The Development of a Dual Extrusion Blending Process and Composites Based on Thermotropic Liquid Crystalline Polymers and Polypropylene

By

Edward A. Sabol

Thesis submitted to the Faculty of
The Virginia Polytechnic Institute and State University
in partial fulfillment of the degree of

MASTERS OF SCIENCE

in

Chemical Engineering

APPROVED:

Dr. Donald G. Baird, Chairman

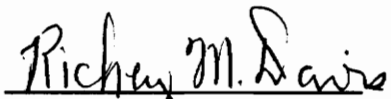

Dr. Richey M. Davis

Dr. Eva Marand

May 26, 1994

Blacksburg, Virginia

The Development of a Dual Extrusion Blending Process and Composites Based on Thermotropic Liquid Crystalline Polymers and Polypropylene

By

Edward A. Sabol

Committee Chairman: Dr. Donald G. Baird
Chemical Engineering

(ABSTRACT)

The overall objectives of this work were to improve a dual extrusion process (DEP) which is used to blend thermotropic liquid crystalline polymers (TLCPs) with thermoplastics, determine the mechanism by which TLCP morphology is developed in the DEP and to determine the optimal properties possible in composite materials generated from the blends. The DEP consists of two single screw extruders within which the TLCP and matrix material are plasticated separately. The two continuous polymer streams are joined and then mixed in a series of static mixing elements. Composite materials were formed from pelletized pregenerated strands by processing at temperatures below the melting point of the TLCP.

The DEP was improved by the addition of a gear pump to the TLCP stream, a multiple port phase distribution system, static mixing design, minimization of residence time, die design, and introduction of thermal control over the entire strand production process. The TLCP material was introduced into the matrix phase by means of a multiple port phase distribution system which injected 12 individual TLCP streams parallel to the flow direction of the matrix stream. This design resulted in improvements in the axial continuity of the TLCP phase during mixing and improved radial mixing as compared with a simple T-injection system. Both Kenics and Koch static mixer designs were evaluated in this investigation and it was found that the use of either could produce similar mechanical property enhancement in the resulting blends provided that an excessive number of elements were not used. Furthermore, it was found that the most stable strand materials were formed

when the die was designed with respect to the flow exiting the static mixer elements. For example, a dual strand die with each capillary having an L/D ratio of 1 produced the most stable strands when used with the Kenics mixing elements. Finally, it was found that drawing the molten blend strand in a vertical drawing chimney provided a favorable thermal environment and resulted in much higher draw ratios and high mechanical properties of the strand.

The other objectives of this work including the development of morphology and composite materials produced from pregenerated strands is presented in two manuscripts formatted for submission to appropriate journals. Detailed abstracts dealing with these two topics are included therein.

Acknowledgments

The author wishes to express his appreciation to Dr. Baird for his guidance and the freedom he allowed in the completion of this work. Additionally, I would like to thank my research committee Dr. Eva Marand and Dr. Richey Davis.

The author also wishes to thank the following:

- Foremost, my family for instilling in me the work ethic required to complete my degree and to my wife, Tracey, for giving me the motivation to finish.

- Mr. Billy Williams, who helped design and built the equipment required in this work.

- Soon-to-be, Dr. Tina Handlos, for our team work in improving and running the dual extrusion process and the countless hours that we spent together in smoke filled rooms (smoke from burning polymer).

- Soon-to-be, Dr. Gerhard Gunther, who was always willing to offer assistance and who always gave more than was asked.

- Dr. Preston Durrill and Dr. Robert Pusey, for making my work in Unit Operations Lab both rewarding and enjoyable.

- Finally, I would like to thank Gus who helped maintain my sanity through much of this ordeal.

Original Contributions

The following are considered to be the significant original contributions of the work presented in this thesis:

- The design of the multiple port injection nozzle that enhances the development of a fibrillar TLCP morphology in blends generated using the dual extrusion process.

- The design of a multiple step compression molding process that can be used to produce composite materials, based on blends of TLCPs and thermoplastics, with the highest possible planar isotropic mechanical properties. The process maintains the high molecular orientation and elongated morphology of the TLCP phase of pregenerated strands (produced using the dual extrusion process) in a composite structure where the reinforcement is arranged randomly on a global scale.

Table of Contents

List of Figures

List of Tables

1.0 Introduction

The purpose of this chapter is to introduce the reader to the dual extrusion process and composites materials based on drawn blend strands and the improvements they offer over conventional methods of in situ composite formation (Section 1.1). Important process considerations for the development of reinforcement in blends of thermotropic liquid crystalline polymers (TLCPs) are discussed in Section 1.2. In addition, equations are given in Section 1.3 that are subsequently used to compare the properties of in situ composite strands and composites based on blends of TLCPs and thermoplastics to provide a theoretical limit for the possible properties developed with these methods. Lastly, the objectives of this research are given in Section 1.4.

1.1 Composites Based on TLCP / Thermoplastic Blends

A brief review of the development of in situ composites is given in this section. It is focused on the methodology of their development and pertinent properties and processes that have led to advancements in this area. Conventional in situ composite generation and the dual extrusion system are described in Sections 1.1.1 and 1.1.2, respectively. Finally, secondary processing methods that utilize in situ composite strands to produce composite materials with planar isotropic mechanical properties are

presented in Section 1.1.3.

1.1.1 Conventional In Situ Composites

The reinforcing component of the composites important to this study are thermotropic liquid crystalline polymers (TLCPs). The molecular architecture of TLCPs is composed of highly symmetric aromatic constituents that are sufficiently rigid to provide high strength yet flexible enough to allow for melt processing (1,2). TLCPs exhibit many desirable properties including high strength and modulus, good thermal endurance, excellent barrier properties, good surface appearance, low linear coefficient of thermal expansion, excellent dielectric properties and high chemical resistance (3-5). The properties of these materials typically show a high degree of anisotropy (directional dependence) because of their rodlike architecture being easily aligned in the flow direction during processing. This effect is desirable in processes such as fiber spinning but proves to be a disadvantage in the production of materials such as films and injection molded parts where isotropic properties are typically desired. Although TLCPs exhibit some excellent mechanical properties, their use has been limited because of their high cost in comparison with more widely utilized thermoplastic materials. The cost, though, is expected to decline as the products mature and superior cost effective processes and products are developed (3).

To overcome the limitation of cost and to tailor materials to specific needs, researchers have utilized TLCPs as the reinforcing phase of in situ composite blends (3,6,7). The dispersed TLCP phase in these blends can form oriented high strength fibrils during processing which provides for the mechanical reinforcement of the thermoplastic matrix. Because the reinforcement develops during processing, these materials are often described as *in situ composites*.

There are two broad categories of in situ composite formation. The first is to simply dry blend pellets of the respective polymers prior to processing. This method relies on the processing equipment (for example the screw in an injection molder) to disperse the TLCP phase within the matrix material.

The second method utilizes independent plasticating and mixing equipment such as single or twin screw extruders or batch mixers to first disperse the TLCP within the matrix material prior to in situ composite formation. This pre-blended material is then processed to form the final composite material (i.e., fiber, injection molded part, sheet, etc.). In both cases, the TLCP reinforcing morphology is developed in the final stages of composites formation.

The conventional methods for in situ composite generation are severely limited. These methods require that the TLCP and matrix material have overlapping processing temperatures. This is a limitation because TLCPs of the highest strength typically have melting temperatures in excess of the thermal processing window of many thermoplastic polymers such as polypropylene (PP) and polyethylene. Another disadvantage of these methods is that the formation of TLCP fibrils is dependent on the deformation and coalescence of dispersed droplets of TLCP in the presence of an elongational flow field (3,8-10). These phenomena are quite complex and the above processes do not readily allow for a large degree of control over the formation of TLCP fibrils.

The inability of blending polymers of different processing temperatures has motivated the development of a novel blending process which does not rely on the same processing equipment to plasticate the TLCP and the thermoplastic polymer. This process is described as the dual extrusion method and is described in the following section.

1.1.2 The Dual Extrusion Method

The dual extrusion process (DEP) was initially developed and patented by Baird and Sukhadia (11-13). This process (Fig. 1-1) utilizes two single screw extruders. One extruder plasticates the matrix material while the second plasticates the TLCP. The molten polymer streams

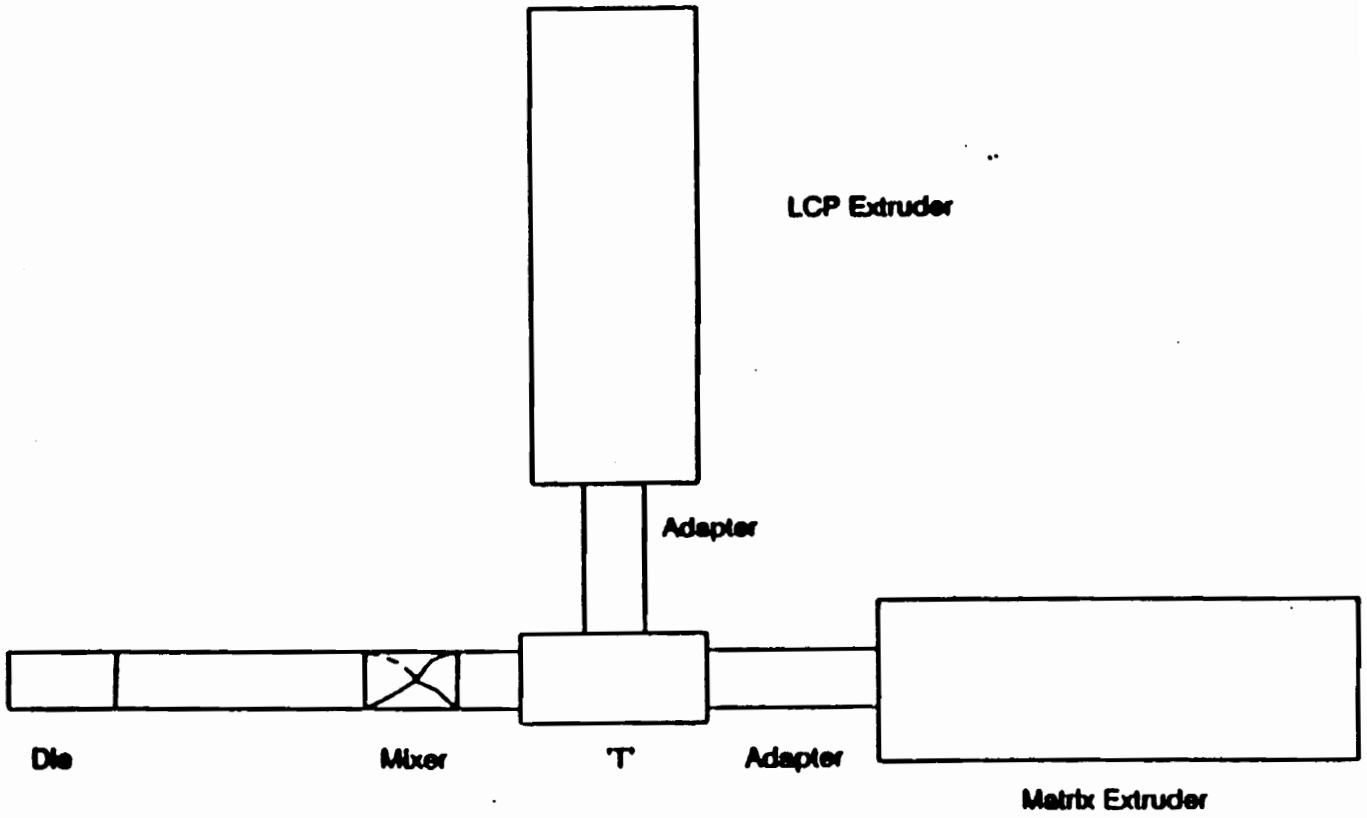

Figure 1-1: A schematic of the dual extrusion as presented by Sukhadia and Baird (6).

are then joined in a tee that leads into a series of static mixing elements that distribute the TLCP within the matrix phase. The blended material is then extruded through a die for final shaping of the in situ composite. Several advantages of the dual extrusion process over conventional methods of in situ composite formation are:

1) the TLCP and matrix materials can be processed with no overlap of processing temperatures and minimal degradation of the matrix phase;
2) the formation of the reinforcing fibrils relies on the division and geometric rearrangement of continuous polymer stream in a series of static mixing elements as opposed to the deformation of dispersed TLCP droplets; and
3) independent thermal histories can be imparted to the polymer streams prior to the mixing process.

The importance of these advantages will be fully described in Section 1.2.

The dual extrusion method has been used to produce in situ composite strands with tensile properties higher than those for blends mixed in a single screw extruder (13). For example, Sukhadia et al. produced strands of a 30 wt.% blend of a thermotropic liquid crystalline copolyester based on hydroxybenzoic acid (HBA) and 2-hydroxy 6-napthoic acid (HNA), commercially known as Vectra A, in a poly(ethylene terephthalate) (PET) matrix using both single and dual extrusion techniques. Under similar post extrusion conditions the dual extrusion strands had a tensile modulus of 19 GPa while strands produced form blends mixed in a single screw extruder had a modulus of 13 GPa. This represents a 46% improvement in properties due to the dual extrusion processing method alone.

The improvements in properties were attributed to morphological (TLCP phase structure) differences caused by the unique dual extrusion method. It was found that strands produced from blends mixed in a single screw extruder exhibited a "skin-core" type of morphology. This morphology is

characterized by the material close to the surface containing highly elongated TLCP fibrils while the material close to the center contains predominately droplets of TLCP that provide little reinforcement to the matrix. Skin-core morphology has been widely observed in in situ composites processed by conventional methods and is not the optimal morphology for self reinforcement because the droplets provide little reinforcement to the matrix (3,8,14,15). In contrast, the strands produced using the dual extrusion method exhibited a TLCP reinforcing phase which consisted of predominately axially continuous fibrils and was devoid of a skin-core morphology (13).

Although strands produced using the dual extrusion process showed large improvements in the properties of strands, little improvement was observed in the properties of sheets produced with the same method (13). Poor property enhancement in conventional in situ composite sheets has been observed by other researchers as well (16-18). For example, Crevecouer (16) produced in situ composites sheets and fibers of 20 wt.% of Vectra A, in a matrix blend of polystyrene and poly(phenylene-ether). The modulus of the films was 4 GPa while fibers of the same composition exhibited a modulus in excess of 10 GPa. Additionally, the properties of the sheets were highly anisotropic.

Thus, achieving outstanding properties with in situ composites seems limited to the production of strands and fibers because these processes provide a strong drawing step which orients the TLCP fibrils. Furthermore, it was found that the dual extrusion process could be used to produce properties in strands which were higher than those seen in conventional in situ composites. The high mechanical properties of the blend strands produced using the dual extrusion process has motivated the used of these materials to form subsequent composite materials.

1.1.3 Composites Based on Drawn Blend Strands

Secondary processing technology which utilizes the high mechanical properties of in situ composite strands to form more usable materials was investigated by Bassett and Yee (19). The process investigated by these researchers uses in situ composite fibers to form a composite "pre-preg" material. The pre-preg is formed by arranging the in situ composite fibers into a tow or cloth. The pre-preg is then consolidated in a hot press at a temperature below the melting point of the TLCP but above the melting temperature of the thermoplastic matrix. They utilized this process to produce uniaxially aligned compression molded composites of 40 wt.% of a TLCP copolyester-amide composed of HNA, terephthalic acid (TA), and aminophenol, sold under the trade name Vectra B, in a polystyrene matrix. The moldings exhibited properties that approached the properties of the original in situ composite strands. Similarly, Handlos and Baird (20) showed that uniaxially and biaxially aligned composites could be produced from in situ composite strands generated by using the dual extrusion method. The composites in this case were a blend of Vectra A in a PP matrix. In this study as well, the uniaxially aligned composite plaques showed tensile properties similar to the original strand properties and properties approximately half the strand properties for the biaxially arranged fiber composites.

The utilization of in situ composite fibers and strands as composite pre-preg material has many potential advantages over conventional composites materials. The studies reported above, clearly indicate that the properties achieved in the in situ composite strands are directly transferable to the properties of uniaxially aligned compression molded plaques of the same material. The advantages and implications of using in situ composite strands as composite pre-pregs in comparison with conventional composite sheets have been delineated by Bassett and Yee (19) as follows:

1) the woven cloth could conform to mold configurations in contrast to thermoplastic stiff sheet composites:
2) voids and adhesion problems associated with poor fiber wet out would be avoided

due to the matrix and TLCP being intimately mixed prior to consolidation;

3) the composite material is 100% recyclable; and
4) a potentially low processing cost in comparison with traditional methods of composite preparation.

These attractive possibilities utilize the highest properties attainable in the in situ composite to form a mechanically isotropic material which could be further processed in operations such as thermoforming.

Baird et al. have extended this initial concept of using strands produced from blends of TLCPs and thermoplastics to form composites in processing operations such as injection molding, sheet extrusion, blow molding, etc. (21,22). This method uses pelletized strands produced via the dual extrusion system as the raw material for secondary composite formation. The composite formation is accomplished at a temperature below the melting point of the TLCP. In this way, the TLCP remains as a rigid reinforcing phase that aligns more randomly during processing as compared to conventional in situ composite formation. The random arrangement of the TLCP reinforcing phase could lead to a more globally isotropic property enhancement of the matrix.

Composite materials produced from drawn blend strands could have several advantages over conventional short fiber composites such as fiberglass. The reinforcing phase in the composites could be of a much smaller cross sectional diameter. The diameter of the TLCP fibrils in highly drawn blend strands can be of the order of 1 μm or less whereas common glass fibers used for thermoplastic reinforcement have diameters of the order of 10 μm (23,24). This is important because the properties of the composite material are dependent on the aspect ratio (ratio of the length to cross sectional diameter) of the reinforcing fibers (Section 1.4). Therefore, the aspect ratios of composites based on blend strands can be a full order of magnitude shorter and still have the same relative reinforcing capacity as short glass fibers. Other advantages of composites based on drawn blend strands over short glass filled thermoplastics include: 100% recyclable, improved surface finish, and more process flexibility at a reduced processing cost. Many of these advantages are derived from the TLCP fibrils being somewhat flexible during processing which limits the break up of the reinforcing phase during processing.

A brief discussion of the basic concepts of in situ composites was given in this section. The discussion was focused on the limitations of in situ composite processes, and how the limitations have lead to the development of the dual extrusion process which appears to be a particularly effective methods of generating self reinforcement in blends of TLCPs and thermoplastic polymers. Methods were also discussed in which the optimal properties in blend materials, developed through fiber drawing processes, could be used to produce composites materials with potentially more useful forms. The following section is focused more specifically on the development of the reinforcing TLCP fibrils during processing.

1.2 Aspects of In Situ Composite Processing

This section is focused on several important aspects of the processing of in situ composites with special attention given to processes which produce the highest physical properties. Specifically, the mixing of TLCPs with thermoplastics is described in Section 1.2.1. The effect that extensional flow fields have on the on the properties of TLCPs and their blends with thermoplastics is described in Section 1.2.2. Lastly, relevant issues involving the thermal behavior of TLCPs are described in Section 1.2.3.

1.2.1 Mixing

The method in which the TLCP and thermoplastic are mixed is a crucial component in the formation of an in situ composite. Mixing of molten polymers is highly complex, and the following treatment is superficial at best. It is intended to describe the components that are of the most importance with respect to the formation of in situ composites. The types of mixing generally encountered in the blending of TLCPs and thermoplastics are also compared.

Conventional in situ composite blending depends on high energy intensive dispersive mixing equipment such as single or twin screw extruders or batch mixers. Mixing in these devices relies on high strains (deformations) to first elongate the dispersed molten particles of the TLCP phase which subsequently break up into smaller droplets. The initial stages of this process can be illustrated by considering mixing in simple shear flow (Fig. 1-2) where a fluid is sheared between two parallel plates, one stationary and one moving with velocity V (25). A fluid element $ABCD$ deforms to element $A_tB_tC_tD_t$ because the velocity along AC is higher than along BD. The shear rate is defined as the gradient of the velocity field, and in this case is given by

$$\dot{\gamma} = \frac{V_A - V_B}{AB} \qquad (1)$$

The shear strain γ is a measure of the deformation of the fluid element that occurs as a result of a shear rate acting over a period of time. The shear strain for this simple case is given by

$$\gamma = \frac{AA_t - BB_t}{AB} = \tan\beta_t \qquad (2)$$

The thickness of the element described as the striation thickness, δ, is reduced as the shear strain increases, and is given by,

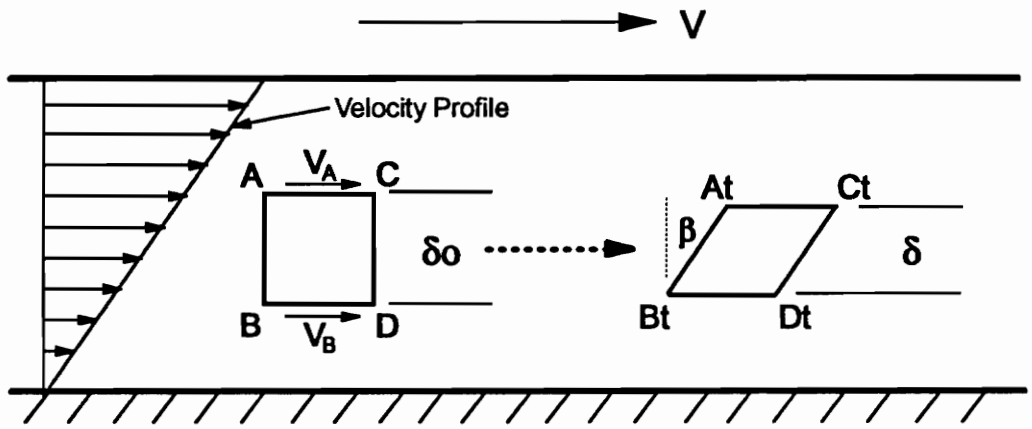

Figure 1-2: Strain induced mixing in simple shear flow.

$$\delta = \delta o \frac{1}{(1+\gamma^2)^{1/2}} \qquad (3)$$

This treatment neglects the interfacial forces and the effects due to the differences in phase viscosity. It is only realistic when the minor phase deforms affinely: that is, the deformation of the matrix and the minor phase are equal. This is true only in the initial stages of mixing and/or when the polymers are totally miscible (i.e., the surface tension is non existent) and the viscosities of the two phases are identical (25,26).

Blends of thermoplastics and TLCPs are typically immiscible or only partially miscible. Therefore, the deformation of the TLCP phase is counteracted by interfacial forces. In these systems the TLCP phase deforms into long slender bodies. However, the interfacial forces inevitably overcome the viscous forces, and the elongated TLCP phase breaks up into lower surface energy droplets. The breakup of the minor phase is termed dispersive mixing (26).

The phenomenon of droplet deformation and break up is a function of the ratio of the viscosity of the dispersed phase to the viscosity of the matrix phase ($\lambda = \mu_d/\mu_m$). Specifically, it has been found that a viscosity ratio of less than 1 is required for droplet elongation in simple shear flows (1,2). Furthermore, the deformation is dependent upon the Weber number which is the ratio of the viscous stress in the dispersed phase to the interfacial stress between the phases. There is also a dependence on the type of flow field generated within the mixing equipment in that an extensional flow component is more effective at deforming the dispersed phase versus shearing flow alone (2,9,15,28,29).

Another type of mixer that has been used in the blending of TLCPs with thermoplastics is the static (motionless) mixer (12,13,19,30). Static mixers use non-moving mixing elements that continually divide and geometrically rearrange the melt flow thus increasing the surface area and degree of distributive mixing. Static mixers are designed to be placed within process piping, and the energy required for mixing is derived from the excess pressure drop that the mixing elements cause compared

with the flow through the pipe in their absence (31).

One of the simplest static mixers is the twisted tape mixer developed by Kenics (Fig. 1-3) (25,32,33). This mixer consists of helical elements that are oriented 90° relative to each other. Each successive element alternates right and left handed helices. Ideally, the flow is divided in half in each element leading to the following expression for the number of striations,

$$S = 2^{n} \qquad (4)$$

where S is the number of striations and n is the number of Kenics mixer elements. Due to geometric considerations, Eqn. 4 leads to a simple expression for the ideal striation thickness developed in a Kenics mixer:

$$\delta_n = \delta_0 2^{-n} \qquad (5)$$

where δ_n is the striation thickness after n mixer elements and δ_0 is the striation thickness prior to the first element (25). The relative simplicity of the Kenics mixer has lead to some theoretical and numerical modeling of the flow that occurs within the elements (34,35).

A second and more complex type of static mixer is the Koch mixer (Fig. 1- 4) (36). This mixer is composed of a system of bars placed 90° relative to each other and an angle of approximately 45° relative to the axis of the pipe. The bars divides the flow into layers that are distributed over the cross section of the pipe. The mixing action of the Koch mixer is based on the flow around a tilted bar (26). In particular, when a bar is oriented at an angle of approximately 45° relative to the axis of the pipe a fluid stream is divided and remains divided because secondary flow on the back side of the bar fills the space between the secondary streams (Fig. 1-5a). In contrast, when a bar placed perpendicular to the pipe axis the divided streams recombine because there is a stagnant region on the back side of the bar (Fig. 1-5b). The number of striations produced in the Koch mixer increases exponentially with the number of mixer elements but due to the complex flow pattern an exact or even approximate expression quantifying the mixing can not be found in the

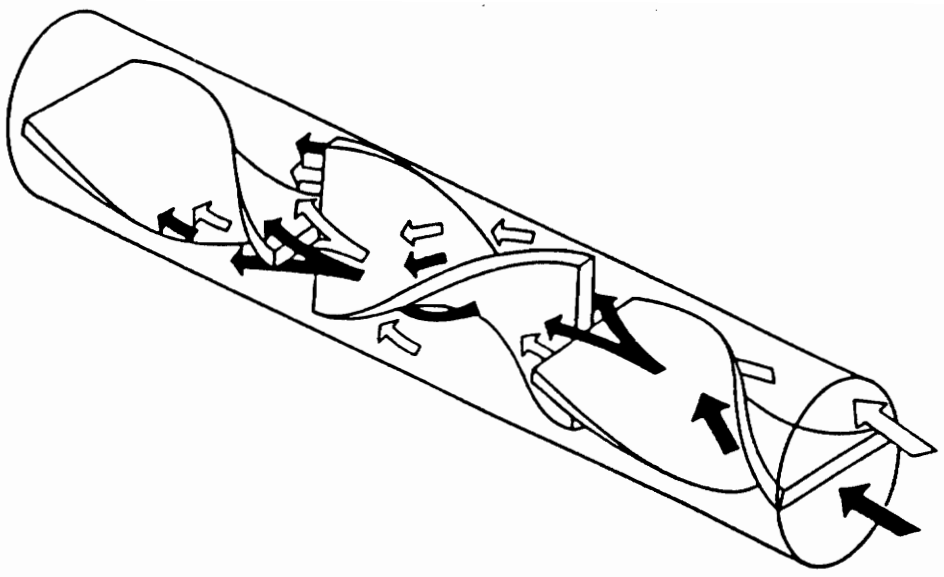

Figure 1-3: Helical elements of the Kenics static mixer (32).

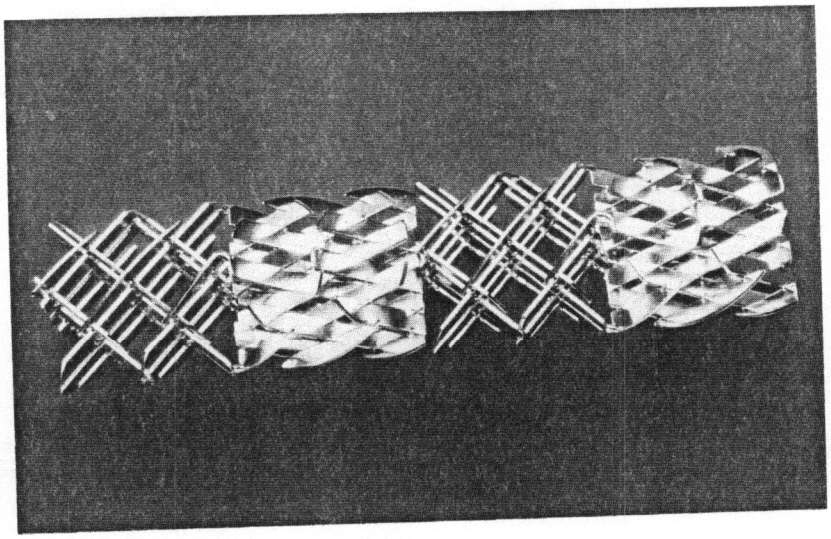

Figure 1-4: A photograph of four elements of the Koch static mixer (36).

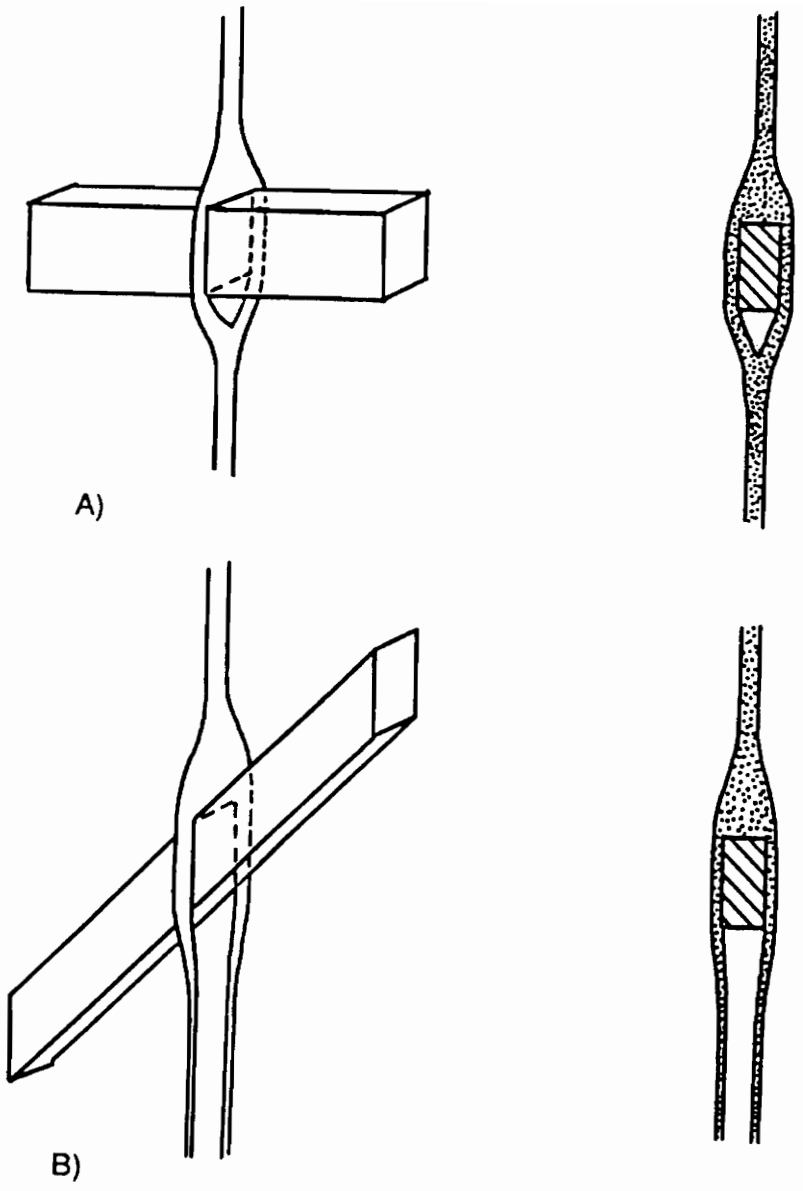

Figure 1-5: Flow splitting with perpendicular (A) and oblique (B) bars (25).

literature. There are numerous other static mixer designs, but the Kenics and Koch mixers show the essential operational characteristics of most of the commercially available models specifically designed to mix high viscosity fluids.

The mixing that occurs in static mixers can be described as laminar distributive mixing. There is certainly some degree of dispersive mixing, but the extent of this type mixing is much less in comparison with the mixing methods described previously. This is due to the relatively low shear rates and residence times encountered in the purely pressure driven flow that occurs in the static mixers in contrast to the high shearing action of mechanically intensive mixing equipment (25,26).

Some studies have been done on the effect that different mixing methods have on the physical properties of the resultant in situ composites. The majority of these studies have investigated different methods of dispersing the TLCP phase within the matrix material prior to final process operations (7,30,37,38). The results of these studies are somewhat contradictory in that there is no clear pattern of improved properties of the in situ composites with type of preblending equipment used or the degree of mixing. The vast majority of studies have focused on comparing internal mixing equipment while relatively few studies have included static mixers.

In the studies which do investigate the effects of static mixers on the morphology and physical properties of in situ composites, they are typically placed between an extruder and the die to improve distributive mixing (19,30). For example, Iseyev and Modic (19) investigated blends of polycarbonate (PC) and 2.5 wt.% of a TLCP copolyester based on HBA and HNA. They found that the physical properties of injection molded plaques produced using pre-blended materials generated by using a single screw extruder and 6 elements of Koch static mixers showed improved mechanical properties as opposed to strands produced using an internal mixer. Specifically, the tensile modulus, yield strength, ultimate strength and toughness (area under the stress strain diagram) of plaques produced using static mixer preblending all showed marked improvement over blends mixed in an internal mixer (Fig. 1-6).

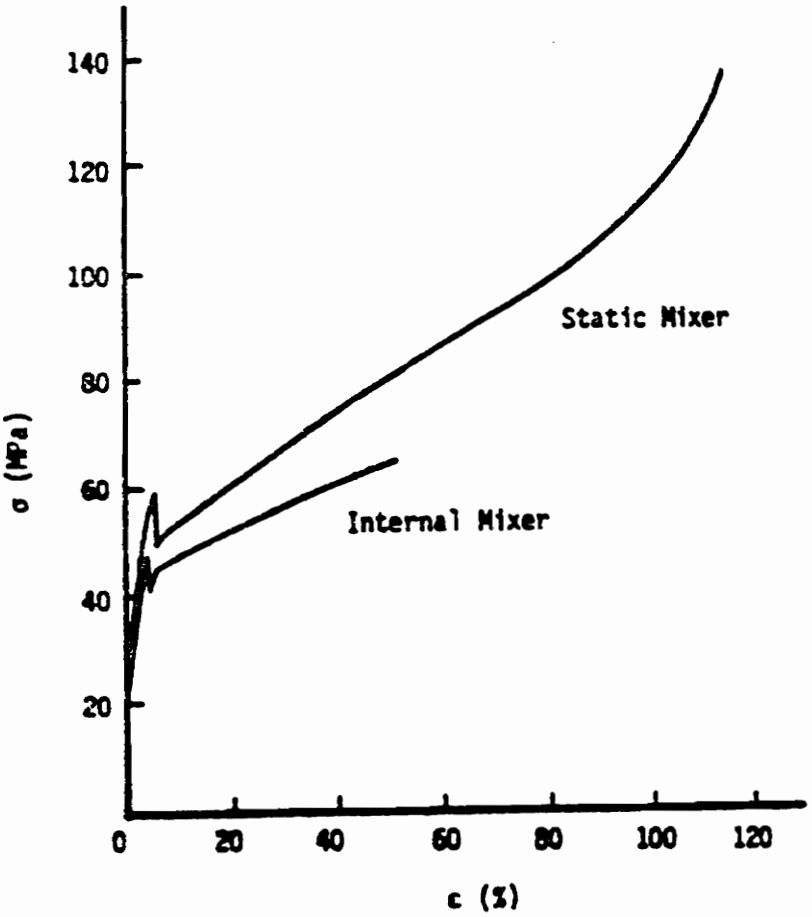

Figure 1-6: Tensile stress as a function of strain for a 2.5 wt. % (HBA/HNA)/PC blend (30).

The only in situ composite process that employs static mixers as the exclusive means of mixing the TLCP and thermoplastic is the dual extrusion process. In the initial studies of this system, 18 Kenics mixer elements were used to distribute the TLCP phase within the matrix phase (12,13). Although this system has been shown to produce strands with excellent mechanical properties, little is known of the optimal type or number of mixing elements needed to produce the highest property strands. Hence, improved mixing technology in combination with the dual extrusion system is a clear avenue to the improvement of mechanical properties of in situ composite strands.

1.2.2 Fibril Formation and Melt Drawing

In Section 1.1 it was stated that TLCPs are easily aligned in certain flow fields. This characteristic of TLCPs in itself does not assure high physical properties in the resultant in situ composites. The mechanical properties of in situ composites are highly dependent on the degree of molecular orientation of the TLCP phase as well as the generation of a fibrillar morphology. Orientation relates to the degree of order of the molecules upon solidification. The degree of molecular order is largely dependent on the type of flow field generated in the processing operation.

Simple elongational flow fields are the most effective at imparting a high degree of molecular alignment and orientation of blends of TLCPs and thermoplastics. This type of flow is characterized by stretching a fluid along only one primary axis in the absence of any shear effects and is developed in polymer processes such as fiber spinning and film extrusion (39). In these processes a molten strand or sheet is extruded from a die then stretched in the absence of any shear effects. The degree of elongation is typically characterized by the draw ratio which is the final velocity of the material divided by the average velocity of the material exiting the die before elongation ($\varepsilon = V_f/V_i$).

The dramatic improvement of physical properties for neat TLCPs with increased draw ratio has

been observed. For example, Nobile et al. (40) showed that the modulus of strands of a TLCP copolyester of PET and HB increased from 2 GPa in the undrawn state to a plateau modulus of approximately 35 GPa for draw ratios over 100 (Fig. 1-7). The dramatic improvement in the mechanical properties of TLCP was the result of increased molecular orientation caused by increased draw ratio.

The improvement of tensile properties with increased draw down ratio is also clearly seen in in situ composite strands and fibers (3,6,13,40-45). For example, Dutta et al. (41) studied the effect of draw ratio on fibers produced from a blend of 20 wt.% of a TLCP based on HNA, HBA, hydroquinone (HQ), and TA in a matrix of PC. They observed an order of magnitude increase in fiber modulus as the draw ratio was increased from 1 to 1000 (Fig. 1-8). The reinforcement of the matrix material was due to dispersed fibrils of TLCP being elongated and oriented providing improved reinforcement to the matrix as the draw ratio was increased.

In addition to the molecular orientation of the TLCP phase, the increase in the mechanical properties of in situ composites with increased draw ratio is due to the development of a fibrillar TLCP morphology. Droplet elongation was briefly introduced in Section 1.2.1 and the same phenomenon that leads to strain mixing also leads to the formation of the reinforcing TLCP fibrils in a conventional in situ composite. Initial investigations into the development of a fibrillar morphology in polymer blend was investigated by Tsebrenko et al. (10). A schematic of their proposed mechanism for the development of a fibrillar morphology includes four distinct regions (Fig. 1-9). Specifically, the regions can be described as: A) tension and fiber forming; (B) flow narrowing; (C) relaxation zone; and (D) flow in the shear field. This mechanism also indicates the need for a low L/D ratio for the die. In particular high L/D ratio die allow for the relaxation of the newly formed fibrils which either break up or return to a spherical shape as a result of interfacial forces.

The development of a fibrillar TLCP morphology is also dependent on coalescence of the dispersed droplets in the fibrils forming process. For example, at higher TLCP concentrations the

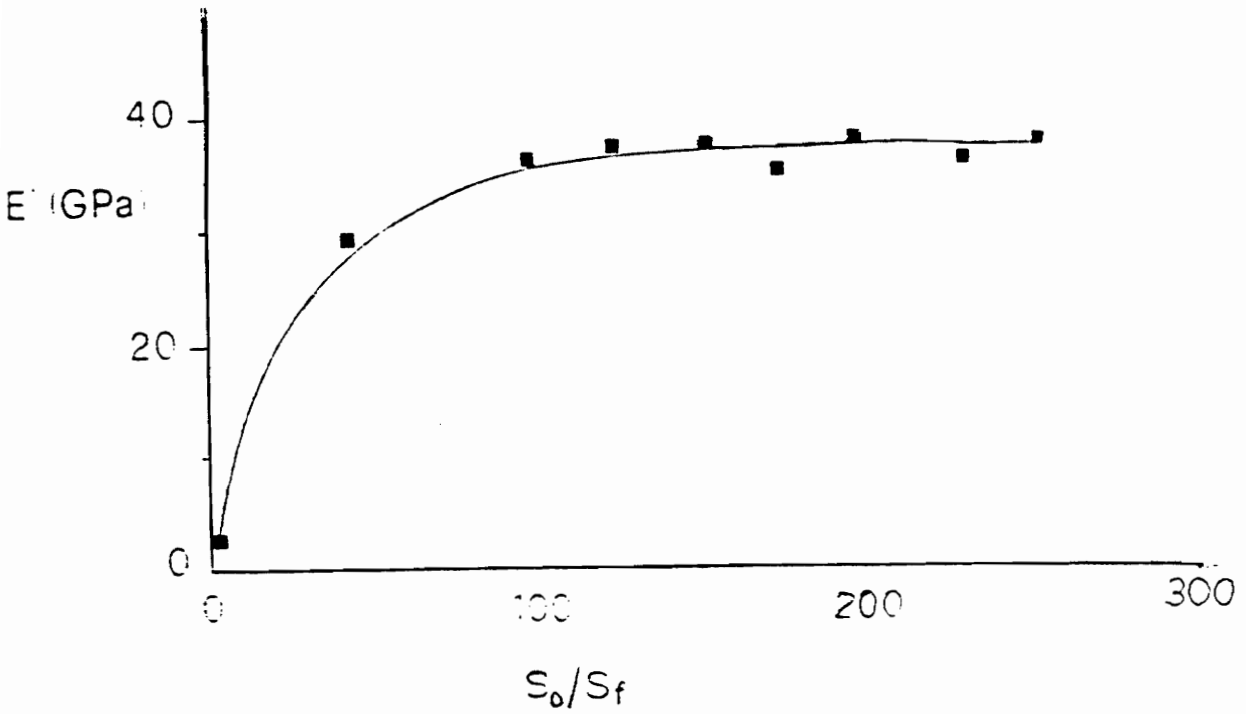

Figure 1-7: Modulus development in a TLCP copolyester based on PET/HB where S_0/S_f is the draw ratio (28).

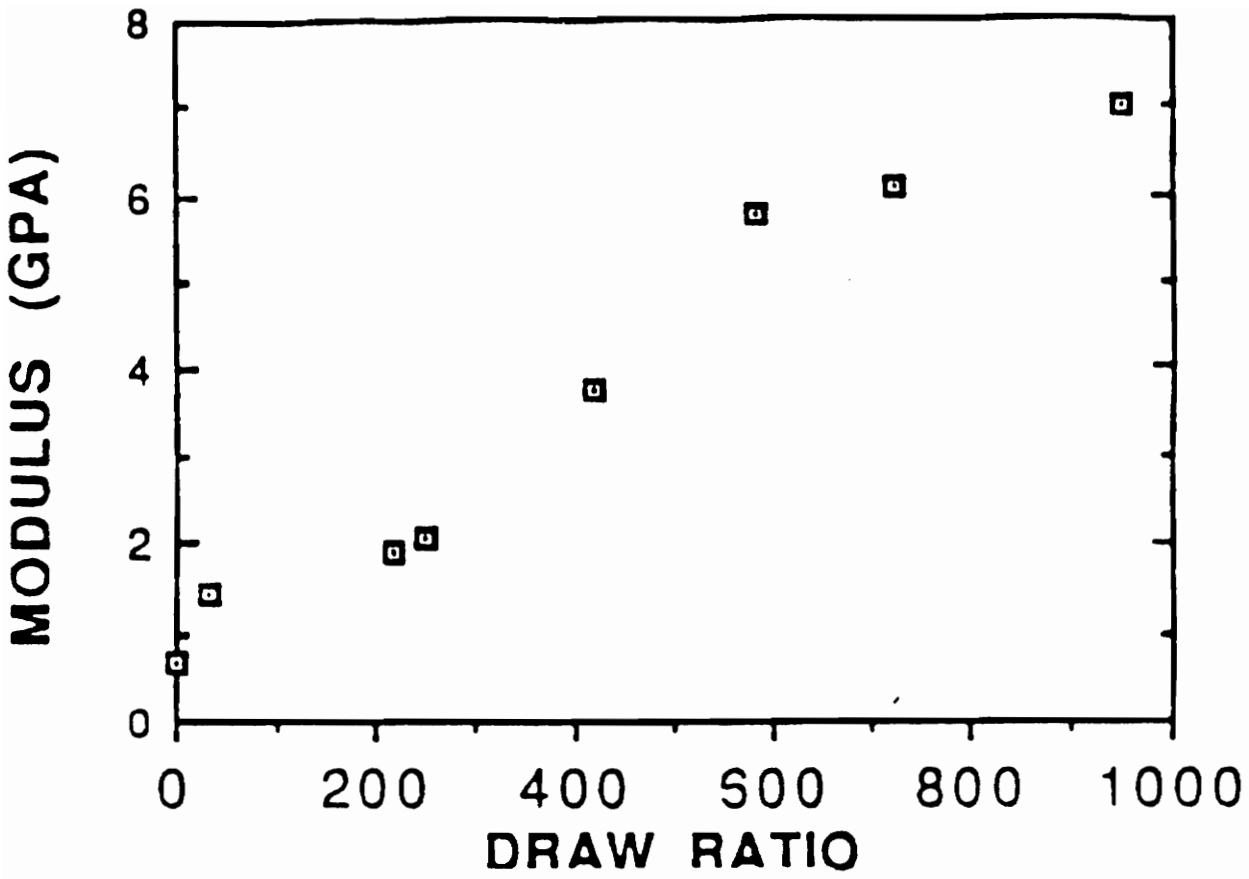

Figure 1-8: The effect of draw ratio on the tensile modulus of in situ composite fibers of 20 wt. % of a TLCP based on HNA, HBA, HQ and TA in a PC matrix (29).

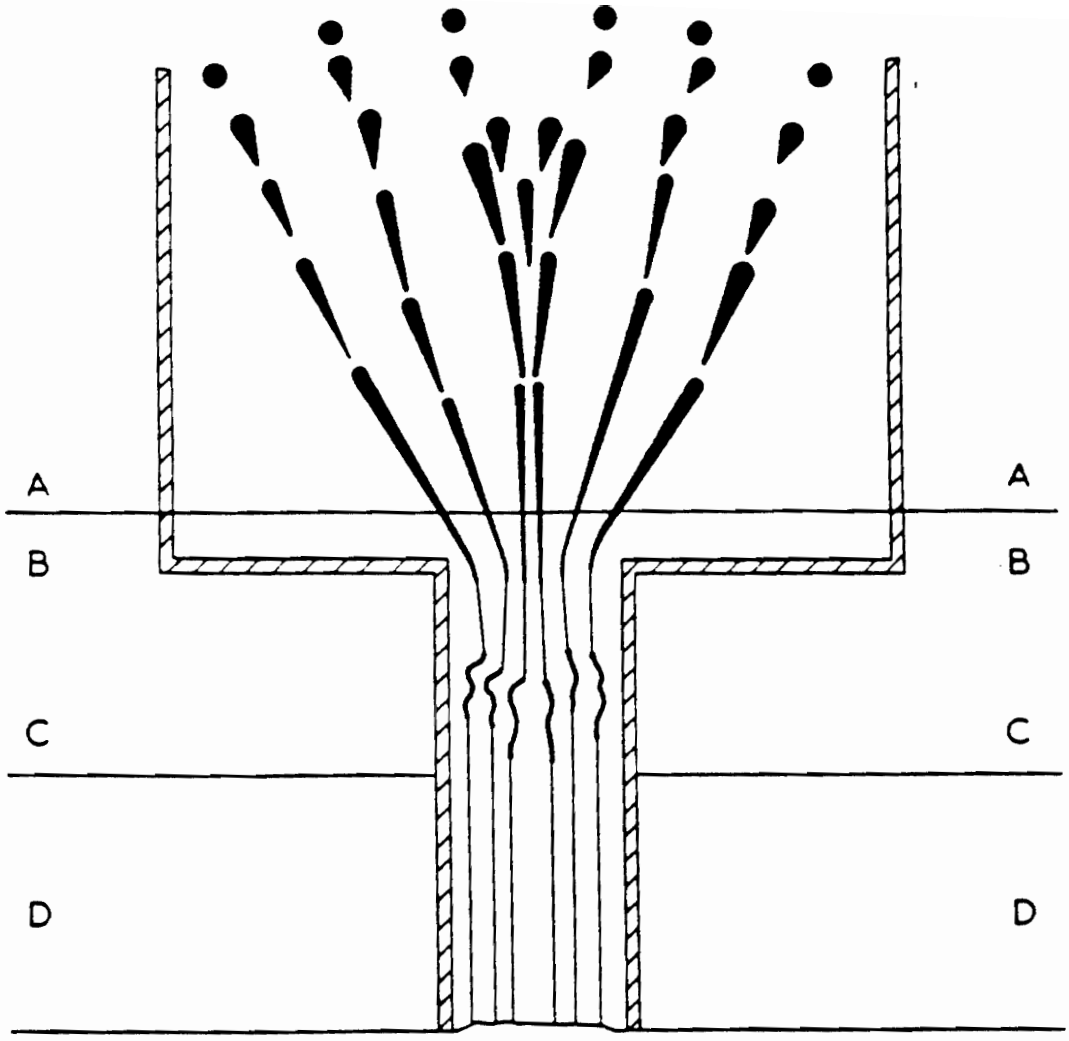

Figure 1-9: Fibril formation of a polymer blend in a capillary die with (A) tension and fiber forming, (B) flow narrowing, (c) relaxation zone and (D) shear flow (10).

TLCP droplets interact in a dynamic cycle of droplet coalescence, deformation and break up. Therefore coalescence can lead to the formation of fibrillar morphology simply due to droplets combining in the entrance region of the die. However, droplets can be generated which are quite small with correspondingly high interfacial surface tension. These small droplets can not deform as easily as larger droplets and (in the absence of coalescence) can not form a fibrillar morphology. This dependence on concentration is supported by many investigators which have found that there exists a minimum TLCP concentration before fibrils can form (8,15,40,47,48).

The mechanism of fibril formation described above is somewhat different from the mode of TLCP fibril formation proposed for the dual extrusion method (13). In this process it is believed that TLCP fibrils are formed from the continual division and geometric rearrangement of continuous polymer streams within the mixing elements. These fibrils are further elongated and oriented as the flow contracts into the capillary die and is drawn as a strand. The evidence for this mechanism is that strands produced with this method show no skin-core morphology and that the TLCP fibrils are truly axially continuous (13).

1.2.3 Thermal Effects

The thermal history of thermotropic TLCPs can profoundly affect their rheological behavior. Two phenomena that are particularly significant to the processing of TLCPs and their blends with thermoplastics include preheating and supercooling effects. When some TLCPs are preheated to a higher temperature then dropped to the testing temperature, the rheological behavior is markedly different when compared to a sample heated directly to the testing temperature. The preheated material has been shown to have a reduced viscosity (49-51). The second thermal effect, supercooling, occurs when a sheared TLCP can be cooled to temperatures well below the melting point but still remains fluid for an extended

period of time (51,52).

The preheating effect was been described in an early study by Wissburn (51) for a thermotropic liquid crystalline copolyester based on PET and HBA in a 40/60 molar ratio. It was found that if the material was preheated to 300°C then dropped in temperature to 210°C, the measured viscosity (in some cases) was found to drop by over an order of magnitude in comparison with a sample directly heated to 210°C (Fig. 1-10). The drop in viscosity was attributed to the preheating which melted residual crystals of the HBA component. Similar results have been observed in other TLCP systems (49,50).

The preheating effect could be quite useful in the processing of in situ composites. For example, the elongation of dispersed droplets of TLCP in a thermoplastic matrix is dependent on the viscosity ratio of the TLCP phase to the matrix phase ($\lambda = \mu_d/\mu_m$) as discussed in Section 1.2.1. Specifically, it has been found that λ must be equal or less than unity for a dispersed TLCP droplet to deform into a fibril in an extensional flow field (1). The only method of in situ composite generation that allows for the independent control of viscosity through preheating is the dual extrusion system. In all other methods the matrix and TLCP are plasticated in the same equipment. Therefore, the temperature is necessarily the same for each phase allowing little control over the viscosity ratio of the constituents.

The supercooling behavior of several TLCPs has been studied by Done and Baird (52,53) In one such study, (53) the viscosity of a TLCP copolyester based on PET and HBA in a 40/60 molar ratio was measured while the sample temperature was dropped at a rate of 5°C/min. In this case, it was found that the material did not solidify until 85°C below the melting point of the polymer. The study also investigated other TLCPs that showed various degrees of supercooling. This phenomenon could prove very useful as a processing tool for the production of in situ composites. Taking advantage of the supercooling effect would allow for the processing of in situ composites at a temperature below the melting point of the TLCP further reducing the possibility of degradation of

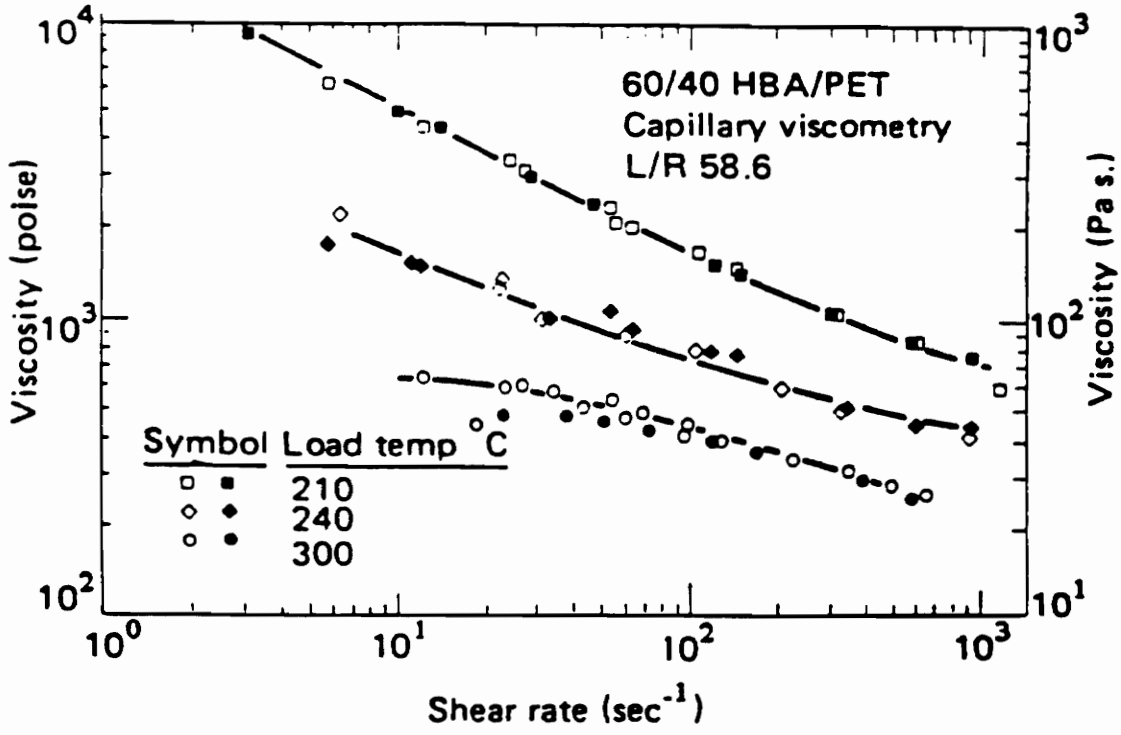

Figure 1-10: Effect of preheating on the viscosity of liquid crystalline copolyester composed of 60/40 PHB/PET (51).

the matrix material.

This section was intended to give an introduction to some of the important processing considerations that could be useful in the generation of mechanical reinforcement in blends processed in situ composites using the dual extrusion method. It was found that mixing is of central importance in the development of in situ composites. Additionally, it was also found that drawing and thermal effects are powerful tools in the pursuit of high strength strands produced from blends of TLCPs and thermoplastics. The following section deals with composite theory that can be used to predict the upper limit of composite properties attainable in an in situ composite.

1.3 The Theory of Fiber Reinforced Composites: Mechanical Property Limitations

A brief review of the equations that have been used to predict the physical properties of in situ composites is given in this section. The theories that are described were originally derived to predict the properties of traditional fiber reinforced composites. The similarities of in situ composites to fiber reinforced composites allows the equations to find direct utility in the prediction of the properties of composite materials based on blends of TLCPs and thermoplastics materials. The equations described in this section are used to predict the theoretically highest properties attainable in in situ composites within the constraints of the assumptions inherent to their derivation.

The equations used to predict the modulus and tensile strength of uniaxially aligned fiber composites are presented in Section 1.3.1. The properties of randomly oriented fiber composites is described in Section 1.3.2.

1.3.1 Uniaxial Fiber Reinforced Composites

The relationship generally accepted to describe the modulus of uniaxially oriented fiber reinforced composites is the Halpin-Tsai equation (54). The development assumes that the reinforcing phase has a uniform length to diameter ratio and that there is continuity of stress and strain at the fiber matrix interface. The Halpin-Tsai equation provides a direct relationship between the modulus of the reinforcing fiber and the matrix material to the fiber direction modulus of the resulting composite material

$$E_p = E_m \frac{1+2(L/D)\varphi_f}{1-\eta\varphi_f} \qquad (6)$$

$$\eta = \frac{E_f/E_m - 1}{E_f/E_m + 2(L/D)}$$

where E_p, E_f and E_m are modulus of the uniaxial composite (parallel to the reinforcement), reinforcing fiber, and matrix material, respectively, φ_f is the volume fraction of fiber, and (L/D) is the length to diameter aspect ratio of the reinforcing phase. To illustrate the importance that the aspect ratio of the reinforcing phase on the properties of the composite, Eqn. 6 is plotted in Fig. 1-11 where the modulus of the matrix material is taken as 1 GPa while the fiber modulus is taken as 75 GPa. As can be seen in Fig. 1-11, when the fiber aspect ratio approaches infinity there is a linear relationship between the matrix and fiber modulus which is given as,

$$E_p = \varphi_f E_f + (1-\varphi_f)E_m \qquad (7)$$

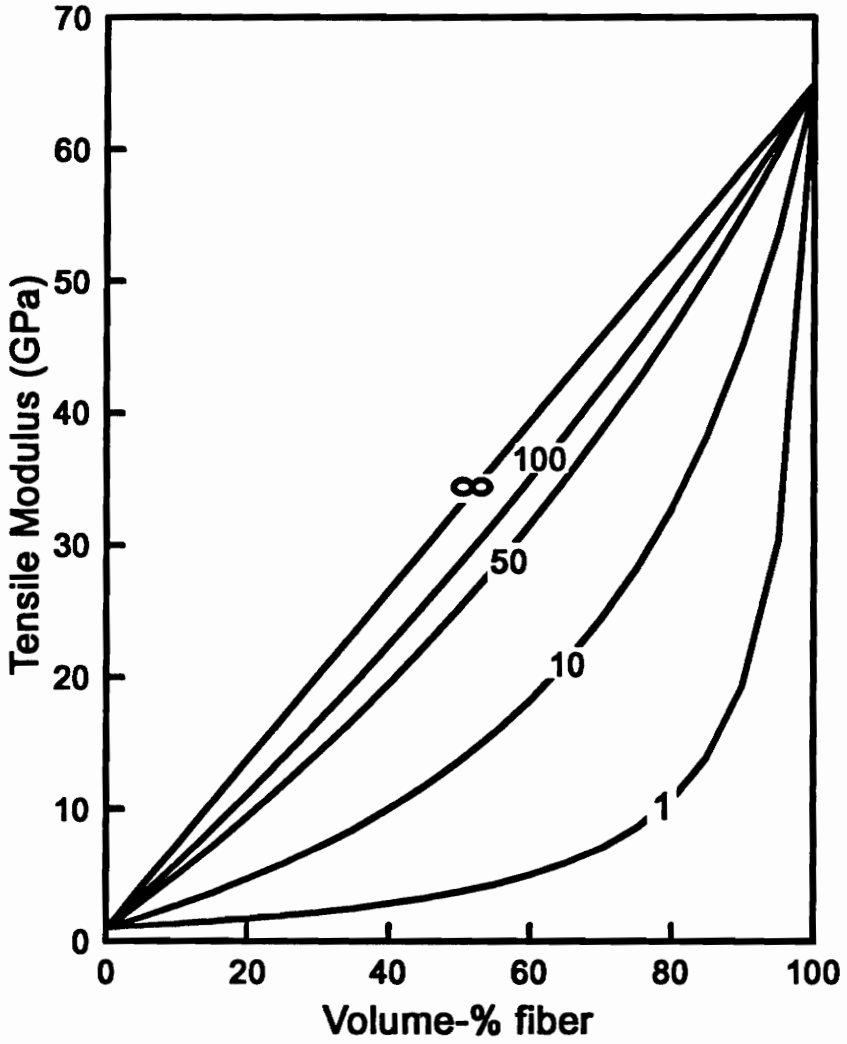

Figure 1-11: **Predicted modulus values for uniaxially aligned fiber reinforced composites as a function of fiber aspect ratio using the Halpin-Tsai equation.**

This simple relationship is referred to as the "rule of mixtures" and is often used to compare in situ composite properties (6,55). Eqn. 7 is particularly useful in the case of in situ composite strands and fibers. This is due to TLCP fibrils being aligned in the machine direction (flow direction) which approximates an uniaxially aligned fiber reinforced composite.

A comparison of the modulus obtained through Equation 7 with experimentally obtained literature values is presented in Table 1-1. The modulus of the reinforcing fiber is taken as the as spun fiber modulus of the neat TLCP as quoted by the manufacturer. It is clear from Table 1-1 that the properties of in situ composite strands are much closer to the composite theory limit as compared with injection molding materials. This is due to the elongational flow field in injection molding being weak which does not allow for the full development of the potential properties of the TLCP. Furthermore, of the in situ composite strand properties listed those produced using the dual extrusion process most closely approach the limit predicted by using composite theory.

Uniaxially aligned fiber composites have highly anisotropic mechanical properties, with considerable enhancement of the tensile properties in the fiber direction but not in the directions perpendicular to the fibers, the transverse direction. In the transverse direction, the composite modulus is dominated by the modulus of the matrix material and is often estimated by an inverse rule of mixtures (56). The tensile modulus, E_t, in this case is given by

$$1/E_t = \varphi_f/E_f + (1-\varphi_f)/E_m \qquad (8)$$

As can be seen from Eqn. 8, the modulus in the transverse direction is significantly less than that of the modulus in the machine direction.

The tensile strength of a uniaxial composite has also been modeled in a similar fashion using composite theory (56). The equation that results from composite theory depends on a critical fiber

Table 1-1: Comparison of actual and predicted modulus values for some in situ composite materials

In Situ Composite	Reported Modulus (GPa)	Processing Method	Eqn. 7 Modulus (GPa)	Ref.
30% Vectra A/PP	2.16	Inj. TB	15.8	58
30% Vectra A/PP	2.94	Inj. PQ	15.8	58
30% Vectra B/PP	3.67	Inj. TB	18.0	59
30% Vectra A/PET	5.50	Inj. PQ	21.3	60
20% Vectra A/PET	3.42	Inj. PQ	15.0	12
30% Vectra A/PET	19.0	DEP Strand (40)	21.6	13
30% Vectra A/PET	13.0	Strand (40)	21.6	13
20% Vectra A/PET	11.1	Strand (80)	15.0	61
28% Vectra B/PP	4.7	Strand (35)	18.7	12
26% Vectra A/PP	13.5	Strand (40)	20.0	12

Methods of processing: injection (Inj.) molded tensile bar (TB) or plaque (PQ), and strands produced using the dual extrusion process (DEP) or conventional in situ composite processes with strand draw ratio given in parentheses

length , L_c, which is the minimum fiber length required for stress transfer between adjacent reinforcing fibers, and is given as

$$\sigma_p = \varphi_f(1 - L_c/2L)\sigma_f + (1 - \varphi_f)\sigma_m \qquad (9)$$

where σ_p, σ_f, and σ_m are the strength at break of the composite (fiber direction), reinforcing fiber, and matrix material respectively. This equation also reduces to a simple linear rule of mixtures in the limit of continuous reinforcing fibrils, L>>Lc, as given below:

$$\sigma p = \varphi_f\sigma_f + (1 - \varphi_f)\sigma_m \qquad (10)$$

The equations given in this section are simple yet describe the composite properties quite effectively. There are certainly many refinements that have been made in the theories to better predict the properties of uniaxially aligned fiber composites (56,57). However, for our purposes these equations are quite adequate and have been widely used to determine the upper limit that might be realized of in situ composite properties (6,54).

1.3.2 Randomly Oriented Fiber Composites

The methodology used by Halpin-Tsai in Section 1.3.1 for uniaxially reinforced composites can be extended to fiber reinforced composites where the fibers are isotropically oriented in the plane of the sample (57). For this case the modulus of a random composite, E_r, is given by

$$E_r = \frac{3}{8}E_p + \frac{5}{8}Et \qquad (11)$$

where E_p and E_t are the moduli parallel and transverse to the fiber direction, respectively. In the case of composite reinforcement with aspect ratios approaching infinity Eqn. 7 and 8 can be used to predict E_p and E_t respectively. The use of Eqn. 11 could provide a useful tool in predicting the limits of realistic properties in composites based on randomly oriented drawn blend strands.

This chapter was focused on the development of mechanical reinforcement in blends of thermoplastics and TLCPs. Special attention was given to the process that leads to the development of the highest properties in these systems (i.e., in situ composite fibers produced using the dual extrusion method). Finally, equations were summarized which provide a theoretical limit for the properties that might be expected in blend strands as well as composites bases on pregenerated strands. The next section will establish the objectives of this research.

1.4 Research Objectives

The dual extrusion method offers several advantages over conventional in-situ composite formation. These advantages include: (1) the ability to blend thermoplastic polymers with TLCPs that have nonoverlapping processing temperatures; (2); truly axially continuous reinforcing TLCP micro fibrils; and (3) ultimately higher tensile properties as compared to blends of identical composition produced using other processing methods. Furthermore, the development of a process that maintains the high properties of strands produced using the dual extrusion process in a composite material with more

isotropic reinforcement in the final compoite could prove to be economically attractive. With this introduction, the objectives of this research are given below.

Objective One

Optimize the mechanical properties of strands produced with the dual extrusion method through improvements in: concentration control, mixing technology, strand die design, strand drawing, and temperature control throughout strand production process.

Objective Two

Determine the mechanism by which the TLCP reinforcing fibrillar morphology is developed during the dual extrusion process and compare that to blending in a single screw extruder.

Objective Three

Determine the optimal physical properties attainable in a planar isotropic composite produced from pregenerated blend strands.

The achievement of the objectives of this work is presented in the following three chapters. The dual extrusion process is described in Chapter 2 and analysis of the design changes is discussed in all of the following chapter. In addition, the second objective, the mechanism of morphology development in the dual extrusion system, is investigated in Chapter 3. Finally, objective three, composites based on drawn strands, is presented in Chapter 4.

2.0 Materials, Processing and Characterization Techniques

This chapter is focused on the materials and methodology used in the accomplishment of the objectives of this research. The polymers used in this study are described in Section 2.1. In Section 2.2, processing equipment and techniques are described. Special attention is given to the dual extrusion system and the modifications that have been implemented to optimize the system. Additionally, a compression molding technique is described. This secondary processing method has been shown to be quite successful in producing high strength isotropic plaques from the dual extrusion strands. Finally, the characterization methods used in rheological, mechanical property, and morphological evaluation of the materials processed in this study are discussed in Section 2.3.

2.1 Materials

Two TLCPs were used in this study. HX1000, supplied by DuPont, is an amorphous copolyester based on hydroquinone, terephthalic acid and other hydroquinone derivatives (3). It has a glass transition temperature of approximately 185°C (38) and a density of 1.25 g/cm^3. This material is typically processed

in the range of 290 to 365°C. The second TLCP, Vectra B950 (VB), was purchased from the Hoechst Celanese Company. VB has a glass transition temperature of 110°C and a melting point of 280°C with a density of 1.41 g/cm^3 (62,63). The rheology of HX1000 and VB, pertinent to processing via the dual extrusion method is discussed in references 17 and 15, respectively.

Polypropylene (PP) was used as the matrix in this study and was Profax-6823 purchased from the Himont Company. The PP has a melt flow index of 0.8 and the following characteristics: T_m =161°C, M_w ≅ 600,000, M_w/M_n = 5 and a density of 0.902 g/cm^3 (64). For the VB/PP blends the matrix PP was sometimes mixed with 10 wt.% maleic anhydride grafted polypropylene (MAP) supplied by Uniroyal. The MAP has a melt flow index of 50 and has been shown to contain 0.75 wt.% maleic anhydride (63). MAP was added to the blend by dry blending it with the PP prior to processing. Glass reinforced PP was also processed to provide a comparison of properties to composites based on pelletized drawn strands. The glass filled PP (PF072-2) was purchased from the Himont Company and contains 20 wt.% glass fibers.

2.2 Strand Formation Processing

A detailed description of the equipment, processing techniques and conditions used in this work are given in this section. Single screw extrusion of both neat materials and blends are discussed in Section 2.2.1 while the dual extrusion process is described in Section 2.2.2. The discussion of the dual extrusion process is intended to justify the alterations that have been implemented as a result of this work. Where possible design criteria have been provided. Many of the changes are supported by morphological and mechanical property investigations with the data discussed in subsequent chapters.

2.2.1 Single Screw Extrusion

Blends of the PP and HX1000 were generated using a 1" Killion extruder, model KL-100, with L/D = 24 and a compression ratio of 3:1. In some cases, 0.5" Kenics static mixer elements were placed between the extruder exit and the die to improve distributive mixing. The die used for this processing method was 0.125" diameter with an L/D equal to one. This arrangement was used to compare the materials generated using the dual extrusion system to those produced using single screw extrusion. For comparison purposes, neat TLCPs were extruded through a 0.125" diameter (L/D = 1) die and drawn to ascertain the properties of the neat materials.

2.2.2 The Dual Extrusion Process

The dual extrusion process, initially developed and patented by Baird and Sukhadia [5], has been substantially improved as a result of this study. The optimized dual extrusion process and some important details regarding the process modifications are described in this section. Many of the justifications and implications of system alterations are discussed in subsequent chapters. A detailed operating procedure is provided in Appendix A.

The dual extrusion process is depicted schematically in Fig. 2-1. The system is composed of two single screw extruders in which the TLCP and matrix materials are plasticated separately. The TLCP extruder is connected to a gear pump that meters the flow of TLCP prior to mixing. The TLCP stream joins the matrix material in a specially designed phase distribution system. The materials are subsequently dispersed in a series of static mixer elements. Finally, the blend material is extruded though a die to form the in situ composite strand or strands. The extrudate is then drawn inside a vertical drawing chimney to increase TLCP fibrillation and orientation. After drawing, the material is quenched

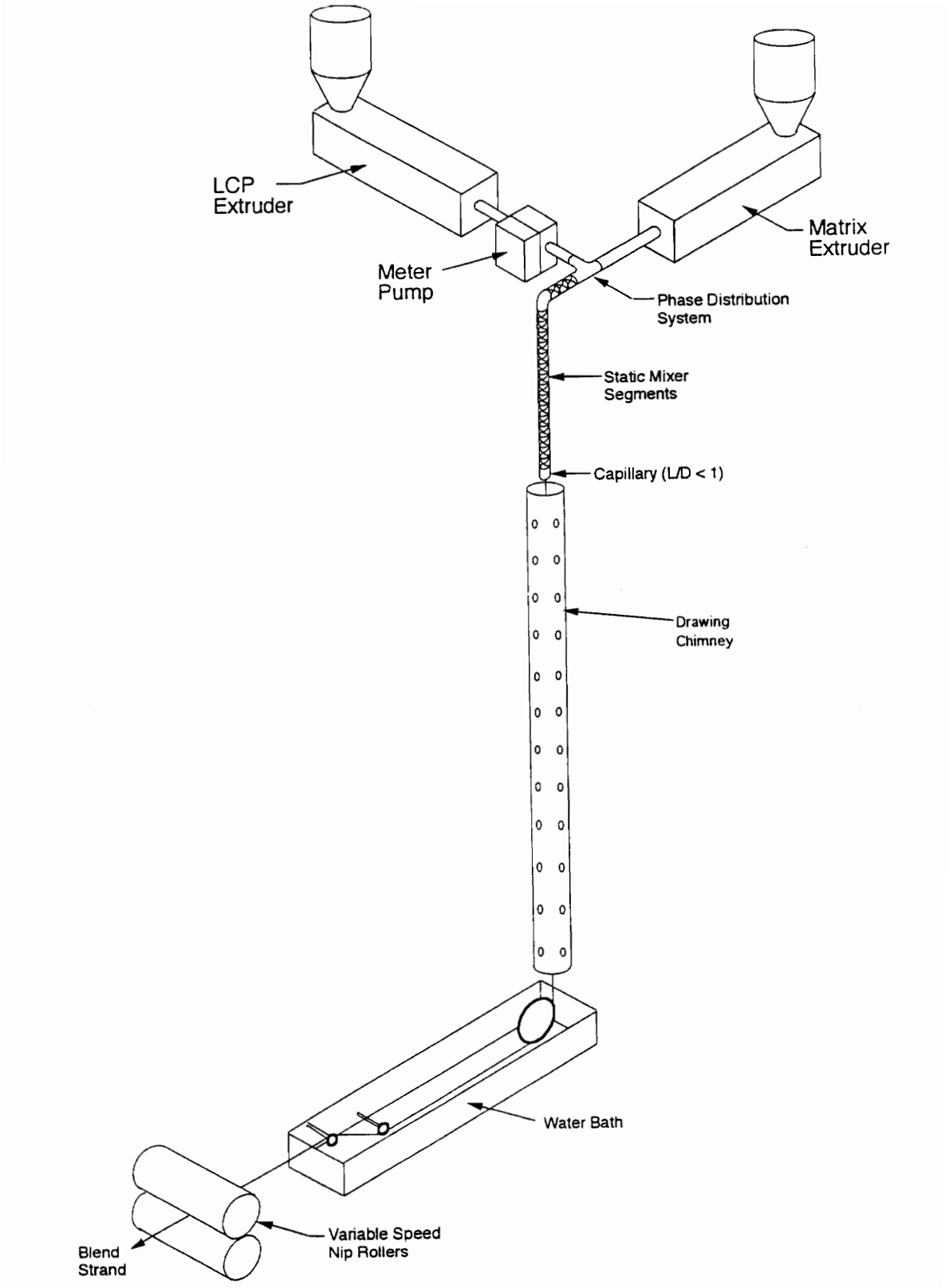

Figure 2-1: A schematic of the dual extrusion process.

in a water bath to solidify the molten blend strand and set in the resultant morphology and orientation.

The process was developed using three specific design criteria. These included the minimization of residence time during mixing, maximization of extensional flow characteristics, and control of temperatures throughout the process. The residence time in the system was minimized to limit the degree of degradation of the matrix material as well as limit solidification of the TLCP during the blending process. Furthermore, reduced residence time in conjunction with increased extensional flow limits the degree of relaxation of the TLCP phase during processing. Relaxation of the TLCP phase would lead to the formation of dispersed droplets due to interfacial forces, thus limiting the formation of TLCP fibrils prior to drawing. Finally, accurate monitoring and control of the temperatures within the dual extrusion process were also desired to minimize the degree of degradation of the matrix material.

The components of the system are now described in more detail. When appropriate, the methodology of how the overall design objectives were incorporated into the specific component is described.

Extruders: Both extruders are Killion model KL-100 single screw extruders. The screw diameters are 1" with L/D=24, and the compression ratio is 3:1.

Metering Pump: The metering pump is a Zenith gear pump model HD-556 with a pumping capacity of 1.752 cm^3/rev and variable speed 1/2 horse power drive. The pumping system was purchased from the Parker Hannifin Corporation. This pump is capable of maintaining a constant flow rate of polymer provided the pump is supplied with a sufficient flow rate of material.

The metering pump was introduced into the system to provide accurate control of the blend composition. The composition of the in situ composite material produced using the original dual extrusion system relied on calibrations of the extruders [13]. The calibration of the extruders was accomplished through measuring the disappearance of a known weight of polymer pellets from the

respective extruder feed hoppers. This process is inaccurate due to the variation in extruder output due to system variations (i.e., temperature and pressure fluctuations and feeding problems). These complications were further intensified because the two extruders are connected causing variations in the flow rates of both extruders. The addition of the metering pump has allowed for the precise control of one of the inlet streams. The composition is now determined by pumping a known flow rate of TLCP into the mixing system and monitoring the total exiting flow rate from the system. This pump is highly reliable and maintains a constant TLCP flow rate. Pump calibrations for the TLCPs used in this study (Fig. 2-2) clearly illustrate the accuracy and reproducibility TLCP flow rate metered using this type of pump. Using the calibration curves and the procedure just described, the composition exiting the die is accurately controlled. Additionally, the metering pump allows for the accurate application of low flow rates of TLCP where the extruder flow rate is quite erratic.

Multiple Port Phase Distribution System: The phase distribution system (Fig. 2.3) was specifically designed and fabricated for this application. The phase distribution system is constructed of 304 stainless steel and connects to the other process piping and subsequent static mixer segments by NPT-M pipe thread fittings. In this system the TLCP enters through a 0.203" diameter injection stem and is distributed into the matrix material by twelve 0.0625" diameter injection ports. The injection ports are located symmetrically in front of the first element in a series of three 0.5" Kenics static mixer elements. The three Kenics elements are placed immediately against the injection stem. This placement was designed to reduce the possibility of the TLCP streams rejoining after they enter the matrix material due to hydrodynamic and interfacial forces. This construction also minimizes the residence time of the materials before being mixed in the static mixers. The size and number of injection ports was limited by available space and difficulty in construction. The ports were designed to maintain an average TLCP injection velocity of approximately three times the average velocity of the matrix material for a 25 vol. % TLCP/matrix blend. As the TLCP enters the matrix material, the diameter of the matrix phase inlet

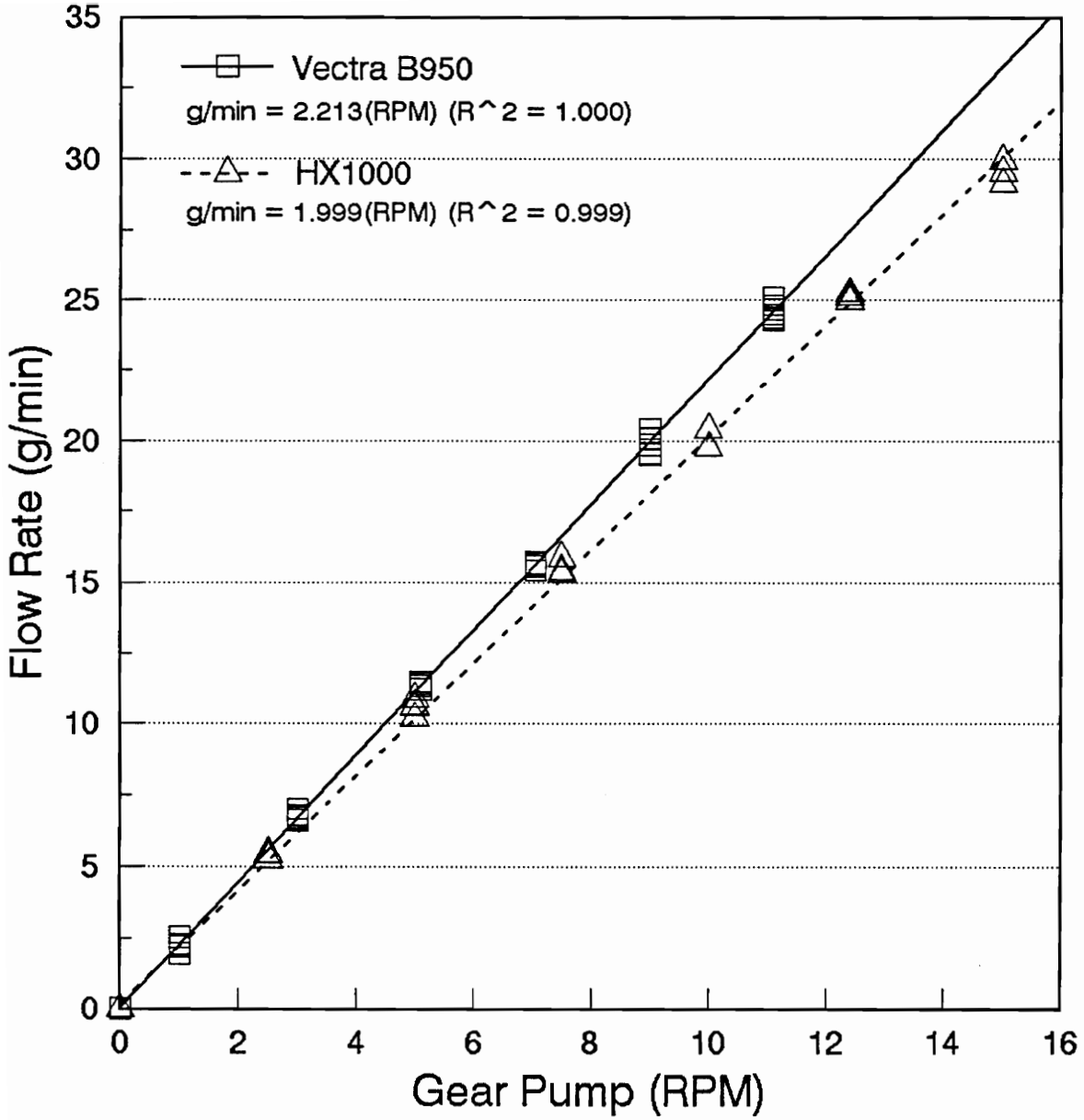

Figure 2-2: Flow rate versus gear pump RPM for HX1000 and Vectra B950.

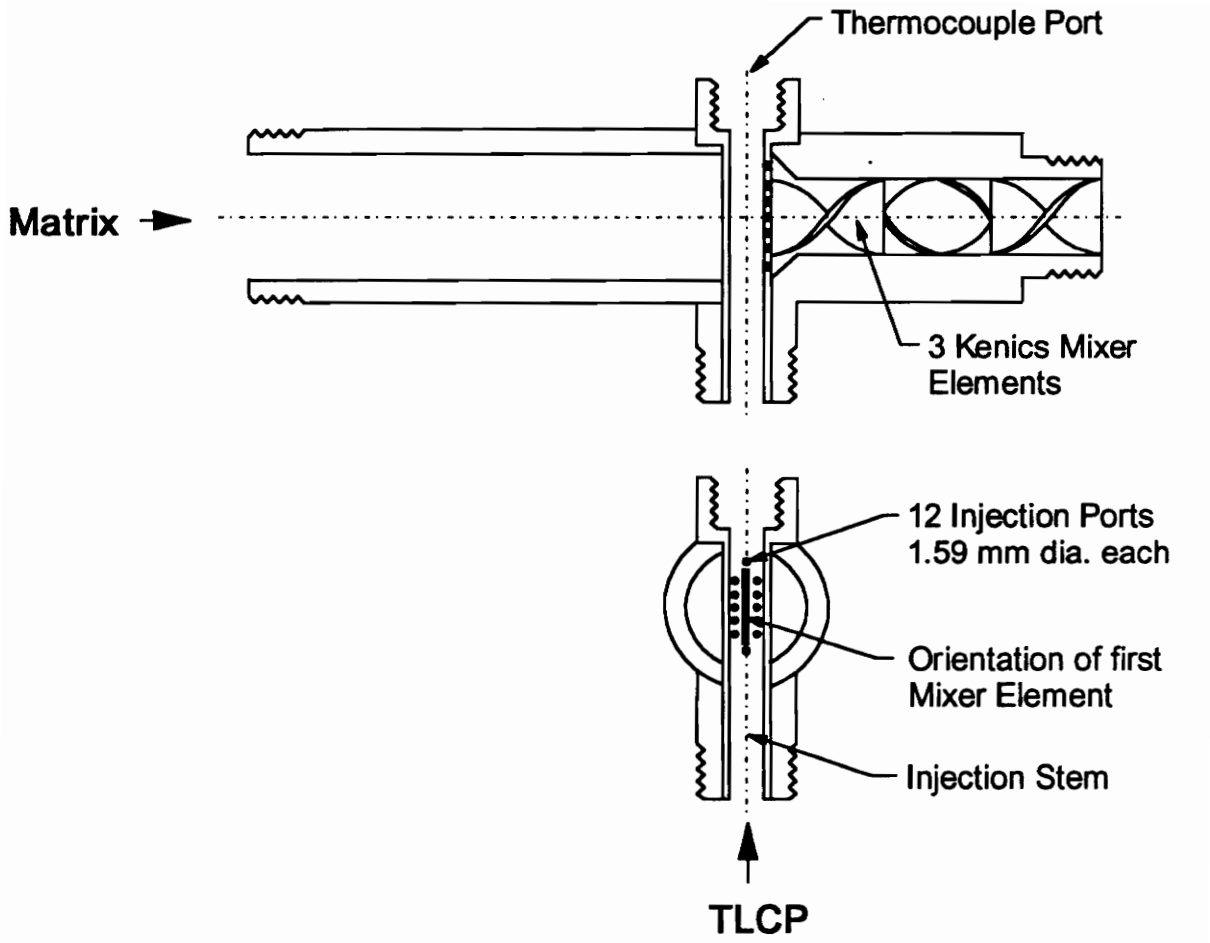

Figure 2-3: **A schematic of the multiple port phase distribution system.**

reduces from 0.75" to 0.5". The diameter reduction increases the extensional nature of the flow field as the blend enters the Kenics mixers. This reduces the likelihood possibility of the TLCP phase relaxing and forming droplets.

Melt temperature control was also important in the design of the phase distribution system. The thermocouple port at the end of the injection stem allows for direct measurement of the TLCP temperature before it enters the matrix material. The port is also useful in the cleaning of the injection stem during system maintenance. The melt temperature of the matrix material is monitored by using the themocouple port located in the matrix phase inlet.

Static Mixer Segments: The two types of mixers used in this study were the Kenics and Koch designs (Figs. 1-3 and 1-4). Various lengths of 0.5" Kenics mixers were permanently housed in appropriate sections of 0.5" nominal 304 stainless steel schedule 80 piping. Kenics mixer segments of 3, 3, 5, 6, and 8 elements were built for this study. The mixer segments are connected to each other through NPT pipe thread fittings and are constructed so they can be joined in only the proper alternating helical configuration. Several of the mixer segments include thermocouple ports so that the melt temperature can be measured. Two segments of four elements each of the Koch mixers were also fabricated. The Koch mixers are 1" in diameter and of cast stainless steel construction. They were housed in 1 1/4" nominal 304 stainless steel pipe bored to 1" inside diameter to accommodate the Koch mixer elements. Appropriate adapters were also manufactured so that these segments were compatible with the Kenics mixer segments and the dies used.

Extrusion Dies: The extrusion dies used in this study are shown in Fig. 2-4. They were designed so that they could be connected directly onto the mixer segments resulting in minimal time. A single 0.125" diameter capillary die (Fig. 2-4a) was predominantly used in this work. This design was shown to be less

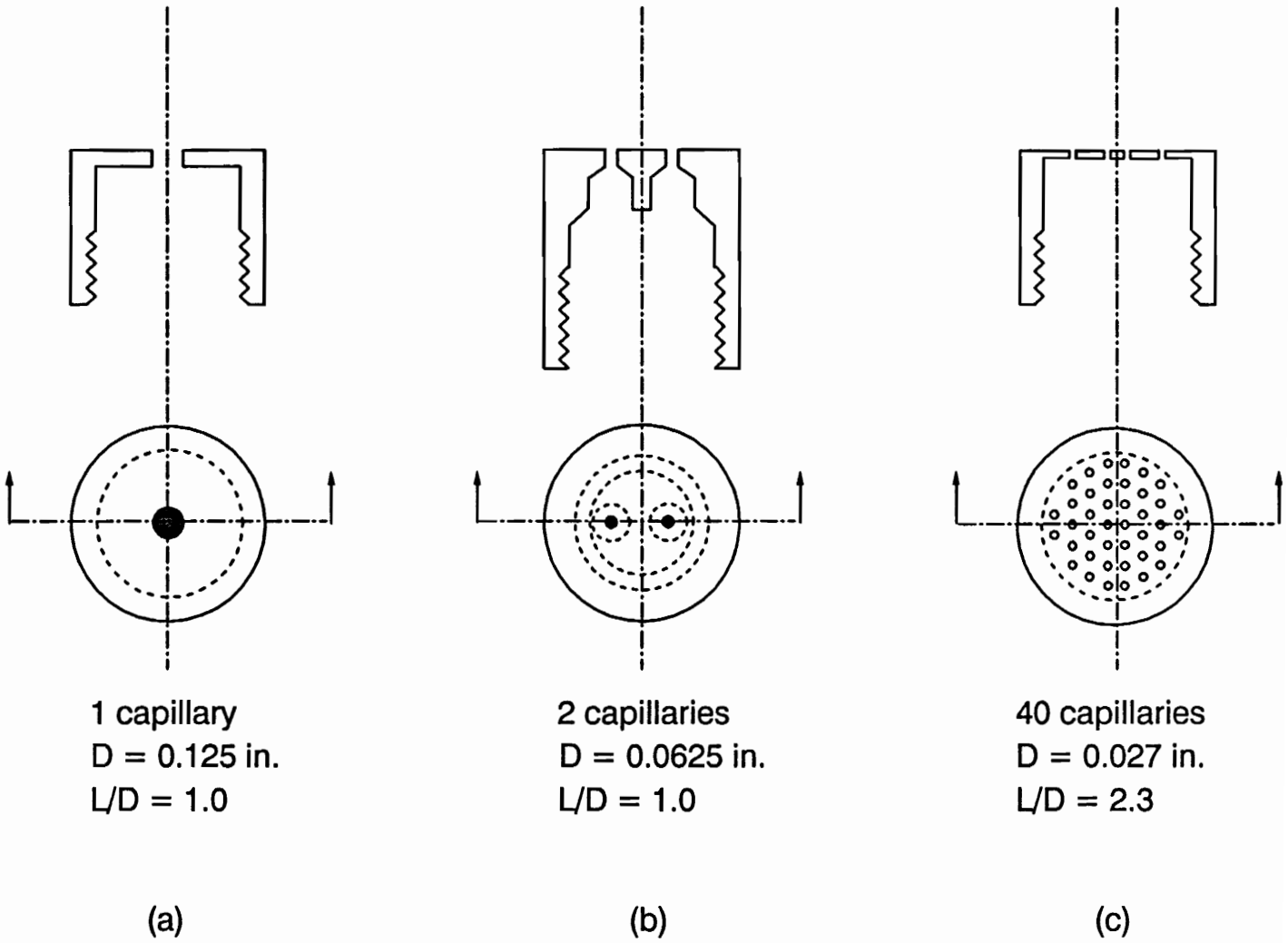

Figure 2-4: Extrusion dies used for the generation of in situ composite strands.

than optimal when used in combination with the Kenics static mixers. Specifically, the blend stream exiting the final Kenics mixer element is split and must reform a single stream before exiting the die. The continuity of the rejoined blend stream is controlled by molecular diffusion. The time scale for this process is quite long compared to the residence time of the material between the last mixer element and the die exit. In some cases, continuity of the reformed streams was not established and the extrudate strand split upon exiting the die. This prompted the design a double capillary die (Fig. 2-4b). This die is positioned so that each 0.0625" diameter capillary is fed by either side of the mixer element blade. The last die designed for this work consists of 40 capillaries of 0.027" diameter each (Fig. 2-4c). This die has also been designed with respect to the flow exiting a Kenics mixer. The hole pattern of this die is symmetric about a center line passing through the center of the die. During operation the center line of this die is aligned with the trailing edge of the last mixer element. This allows each die half to be fed from either side of the last mixer element. In both of the multiple hole dies, the requirement that the melt stream reforming after the final mixer element was eliminated.

The dies were designed to minimize the length to diameter ratio of the capillaries. The L/D ratio of the single and double capillary dies is equal to one while the L/D of the capillaries in the 40 was limited by machining constraints and is equal to 2.3. The L/D was kept as low as possible to minimize the residence time and the possibility of relaxation of the TLCP fibrils inside the capillary. The severe contraction of the blend stream in these dies leads to a strong extensional flow field as the molten polymer enters the capillary for final shaping. The extensional flow field is then continued as the blend is drawn upon exiting the die. Some of the extensional effect due to the contraction would be lost if the L/D of the capillaries were higher as the flow would be transformed into shearing flow in the long land region of the capillary.

Drawing Chimney: The drawing chimney consisted of various lengths of 2 1/2" and 4" nominal PVC schedule 40 pipe. The temperature inside the chimney is higher than ambient conditions due to the

insulating effect of the pipe. Polymer strands suspended in the chimney remained molten for a longer period of time due to the higher temperature. This allowed for the possibility of higher draw ratios. The addition of the chimney also insulated the strand from air currents in the room. Air currents caused premature freezing of the strand and intensified instabilities at high take-up velocities. The smaller diameter pipe was 2.5' long and located directly under the die. This was used to greatly reduce the amount of cooling that took place in the initial phase of strand drawing. The smaller pipe was followed by a 10' section of 4" pipe. This section was perforated by four 0.75" diameter holes located symmetrically about the pipe circumference and axially every 8". The temperature profile in this section of the drawing chimney was roughly controlled by covering sections of the perforations using adhesive tape. Many experiments were conducted using only a short drawing chimney or no chimney at all. The elaborate chimney system described above was only required when extremely high draw ratios were investigated

Water Bath: A 8" × 8" × 4' water bath was constructed to quench the molten polymer strand. The strand is guided in the water bath by a stationary 4" roller fixed at the front of the water bath. The strand is guided out of the water by two freely rotating 1 1/2" rollers. In some cases a second water bath was required to adequately cool the strand before being taken up by the variable speed nip rollers.

Drawing Rollers: Nip rollers capable of maintaining strand velocities from 0 to 320 m/min were used in this system. The bottom roll was coated by a layer of cork gasket material which increased the friction between the strand and the roller allowing for accurate transfer of the velocity of the rollers to the strand.

Temperature Control: The temperature of the material was monitored and controlled throughout the dual extrusion process. A significant improvement in the system consisted of the installation of thermocouples directly into the various molten polymer streams as described previously for several of the

individual components of the system. The placement of thermocouples in the original dual extrusion system allowed for the measurement and control of the temperature of the outside of the piping. This practice has been shown to greatly underestimate the actual temperature of the melt (in some cases by greater than 100°C).

Typical processing temperatures and settings are presented in Table 2-1. As indicated in the table, the temperature of the TLCP materials was higher within the extruder compared with the temperature just prior to mixing. The materials were subsequently cooled in the process piping and metering pump before being blended with the matrix material. These conditions were chosen to facilitate processing and to take advantage of the preheating phenomena described in Section 1.2.3. Blending was accomplished at the lowest possible temperature while maintaining a molten TLCP phase. The blend was then heated to a higher temperature just before being extruded from the die. This was required to maintain a uniform extrudate that could then be drawn. More detail concerning the individual heaters, control zones and controller set points is given in Appendix A.

2.3 Composites Formation

Composite materials were formed from drawn strands through several processing operations. The goal was to produced materials with more isotropic property enhancement as compared with in situ composite formation. The stands in this case were generated using the dual extrusion system and subsequently processed via compression molding, sheet extrusion and compression molding. The specific processing operations and conditions are discussed in the subsequent sections.

Table 2-1: Set point and melt temperatures for the dual extrusion process

Temps. in (^{0}C)	Extrusion				Blending		
	Feed Zone	Melting Zone	Metering Zone	Melt	Prior to Static Mixers	Static Mixer Section	Blend Exiting Die
PP	125	220	260	275	260	-	-
HX1000	250	310	330	350	310	270 to 280	290 to 300
Vectra B950	240	300	310	335	300	260 to 270	285 to 295

2.3.1 Compression Molding

Strands generated using the dual extrusion system were further processed through compression molding in a water cooled Carver Laboratory Press (model 2696). Compression molded plaques were produced in which the strands were aligned both uniaxially and randomly. For uniaxially aligned composite plaques approximately 11.5 g of in situ composite strands were cut to a length of 2.75". The strands were then placed in a 3" × 3" picture frame mold and aligned. The mold was then heated using plate heaters to a temperature of 190°C. The temperature of the strands in the mold was monitored using a 1/16" thermocouple temperature probe. The mold was then removed from the heating plates and pressed at an initial clamping pressure of 300 psig to form the final uniaxially aligned composite plaque. The pressure dropped as the sample cooled. The mold was allowed to continue to cool for approximately 5 minutes prior to the plaque being removed from the mold.

A second compression molding process was developed to produce long fiber plaques with isotropic mechanical properties. This process (Fig. 2-5) uses dual extrusion strands arranged in a random fashion. This process involves multiple compression molding steps. Initially, 4 g of strands are cut and randomly arranged in a 6" × 6" picture frame mold. The material is then heated to 220°C and pressed at an initial pressure of 700 psig. Three 6" × 6" plaques were made in this fashion. These thin plaques were then cut into four 3" × 3" laminates. The twelve total laminates were then placed in a 3" × 3" picture frame mold. The mold is then heated to 205°C and pressed under an initial pressure of 875 psig to form the final plaque which exhibits a random orientation of the reinforcing phase in the plane of the plaque.

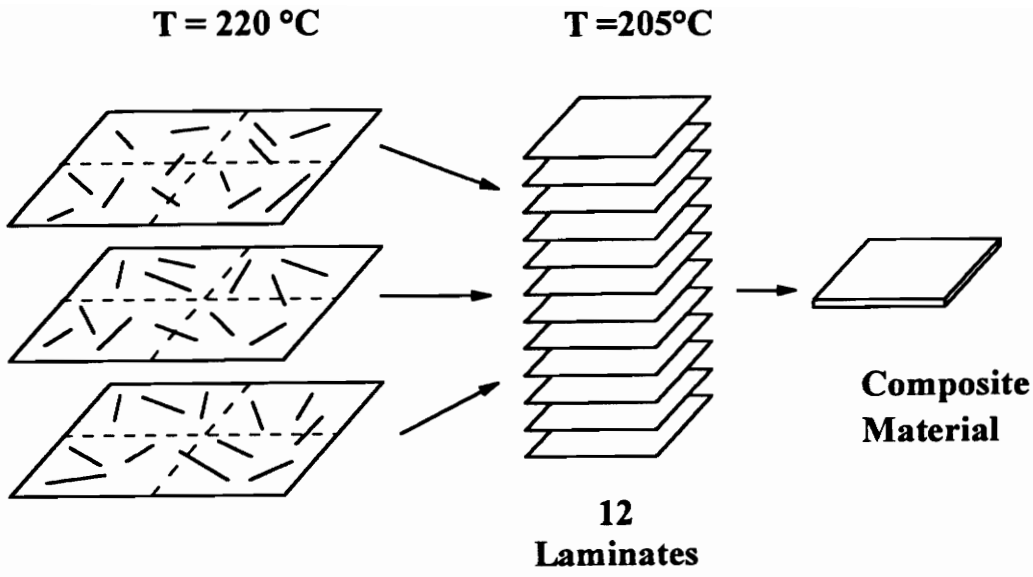

Figure 2-5: A schematic of the compression molding of randomly oriented blend strands.

2.3.2 Extrusion of Sheets

Pregenerated strand produced using the dual extrusion system strands were further processed through sheet extrusion to form short fiber reinforced composites. This was done using a 4" sheet die (coat hanger distribution system) with a gap thickness of 0.05". The die was attached to the 1" single screw extruder. The die was maintained at 190°C while the extruder heater zones were set at 125, 190, and 200°C for the feed, melting and metering sections, respectively. The melt temperature was maintained at approximately 210°C for these experiments. The sheets produced with this method had an irregular surface appearance. Therefore, it was necessary to compression mold the samples before mechanical property testing. The compression molding was done at approximately 180°C to minimize the alteration of the TLCP fibrils.

2.3.3 Injection Molding

Injection molding of dual extruder strands was carried out in an Arburg Allrounder injection molder (model 221-55-250). Strands were initially cut to lengths of approximately 0.25", then used as the feed for the molding process. Plaques were made in an end-gate mold with dimensions of 3" × 3" with mold thickness equal to 0.060". The injection molder is equipped with a total of 4 heating zones: 1-3 along the barrel of the molder and a fourth for the injection nozzle. Processing temperatures were the primary variables tested for this process.

2.4 Material Characterization

The rheology of the blend constituents and the tensile and flexural mechanical properties of the processed materials were characterized when feasible. The blend morphologies were also monitored at all locations throughout processing operations. The testing methods used to characterize the rheology of the polymers is described in Section 2.3.1. Mechanical property characterization is discussed in Section 2.3.2. Lastly, the methods used to study the morphology of the blends are discussed in Section 2.3.3

2.4.1 Rheology

The complex viscosity of HX1000 as a function of frequency and time was determined using a Rheometrics Mechanical Spectrometer (model RMS-800) with a cone and plate geometry (cone angle and diameter equal to 0.1 rad and 12.7 mm, respectively). Frequency sweeps were conducted following thermal histories similar to those occurring in the blending processes. Specifically, the thermal history of the TLCP in the dual extrusion process was modeled by first heating the HX1000 sample to 350°C and maintaining that temperature for 3 minutes. After the preheating step, the temperature of the sample was then dropped to 310°C (cooling time ≅ 2 minutes) and isothermal frequency sweeps were carried out. Similarly, the thermal history of the HX1000 experienced during single screw processing was replicated during rheological testing. In this case the HX1000 was heated directly from ambient conditions to 310°C where frequency sweeps were performed. Furthermore, time sweeps at a fixed frequency of 1 rad/sec were conducted at 350°C to determine if HX1000 was thermally stable at the processing temperatures.

Prior to the rheological tests described above strain sweeps were carried out on HX1000 at 350°C to determine subsequent testing conditions. Strain sweeps indicated that HX1000 is linearly viscoelastic

for strains up to 10 %. Therefore, all dynamic data were taken at 5 % strain which is well within the linear viscoelastic region.

Frequency sweeps were performed on neat PP with thermal histories similar to those seen for the matrix material during the initial stages of mixing. Specifically, the PP was heated from ambient conditions directly to 300 and 260°C which are the initial temperature of mixing in the dual and single screw blending processes, respectively. Again strain sweeps were conducted on the materials at the processing temperatures and indicated that they were linearly viscoelastic for strains up to 15%. Therefore, strain sweeps were conducted at strains of 10% which is within the viscoelastic regime.

2.4.2 Mechanical Properties

Mechanical properties of the materials produced in this study were assessed using an Instron mechanical tester model-4204. Materials were tested in accordance with the ASTM standards wherever possible although some modifications to the tests were needed. Tensile properties of strands were assessed using a single-strand method (ASTM D 3376-75). The strands were placed directly in the grips with a gauge length of 148 mm. A constant crosshead speed of 0.5 mm/min was maintained for most tests. Neat PP and 5 wt. % in situ composite strands were tested using a crosshead speed of 10 mm/min to facilitate sample failure in the time prescribed by the ASTM standard (~1 minute).

The cross section of all strands was typically elliptical. Therefore, the cross sectional areas of the strands were calculated using the largest and smallest diameters of the strands and equation for the area of an ellipse

$$(A_s = \pi/4\, D_1 D_2) \qquad (1)$$

where A_s is the cross sectional area of the strand and D_1 and D_2 are the major and minor diameters of the strand. This area was in turn used to calculate the physical properties of the strands. The draw down ratio was determined by taking into account the elliptical nature of the cross section. The draw ratio was calculated using

$$\lambda = {(D_d)^2}/{D_1 D_2} \qquad (2)$$

where λ is the draw down ratio and D_d is the diameter of the die. For samples that failed due to brittle fracture, the diameters were assessed at the point of break after the sample had been tested. If the tested strand exhibited a yield point, the diameters were determined from the middle of the test specimen before testing.

The reported data relating the mechanical properties of strands to the draw ratio were obtained using a global averaging technique. The reported properties are the average of properties over a specific range of draw ratios. The number of data averaged for each reported value vary depending on the number of samples tested in the specific range of draw ratios. The number of sample data averaged for each reported property value varies from 2 to 6. The total number of strands tested for each set of mechanical property versus draw ratio data range from 50 to 80.

The tensile and flexural properties of the plaques generated from the dual extrusion strands were also evaluated. The plaques (injection molded, compression molded strands or compression molded sheets) were cut into 8 mm wide strips and sanded to minimize cutting marks. The tensile properties of these plaques were evaluated using the Instron testing machine and an extensiometer (Instron model 2630-25). The crosshead speed was maintained at 1.27 mm/min for all samples tested (ASTM D-638M-87b). Reported values are the average of at least 6 samples. The strips were also tested for flexural properties using a three point bending test (ASTM D 790M-86). The crosshead speed was determined by the sample thickness in accordance with the ASTM guidelines.

2.4.3 Morphology

Blend morphology was characterized at various points in the extrusion processes. The samples were prepared by removing the die and various mixer segments and allowing the extrudate to fall directly into a quenching water bath. The rods were subsequently cut using a band saw and the end polished with various grits of sand paper. They were then polished using 600 grit silicon dioxide polishing paper. The polished ends were glued onto microscope slides using a cyanoacrylate adhesive and allowed to cure for at least 10 hours. The samples were then cut parallel to the slide surface using a band saw leaving a 0.125" cross section of the extrudate adhered to the slide. The top surface of the cross sections were then sanded and polished to a final thickness of less than 0.03". Finally, the extrudate was partially back lit and photographed using a Olympus 35 mm camera with a wide angle lens.

When higher resolution was desired (strand and plaque samples), the morphology was observed using optical and scanning electron microscopy. Microtomed slices of blend materials were observed using a Zeiss Polarizing light microscope. Optical images were enhanced by using immersion oil ($n_D = 1.5$). Scanning electron microscopy was done using a Stereoscan-S200 with an accelerating voltage of 15kV. Samples were prepared by cryogenic fracture after immersion in liquid nitrogen for at least 5 minutes. The fractured samples were mounted on aluminum stubs and coated with a layer of gold using a SPI Sputter Coater to enhance conductivity.

This concludes the description of the materials, equipment and characterization techniques used in this research. Special consideration was given to the dual extruder system (improved as a result of this study) and the random compression molding process due to their importance in the realization of the objectives of this research. The process property relationships for the materials of interest to this study are described in the following chapters. Through the subsequent analysis, the improvements in properties that have resulted from the system modifications described in this chapter become evident.

2.5 References (Chapters 1 and 2)

1. G. W. Calundann and M. Jaffe in, *"Proceeding of the Robert A. Welch Conferences on Chemical Research, XXVI. Chap. VII, Synthetic Polymers"*, Houston, Texas, 247 (1982).
2. S. Chandrachekhr, *"Liquid Crystals"*, Cambridge University Press, Cambridge (1977).
3. F. P. La Mantia, *"Thermotropic Liquid Crystalline Polymer Blends"*, Technomic, PA (1993).
4. F. N. Cogswell in, "Recent Advances in Liquid Crystalline Polymers", L. L. Chapoy (Ed), Elsevire, London (1985).
5. M. K. Cox, *Mol. Cryst. Liq. Cryst.*, **153**, 415 (1987).
6. R. A. Weiss, W. Huh and L. Nicolais, *Polym. Eng. and Sci.*, **27** 684 (1987).
7. G. Kiss, *Polym. Eng. and Sci.*, **29** 410 (1987).
8. K. G. Blizard, C. Federici, O. Federico and L. L. Chapoy, *Polym. Eng. and Sci.*, **30** 1442 (1990).
9. M. V. Tsebrenko, *Inten. J. Polymeric Mater.*, **10** 83 (1983).
10. M. V. Tsebrenko, A. V. Yudin, T. I. Abazova and G. V. Vinogradov, *Polymer*, **17** 831 (1976).
11. D. G. Baird and A. M. Sukhadia, U. S. Patent No. 5,225,488 (1993).
12. A. M. Sukhadia, Ph.D. Thesis, Virginia Polytechnic Institute and State University (1991).
13. A. M. Sukhadia, A. Datta and D. G. Baird, *Intern. Polym. Process.*, **7** 218 (1992).
14. D. Beery , S. Kenig, and A. Siegmann, *Polym. Eng. and Sci.*, **33** 1548 (1993).
15. K. G. Blizard, D. G. Baird, *Poly. Eng. Sci.*, **27** 653 (1987).
16. G. Crevecoeour, Ph.D. Thesis. Katholiede Universiteit Leuven (1991).
17. A. I. Isayev, Y. Holdengreber, R. Vismanathan and S. Akhtar, SPE Antec '92 Prep., 2654 (1992).
18. D. Dutta, R. A. Weiss and D. Kristal, *Polym. Eng. and Sci.*, **33** 838 (1993).
19. B. R. Bassett and A. F. Yee, *Polym. Composites*, **11** 10 (1990).
20. A. A. Handlos and D. G. Baird, SPE Antec '93 Prep., 1170 (1993).
21. A. A. Handlos, E. A. Sabol and D. G. Baird, SPE Antec '94 Prep., 1594 (1994).
22. A. A. Handlos, Ph.D. Thesis, Virginia Polytechnic Institute and State University (1994).
23. C. E. Knox in *Handbook of Composites.* ed. G. Lubin, Van Nostrand Reinhold Co., New York (1982).
24. A. A. Coller and D. W. Clegg eds., *Mechanical Properties of Reinforced Thermoplastics.* Elevier, London (1986).
25. C. Ruawendaal in *Mixing in Polymer Processing,* C. Ruawendaal Ed. Marcel Dekker, Inc., New York (1991).

26. J. J. Elmendorp in *Mixing in Polymer Processing,* C. Ruawendaal Ed. Marcel Dekker, Inc., New York (1991).
27. Z. Tadmor and C. G. Gogos, *Principles of Polymer Processing,* Wiley Int. New York (1976).
28. S. Wu, Polym. Eng. and Sci., 27 335 (1987).
29. R. G. Cox, J. Fluid Mech., **37** 601 (1969).
30. A. I. Isayev and M. Modic, *Polym. Composites,* **8** 158 (1987).
31. P. T. Allocca, *Fiber Producer,* April (1983).
32. S. J. Chen and A. R MacDonald, *Chem. Eng.,* March, 105 (1973).
33. C. D. Grace, *Chem. and Proc. Eng.,* July 57 (1971).
34. T. Tung , Ph.D. Thesis, University of Massachusetts (1976).
35. J. Arimond, M.S. Thesis, M.I.T. (1983).
36. M. Mutsakis, F. A. Streiff and G. Schneider, *Chem. Eng. Prog.,* July, 42 (1986).
37. H. J. O'Donnell and D. G. Baird, Presentation, at the SPE Antech Tech. Conference March (1993).
38. S. S. Bafna, T. Sun, J. P. De Souza and D. G. Baird, *Polymer,* **34** 708 (1993).
39. R. B. Bird, R. C. Armstrong, and O, Hassager, *Dynamics of Polymeric Liquids, Vol.1, Fluid Mechanics,* John Wiley & Sons, Inc., New York (1987).
40. M. R. Nobile, E. Amendola, L. Nicolais, D. Acierno and C. Carfagna, *Polym. Eng. and Sci.,* **29** 244 (1989).
41. D. Dutta, H. Fruitwala, A. Kohli and R. A. Weiss, Polym. Eng. and Sci., 30 1005 (1990).
42. Q. Lin, J. Jho and A. L. Yee, *Polym. Eng. and Sci.,* **33** 789 (1993).
43. W. C. Lee, A. T. Dibenedetto and J. M. Gromek, *Polym. Eng. and Sci.,* **33** 156 (1993).
44. S. Menhta and B. L. Deopura, *Polym. Eng. and Sci.,* **33** 931 (1993).
45. M. Kyotani, A. Kaito and K. Nakayama, *Polymer,* **33** 4756 (1992).
46. D. G. Baird and T. Sun in, Liquid Crystalline Polymers. R. A. Weiss and C. K. Ober (Eds.), ACS Symposium Series (1990).
47. A. M. Sukhadia, D. Done and D. G. Baird, *Polym. Eng. and Sci.,* **30** 519 (1990).
48. T. Chung, *Plast. Eng.,* Oct., p. 39 (1987).
49. K. F. Wissburn, G. Kiss and F. N. Cogswell, *Chem. Eng. Comm.,* **53** 149 (1987).
50. S. Drappel, W. A. Yeung, P. R. Sundrarajan and A. Rudin, *J. Rheol.,* **37** 89 (1993).
51. K. F.Wissburn, *Brit. Polym. J.,* December 163 (1980).
52. D. Done and D. G. Baird, *Polym. Eng. and Sci.,* **27** 816 (1987).
53. D. Done and D. G. Baird, *Polym. Eng. and Sci.,* **30** 989 (1990).
54. A. A. Handolos and D. G. Baird, submitted to: *Macromolecular Reviews* (1994).
55. J. C. Halpin and J. L . Kardos, *Polym. Eng. and Sci.,* **16** 344 (1976).

56. H. W. Rayson, G. C. McGrath in, *Mechanical Properties of Reinforced Thermoplastics,* A. A. Coller and D. W. Clegg (Eds.) Elevier, London (1986).
57. P. K Mallick, *Fiber Reinforced Composites.* Marcel Dekker, New York (1988).
58. H. J. O'Donnell, A. Datta and D. G. Baird, SPE Antec '93 Prep., 1170 (1993).
59. A. Datta, H. H. Chen and D. G. Baird, *Polymer,* **34** 759 (1993).
60. J. Seppala, M. Heino and C. Kapanen, *J. Appl. Polym. Sci.,* **44** 1051 (1992).
61. M. Kyotani, A. Kaito and Nakayama, *Polymer,* **33** 4756 (1992).
62. Product Literature from Hoechst Celanese.
63. H. J. O'Donnell, Ph.D. Thesis, Virginia Polytechnic Institute and State University (1994).
64. Supplier Data Himont Co.
65. A. Kohli, N. Chung and R. A. Weiss, *Polym. Eng. and Sci.,* **29** (1989).

3.0 The Development of Morphology

Preface

This chapter is focussed on the second objective of this work. Specifically, the development of the fibrillar TLCP morphology in the dual extrusion process is discussed and compared to the morphology developed via blending in a single screw extruder. Furthermore, the variations of the dual extrusion system are presented which investigate the effects of the multiple injection port phase distribution system and variations of the static mixer designs (objective one). The chapter organized as a manuscript which will be submitted to the journal *International Polymer Processing* for subsequent publication.

The Development of Morphology in Blends of a Thermotropic Liquid Crystalline Polymer and Polypropylene: A Comparison of Mixing History

E. A. Sabol and D.G. Baird

The Department of Chemical Engineering
Polymeric Materials and Interfaces Laboratory
Virginia Polytechnic Institute and State University
Blacksburg, VA 21041 U.S.A.

(ASTRACT)

This paper is focused on the development of morphology in blends of a thermotropic liquid crystalline polymer (TLCP), HX1000, and PP as a function of the mixing history. The purpose of this work was to determine if a dual extrusion process (DEP) could be used to generate a fibrillar TLCP morphology in drawn strands where blending in a single screw extruder could not. The DEP consisted of two single screw extruders within which the TLCP and matrix material were plasticated separately. The two continuous polymer streams were joined in a phase distribution system and then mixed in a series of static mixing elements including both Kenics and Koch designs. Specifically, a low concentration of TLCP (5.0 wt.%) was used to minimize the effect of coalescence in the formation of TLCP fibrils. It was found that the blending in a single extruder resulted in large axial concentration variations and a poor morphology for mechanical property enhancement. The addition of static mixing elements to the single extruder resulted in droplets of TLCP that provided little reinforcement to the matrix material. In contrast blends produced in the DEP, with an appropriate mixing configuration, exhibited an axially continuous TLCP morphology which developed at the onset of mixing in the phase distribution system and was subsequently refined as the melt passed though the static mixing elements. The axially continuous morphology seen at the entrance of the die was maintained and further developed as the blend contracted into the capillary die and was drawn as a strand. The fibrillar TLCP morphology resulted in drawn strands with tensile properties significantly improved over strands produced through blending in a single screw extruder.

3.1 Introduction

The blending of thermotropic liquid crystalline polymers (TLCPs) with thermoplastics has been the focus of intense academic and industrial interest [1 to 3]. Much of this interest stems from the unique TLCP morphology that can develop in these blends. Specifically, under suitable processing conditions the TLCP phase can form oriented fibrils which act to reinforce the matrix. Thus, the blending of a TLCP with a thermoplastic might provide for an effective method of utilizing their high strength and stiffness along with incorporating some of their other desirable properties (i.e., excellent barrier properties, low coefficient of thermal expansion, low water absorption, and high chemical resistance) into the thermoplastic matrix [1, 4, 5]. Their cost, however, is comparatively high indicating that the development of an effective reinforcing morphology with low concentrations of TLCP is highly desirable.

The best morphology of the TLCP phase for mechanical property enhancement is well distributed high aspect ratio (ratio of length to diameter) oriented fibrils. High molecular orientation of the TLCP phase is required to generate the highest possible properties of the TLCP fibrils and high aspect ratio promotes the most effective transfer of stress from the matrix material to the reinforcing fibrils [6, 7]. For example, the Halpin-Tsai equation, used in the theory of fiber reinforced composites, indicates that a reinforcing phase aspect ratio of 100 is required for optimal modulus enhancement of the resulting composite [8]. The effect of increased aspect ratio of the reinforcing phase is less easily correlated with the tensile strength of the composite due to the strength being further dependent on the adhesion of the TLCP and matrix material, but the optimal enhancement is seen when the fiber length spans the width of the composite structure [9].

The mechanism by which high aspect ratio fibrils are formed in blends of TLCPs and thermoplastics is highly complex. Factors such as hydrodynamic forces, rheological properties of the blend components, interfacial forces between phases, degree of mixing and TLCP concentration all play a role in the development and final form of the reinforcing phase. Many of these factors have been

extensively studied with respect to the development of the reinforcing TLCP fibrils in the resultant in situ composite [1, 2, 10 to 15] and have resulted in several contradictory findings. Specifically, the effects that TLCP concentration and mixing history have on the development of morphology have not been clearly established.

The role of mixing history in the development of morphology in conventional in situ composite processes is associated with the dispersion of the TLCP phase within the matrix material prior to the formation of the reinforcing fibrils. The mixing may only take place within the processing equipment responsible for the formation of the final in situ composite part (for example in the screw of an injection molder) or in some cases "preblending" is used in which the components are mixed in an entirely independent process which utilizes a single or twin screw extruder or an internal mixer. In these processes the actual formation of the reinforcing fibrils is the result of the coalescence and elongational deformation of the droplets during the final processing steps (i.e., strand or sheet formation, injection molding etc.) [2, 16 to 18]. Studies which have investigated the effects of mixing history on the morphology and resultant physical properties of in situ composites have focused mainly on variations in the preblending method [3, 13, 19, 20].

The results of investigations associated with preblending of TLCPs and thermoplastics prior to the final processing operation have been somewhat contradictory. For example, Kiss [3] investigated operations such as batch mixers and single and twin screw extruders to premix a wide variety of TLCP thermoplastic pairs prior to injection molding. This study indicated that there were no measured morphological or property differences in the resultant injection molded parts as a result of the various preblending steps. Furthermore, Kiss concluded that the mixing achieved during the injection molding process was adequate and that preblending step was not necessary. In contrast, Isayev and Modic [13] found that the preblending method did affect the properties of injection molded parts. Specifically, they investigated a blend of polycarbonate (PC) and 2.5 wt.% of a thermotropic liquid crystalline copolyester based on hydroxybenzoic acid (HBA) and 2-hydroxy 6-napthoic acid (HNA) and found that preblending

using a single screw extruder with static mixer produced a more fibrillar morphology and higher mechanical properties compared with preblending in a single screw alone. Another example of contradictory results is illustrated by investigations where multiple passes through a single or twin screw extruder were used as a method to vary the mixing history of a blend prior to injection molding. In some cases, multiple passes through an extruder were shown to improve physical properties of the resulting injection molded materials [19] while in others there was no clear increase as a function of the increased number of passes through the mixing device [20].

In addition to mixing history, the development of a fibrillar TLCP morphology is strongly dependent on the concentration of the TLCP. Specifically, for in situ composites processed through conventional methods there seems to exist a range of compositions in which fibrils can be formed [13, 14, 21 to 24]. For example, Chung [21] found that the morphology of blend rods of nylon 12 and a TLCP changed from a droplet morphology to fibrillar structures as the TLCP concentration was increased. In another study, Blizard and Baird [22] determined that fibrils were present in 30 wt.% TLCP blends with PC while droplets were found at 10 wt.% TLCP. A recent study by Beery et al. [16] showed that blends of a 5 wt.% TLCP in PC produced an elongated droplet morphology which changed from spherical or elongated droplets to continuous fibrils for compositions in the range of 10 to 20 % TLCP. In contrast, Isayev and Modic [13] reported fibril formation only at concentrations of less than 10 % TLCP with droplets at higher concentrations. However, the general finding has been that at low concentrations, typically less than 15 wt.% TLCP, droplets are formed whereas at higher compositions a fibrillar TLCP morphology is observed.

The concentration dependence of morphology is in agreement with the generally proposed mechanism for the development of the fibrous TLCP structure in conventional in situ composite processes. Specifically, at low TLCP concentrations the phase size of the TLCP droplets produced in the melt blending step of the in situ composite formation process can be quite small. Therefore, the viscous stresses during processing can not overcome interfacial forces and the TLCP droplets do not effectively

form fibrils. Additionally, the occurrence of coalescence which would tend to form locally larger droplet sizes during fibril formation is curtailed due the low concentration of dispersed droplets. Thus, the formation of TLCP fibrils in conventional in situ composites is limited because the mixing process could generate TLCP droplets of a size which can not be subsequently deformed into reinforcing fibrils.

In contrast with conventional in situ composite processes, a novel dual extrusion process (DEP) has been developed in which the TLCP fibrils are not generated from dispersed droplets but are formed in the actual melt blending process. The DEP, shown schematically in Fig. 2-1, was originally developed and patented by Baird and Sukhadia [25 to 27] and subsequently improved by Sabol [28]. In this process the TLCP and matrix material are plasticated in separate extruders before mixing in a series of static mixing elements. Initial investigations of this processing method showed that the TLCP phase in in situ composite strands exhibited a wholly fibrillar morphology whereas strands produced using single screw extrusion exhibited a "skin-core" morphology which is characterized by high aspect ratio fibrils near the skin and low aspect ratio droplets in the core. The consequence of the wholly fibrillar morphology in the strands produced using the dual extrusion system was improved mechanical properties. Specifically, Sukhadia et al. [26] investigated strands of 30 wt.% of a TLCP composed of HBA and HNA, commercially known as Vectra A, in a matrix of poly(ethylene terephthalate) produced using both the DEP and blending in a single screw extruder. They found that under similar processing conditions (draw ratio equal to 40), the tensile modulus of strands produced using the DEP was 19 GPa while the modulus of strands produced through blending in a single extruder was 13 GPa.

The unique design of the dual extrusion system provides other advantages over more conventional methods of in situ composite formation in addition to the development of an axially continuous TLCP morphology [26 to 28]. Polymer pairs with no overlap of processing temperatures can be blended with limited degradation of the matrix phase. This is important because TLCPs exhibiting the highest mechanical properties typically have processing temperatures in excess of the thermal processing range of many widely used thermoplastics such as polyethylene and polypropylene. Furthermore,

independent thermal histories can be imparted to the polymer streams before the melt blending process. This is significant in that it can provide a method of controlling the viscosity of the blend constituents during mixing which has been found to play a critical role in the development of a fibrillar dispersed phase morphology [2, 29].

Initial studies of Sukhadia et al. [26] have shown that the dual extrusion system could be used to generate significant mechanical reinforcement in a blend of only 4 wt.% TLCP. However, the morphology and properties of the low concentration strands were not compared with those of strands produced using a conventional melt blending processes, and therefore, the development of reinforcement could not be completely attributed to the mixing history. In this paper, the objective is to determine if the dual extrusion process can be used to generate a fibrillar TLCP morphology where blending in a single screw extruder can not. Specifically, a low TLCP concentration is investigated so that the effects of mixing history on the resulting TLCP morphology can be investigated in the regime where coalescence is minimized. To achieve the objective, the TLCP morphology is monitored in both the dual extrusion process and during blending in a single screw extruder and is compared with the resulting morphology and physical properties of the drawn strands produced from these processes.

3.2 Experimental Procedure

3.2.1 Materials

The thermotropic liquid crystalline polymer (TLCP) used was HX1000 supplied by the DuPont company. HX1000 is an amorphous copolyester based on terephthalic acid, hydroquinone, and two other proprietary hydroquinone derivatives [1]. It has a typical processing temperature in the range of 290 to

365°C and has a room temperature density of 1.25 g/cm^3. HX1000 was dried in a convection oven at 115°C for at least 10 hours prior to processing.

The polypropylene (PP) used as the matrix material was Profax-6823 purchased from the Himont Company. It has a melt flow index of 0.8, melting temperature of 161°C, and a room temperature density of 0.902 g/cm^3. The thermal stability of the viscosity of this material has been reported elsewhere [27]. Of importance to this work, isothermal time sweeps of the PP have shown that the complex viscosity is relatively stable for temperatures up to and including 290°C. However, at temperatures higher than 300°C the complex viscosity rapidly decreases with time indicating that thermal degradation of the polymer is occurring.

The blend of HX1000 and PP was chosen for these experiments because it represents a blend in which the processing temperatures of the constituents do not readily overlap. However, the processing temperature difference does not totally inhibit the blending of these polymers in the same extruder. Thus, the use of this polymer pair allows us to assess the full potential benefits of the dual extrusion process while still allowing a comparison with blending in a single extruder.

3.2.2 Blend Processing

Blends of HX1000 and PP were produced using several variations of the dual extrusion system in order to investigate the development of morphology in this system. The DEP (Fig. 2-1) consists of two single screw extruders (Killion model KL-100, diameter 24.5 mm with L/D=24) in which the matrix material and TLCP are plasticated separately. The continuous TLCP melt stream is metered by a Zenith 1.725 cc/rev gear pump and joined with the matrix material in a phase distribution system. Two variations of injection systems were used to introduce the TLCP into the matrix stream. The first injection system consisted of a simple "T" with all ports of a diameter of 12.7 mm and a multiple port injection

system specially designed for this application (Fig. 2-3). It introduces the TLCP into the matrix material through twelve 1.59 mm diameter injection ports placed symmetrically in front of the first in a series of three 12.7 mm diameter Kenics mixer elements which are an integral part of the multiple injection port system. Additional segments of Kenics static mixing elements (Fig. 1-3) or 25.4 mm diameter Koch mixing elements (Fig. 1-4) were placed directly after the phase distribution system to increase distributive mixing of the HX1000 in the PP matrix. The blend material was then extruded through a 3.175 mm capillary die (L/D =1) to form a strand. The strand was continuously drawn in a vertical 50 cm long by 60 mm diameter perforated drawing chimney which increased the temperature of the drawing environment and reduced premature breaking of the strand due to air currents inherently in the processing area. The strand was then quenched in a water bath to set in the resultant morphology and TLCP orientation.

To monitor the development of the morphology prior to the die, extruded rods (diameter $\cong$ 13 mm) of 5.0, 30 and 60 wt.% HX1000 were generated using the DEP with the die and drawing assembly removed. For these experiments, the strand die was replaced with a section of pipe 12.7 mm in diameter and 40 mm in length which was introduced to reform a continuous extrudate rod from the blend material exiting the final static mixing element. The molten rod was extruded directly into a quench water bath. Kenics mixer segments containing 3, 5, and 8 elements and two segments of 4 Koch mixing elements were used in various combinations. In some cases irregularly shaped cross sections were observed which were attributed to the rods having a relatively large diameter which caused them to solidify in a non-uniform manner.

In order to investigate the development of morphology when coalescence was not significant, strands with low TLCP concentration were produced with various mixing histories. Specifically, extruded rods and drawn strands (diameter < 3.2 mm) of 5.0 wt.% HX1000 were produced using both single and dual extrusion using various static mixer configurations. The mixer configuration used in the DEP consisted of the multiple port injection nozzle and 15 additional Kenics mixer elements and 4 or 8 Koch

mixing element. Single screw extrusion mixing was performed using dry blended polymer pellets and a Killion extruder with a diameter of 25.4 mm. Rods and strands generated using single screw extrusion were produced with and without 18 Kenics mixing elements.

The total flow rate and composition of the blend materials were closely monitored and maintained during the DEP. The composition of the blend was determined by first setting the gear pump rotational speed which maintained the constant TLCP flow rate needed for a specific concentration. The rotational speed of the gear pump was determined from flow rate versus pump RPM data determined prior to the blending experiments. Specifically, it was found for the same temperature and pump inlet pressure (2500 psig) that the flow rate of TLCP, Q in g/min, was given by, $Q = 1.9975 \times$ (gear pump RPM), where the correlation coefficient, r^2, was found to be 0.9989 [33]. The rotational speed of the screw in the matrix extruder was then adjusted to maintain a constant total blend flow rate of 40.0 ± 0.5 g/min. Total flow rate of the blend material for extruded strands was measured immediately before and after the collection of strand materials (strand collection typically took less than 2.5 minutes) to insure the composition did not change during processing. Variations in PP flow resulted in a maximum composition variation of only 1% for the blend strands.

The processing temperatures used for the blending methods are presented in Table 1. The temperature of the HX1000 in the extruder of the DEP was maintained at 350°C and subsequently reduced to 310°C prior to injection into the PP stream. The melt temperature during mixing in the single extruder was maintained at less than 310°C in order to minimize the degradation of the PP but still allow for the plastication of the TLCP [27]. In both single and dual extrusion processes the temperature in the mixing section (if present) was maintained as low as possible while still maintaining the TLCP as a molten phase. The temperature of the blend was then increased in the die section to facilitate subsequent drawing of the extruded strand.

Table 1: Set points and melt temperatures for the mixing of HX1000 and PP in both single and dual extrusion processes.

Temperatures in (°C)		Extrusion				Static Mixer Section		
		Feed Zone	Melting Zone	Pumping Zone	Melt	Prior to Static Mixers	Static Mixer Section	Blend Exiting Die
Dual Extrusion Process	PP	125	220	260	275	260	270 to 280	290 to 300
	HX1000	250	310	330	350	310		
Single Extruder Blending	5.0 wt.% HX1000	125	180	295	300 to 310	300 to 310	270 to 280	290 to 300

3.2.3 Rheology

The complex viscosity of HX1000 as a function of frequency and time was determined using a Rheometrics Mechanical Spectrometer (model RMS-800) with a cone and plate geometry (cone angle and diameter equal to 0.1 rad and 12.7 mm, respectively). Frequency sweeps were conducted following thermal histories similar to those occurring in the blending processes. Specifically, the thermal history of the TLCP in the DEP was modeled by first heating the HX1000 sample to 350°C and maintaining that temperature for 3 minutes. After the preheating step, the temperature of the sample was then dropped to 310°C (cooling time ≅ 2 minutes) and isothermal frequency sweeps were carried out. Similarly, the thermal history of the HX1000 experienced during single screw processing was replicated during rheological testing. In this case the HX1000 was heated directly from ambient conditions to 310°C where frequency sweeps were performed. Furthermore, time sweeps at a fixed frequency of 1 rad/sec were conducted at 350°C to determine if HX1000 was thermally stable at the processing temperatures.

Prior to the rheological tests described above strain sweeps were carried out on HX1000 at 350°C to determine subsequent testing conditions. Strain sweeps indicated that HX1000 is linearly viscoelastic for strains up to 10 %. Therefore, all dynamic data were taken at 5 % strain which is well within the linear viscoelastic region.

Frequency sweeps were performed on neat PP with thermal histories similar to those seen for the matrix material during the initial stages of mixing. Specifically, the PP was heated from ambient conditions directly to 300 and 260°C which are the initial temperature of mixing in the dual and single screw blending processes, respectively. Again strain sweeps were conducted on the materials at the processing temperatures and indicated that they were linearly viscoelastic for strains up to 15%. Therefore, strain sweeps were conducted at strains of 10% which is within the viscoelastic regime.

3.2.4 Mechanical Properties

The tensile modulus and strength of individual strands were measured using an Instron mechanical tester (model-4204). The initial gap length of 148 mm was used with a crosshead speed of 10 mm/min with strain calculated by displacement. The cross sections of the strands were typically elliptical. Therefore, the cross sectional area of the strands and consequently the draw ratios (ratio of the cross sectional area of the die to that of the strand) were determined using the major diameter, D_1, and minor diameter, D_2, of the strand and the equation for the area of an ellipse ($A = \pi/4 D_1 D_2$). The reported tensile properties in this paper are the average of several tests at a single take-up velocity. The standard deviations of the reported tensile properties were on average 4% and 5 % of the average tensile modulus and strength, respectively.

3.2.5 Morphology

Rods (diameter ≅ 13 mm) were prepared for morphological observations by initially cutting the rod either parallel or perpendicular to the rod axis using a band saw. The cut surface was then polished with various grits of silicon dioxide sand paper. The polished surface was then glued onto a microscope slide using a cyanoacrylate adhesive and allowed to cure for at least 10 hours. The sample was then cut parallel to the slide surface using a band saw leaving approximately a 3 mm cross section of the rod adhered to the slide. The newly cut surface was then sanded and polished to a final thickness of less than 0.5 mm. Finally, the rod sample was partially back lit and photographed using an Olympus 35 mm camera with a macro-lens (focal length of 55 mm).

To reveal the morphology of extruded rods and drawn strands on a smaller scale, optical and scanning electron microscopy was used. Thin microtomed sections of rods (diameter ≅ 13 mm) and

strands were examined using a Zeiss Polarizing light microscope. Optical images were enhanced by using immersion oil (n_D = 1.5). Scanning electron microscopy was done using a Stereoscan-S200 with an accelerating voltage of 15kV. Samples were prepared by cryogenic fracture after immersion in liquid nitrogen for at least 5 minutes. The fractured samples were fixed to aluminum stubs and coated with a layer of gold using a SPI Sputter Coater to enhance conductivity.

3.3 Results and Discussion

The results of this work are organized as follows. First the results of the development of morphology prior to the die are discussed. The dual extrusion method is first described followed by blending in a single extruder. In both cases special attention is given to the effect of variations of mixing history on the morphology of the resultant blend materials. The differences in morphology seen with the various mixing histories are then discussed with respect to the viscosity of the blend constituents during mixing. The morphology of low HX1000 concentration strands produced using the various mixing histories is then discussed and finally correlated with the tensile properties of the strands.

3.3.1 Morphology Development Prior to Strand Formation

In this section the morphology developed during blending will be discussed. The discussion of the morphology in the dual extrusion process (DEP) begins with the TLCP injection system followed by the development of morphology through sequential static mixing elements. The development of

morphology during blending in single screw extruder with and without additional mixing provided by static mixers is then discussed. The morphology seen in these systems is subsequently correlated with the viscosity of the blend components during the mixing process. Finally, the objective of this section is to monitor and analyze the development of the morphology in these processes prior to the contraction of the extrudate stream through the capillary die. Specifically, if an axially continuous TLCP morphology is seen prior to the die then this morphology is much more likely to be translated into strands produced with similar mixing history.

The phase distribution system shown schematically in Fig. 2 was introduced into the DEP for many of the same reasons which justify the use of injection nozzles in conventional mixing applications. These benefits include increased distribution of the secondary phase prior to blending in the motionless mixers as well as minimization of the required number of mixer elements. Furthermore, this application required a distribution system that also maximized the axial continuity of the TLCP phase as it entered the static mixing elements. An additional design requirement was to minimize the residence time of mixing which in turn minimizes both the degradation of thermally sensitive matrices and dispersive mixing due to high strains.

Photographs of extruded rods taken directly from of the exit of the multiple port injection system and rods generated by using a simple T-injection system are shown in Fig. 4 (the dark phase is HX1000). The T-injection system included 3 elements of Kenics mixers so that the system could be directly compared with the multiple port injection system. The photographs in Fig. 4 indicate that the degree of radial mixing is increased by the presence of the multiple port injection system. A 5.0 wt.% HX1000 concentration produced using the T-injection system resulted in rods where the TLCP remained primarily at the skin region. Similarly, rods produced using the multiple port system showed several striations of TLCP within the PP matrix. However, the most dramatic improvement in mixing was seen at high TLCP concentrations. The 60 wt.% HX1000 rods produced using the T showed very poor mixing with 4 dense HX1000 regions whereas rods made using the multiple port distribution system show at least 7 striations.

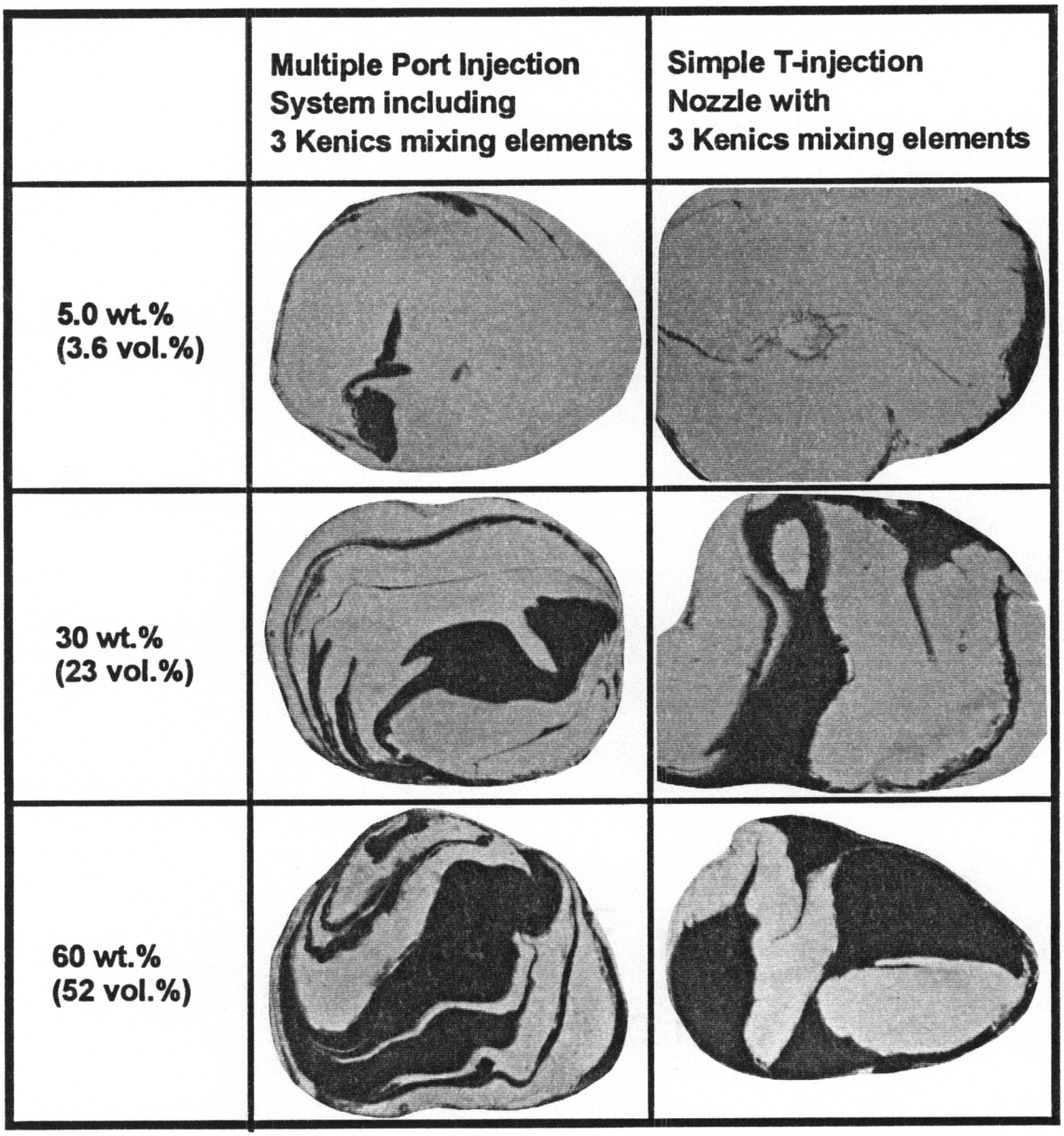

Figure 4: Photographs of the cross sections of 5.0, 30 and 60 wt.% HX1000 rods produced using the multiple port injection system and a simple T-junction with 3 Kenics mixing elements.

The improvement in mixing with increased concentration of TLCP might be caused by differences in the velocity of the TLCP streams as they enter the matrix material. For example, in blends containing 5.0 wt.% HX1000, the TLCP is injected at approximately 1/3 the velocity of the matrix material. However, at 60 wt.% HX1000 the velocity of the individual injected TLCP streams is 13 times the velocity of the matrix material. It is believed that the higher relative velocities of the TLCP relative to the matrix material allow the injected streams to overcome the interfacial and hydrodynamic forces that act to recombine them into a single stream on either side of the first Kenics mixer element. Thus, one clear avenue to an improved injection system might be to reduce the diameter of the injection ports which effectively increases the injection velocity of the TLCP streams relative to the matrix phase. Higher injection velocities might lead to the formation of individual streams of TLCP entering the static mixing elements in comparison with the stratified layers that are currently being formed.

The TLCP phase in the rods produced using the multiple injection port system was seen to be continuous whereas there was little continuity in the rods produced using the simple T-injection system. For example, the rods extruded from the multiple injection port system could be easily split at the interface between the matrix and TLCP phases which allowed the axially continuous TLCP ribbons to be removed from the entire length of the extruded rod. In contrast, the TLCP phase in the rods produced using the T-injection system could not be removed due to the large variation in the concentration along the length of the extruded rod. This observation clearly indicates that the multiple port distribution system increased the axial continuity of the TLCP entering the static mixer system. This effect is attributed to the TLCP being introduced in the matrix material along the flow direction in contrast to the simple T-injection system that introduces the TLCP perpendicular to the flow direction of the matrix material. Perpendicular introduction of a single TLCP stream allows localized variations in the matrix flow rate to disrupt the continuity of the injected stream. Axial continuity of the TLCP phase at this point in the formation of the in situ composite strand is important because it is highly desirable to form strands with uniform axial concentrations and TLCP fibrils of infinite aspect ratio. Thus, if these conditions are

not predominant at this stage of the mixing process then they can not be expected in the resultant in situ composite strand.

From these observations, it was concluded that the multiple injection port nozzle effectively increased the level of mixing and TLCP phase continuity compared with the simple T-injection system. Therefore, all subsequent mixer configurations using the DEP include the multiple port injection system. Configurations including additional Kenics elements are subsequently described with reference to the total number of elements including the three which are permanently housed in the injection nozzle. Mixing systems including Koch mixing elements are described by only the number of Koch elements without reference to the three Kenics mixers in the injection nozzle.

The laminar TLCP morphology initially observed at the exit of the phase distribution system is further developed as the number of static mixer elements is increased. Figure 5 shows photographs of cross sections of rods produced using the DEP as a function of both the number of Kenics elements and the concentration of HX1000. It is clear from Fig. 5 that the TLCP forms laminar striations which increase in number and reduce in thickness as the number of elements is increased. However, even with as many as 18 Kenics elements dense (poorly mixed) TLCP regions still exist in the 60 wt.% HX1000 concentration.

The number and thickness of the striations found experimentally compare only qualitatively with the ideal number and thickness of striations predicted by assuming that each element splits the blend stream into two equal layers. The ideal number of striations for this mixing application (assuming that the TLCP stream is initially equally distributed on either side of the first mixer element) is given by

$$S = 2^n \qquad (1)$$

where S is the number of striations and n is the number of Kenics mixer elements. Using geometric considerations, the expression for the ideal thickness of each striation is,

$$\delta_n = \delta_0 2^{-n} \qquad (2)$$

No. of Kenics Mixing Elements	11	14	18
5.0 wt.% (3.6 vol.%)	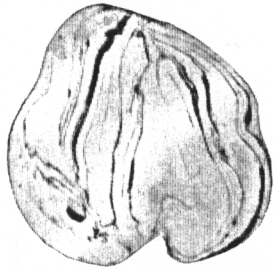		
30 wt.% (23 vol.%)	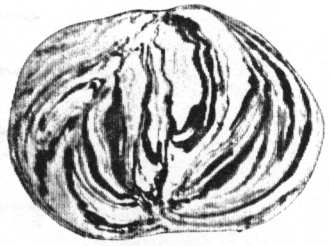	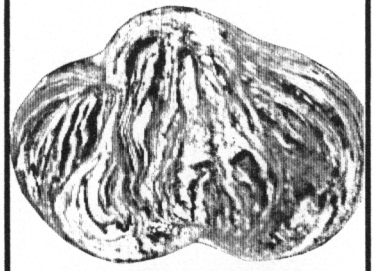	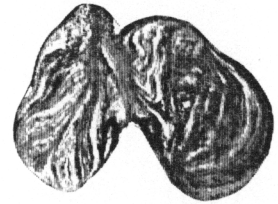
60 wt.% (52 vol.%)	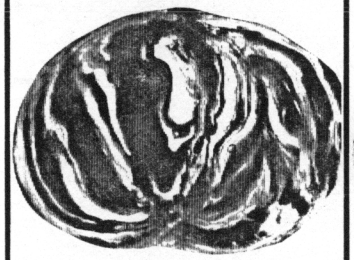	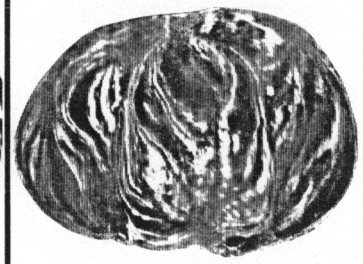	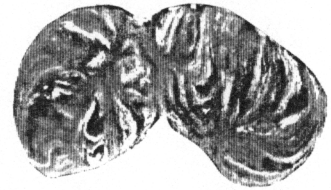

Figure 5: Photographs of the cross sections of 5.0, 30 and 60 wt.% HX1000 rods as a function of the total number of Kenics mixing elements including those in the phase distribution system.

where δ_n is the striation thickness after n mixer elements and δ_0 is the striation thickness prior to the first element. Applying Equations 1 and 2 to the 5.0 wt.% concentration rod indicated that there would be 2.5×10^{11} striations after 18 mixer elements each of a thickness of less than 10^{-3} μm. Clearly, the equations for the ideal number and thickness of striations formed via the Kenics mixer elements do not predict the actual morphology. However, a laminar structure is observed in which the number of striations increased the with number of Kenics elements.

The morphology observed in the cross sections of the rods produced using the Koch mixers is in some cases similar to that seen in cross sections of rods produced using Kenics elements. Figure 6 shows photographs of the cross sections of 5.0, 30, and 60 wt.% HX1000 rods produced using 4 and 8 Koch mixing elements. Comparing rods produced using the various mixer designs indicates that the level of mixing achieved with 4 Koch mixers is similar to that developed with a total 18 Kenics elements. Striations are clearly discernible with dense HX1000 phases present in the 60 wt.% composition. However, the morphology seen in the rod cross sections produced with the 8 Koch mixers is virtually homogeneous with only faint laminar striations seen on the macroscopic scale.

Microtomed sections of the extruded rods were observed in an optical microscope to reveal the morphology on a smaller scale. Figure 7a shows an optical micrograph of an extruded rod cut parallel to the flow direction. The morphology indicates that axially continuous ribbons and droplets of TLCP are formed in the Kenics static mixing elements. This morphology is similar to that shown in Fig. 7b which is an optical micrograph of a rod sample produced using 4 Koch mixing elements. The TLCP morphology in this sample is predominately axially continuous ribbons with interspersed droplets. The morphology of rods produced using 8 Koch mixing elements (Fig. 7c) is different in that the predominant structure of the TLCP phase is dispersed droplets. This indicates that simply increasing the degree of mixing by excessive or more effective motionless mixers is not a viable method of producing well dispersed axially continuous TLCP phases prior to the die. Excessive mixing even in static mixers acts to breakup TLCP fibrils into smaller droplets due to higher strains.

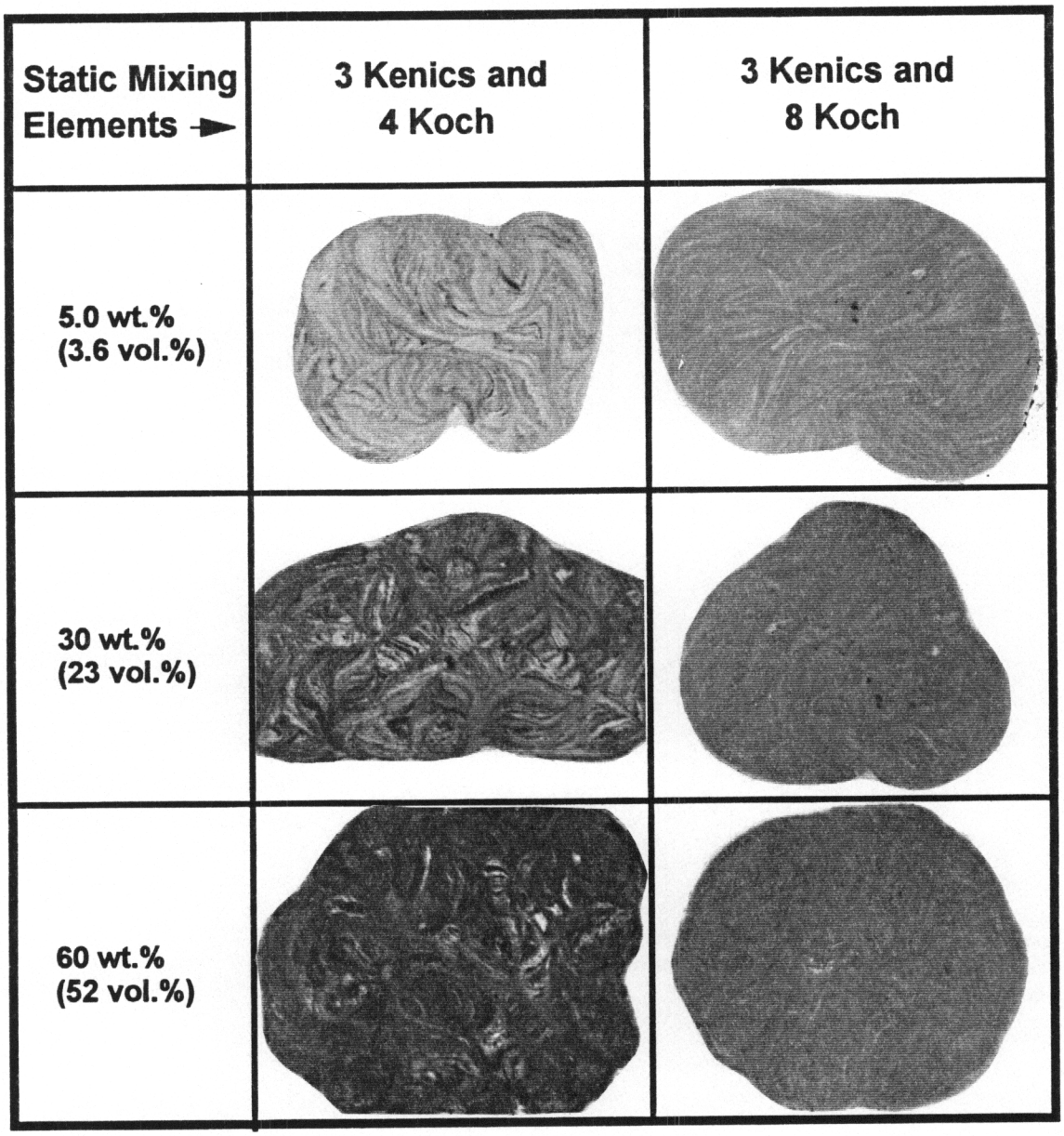

Figure 6: Photographs of the cross sections of 5.0, 30 and 60 wt.% HX1000 rods as a function of the number of Koch mixing elements placed after the phase distribution system.

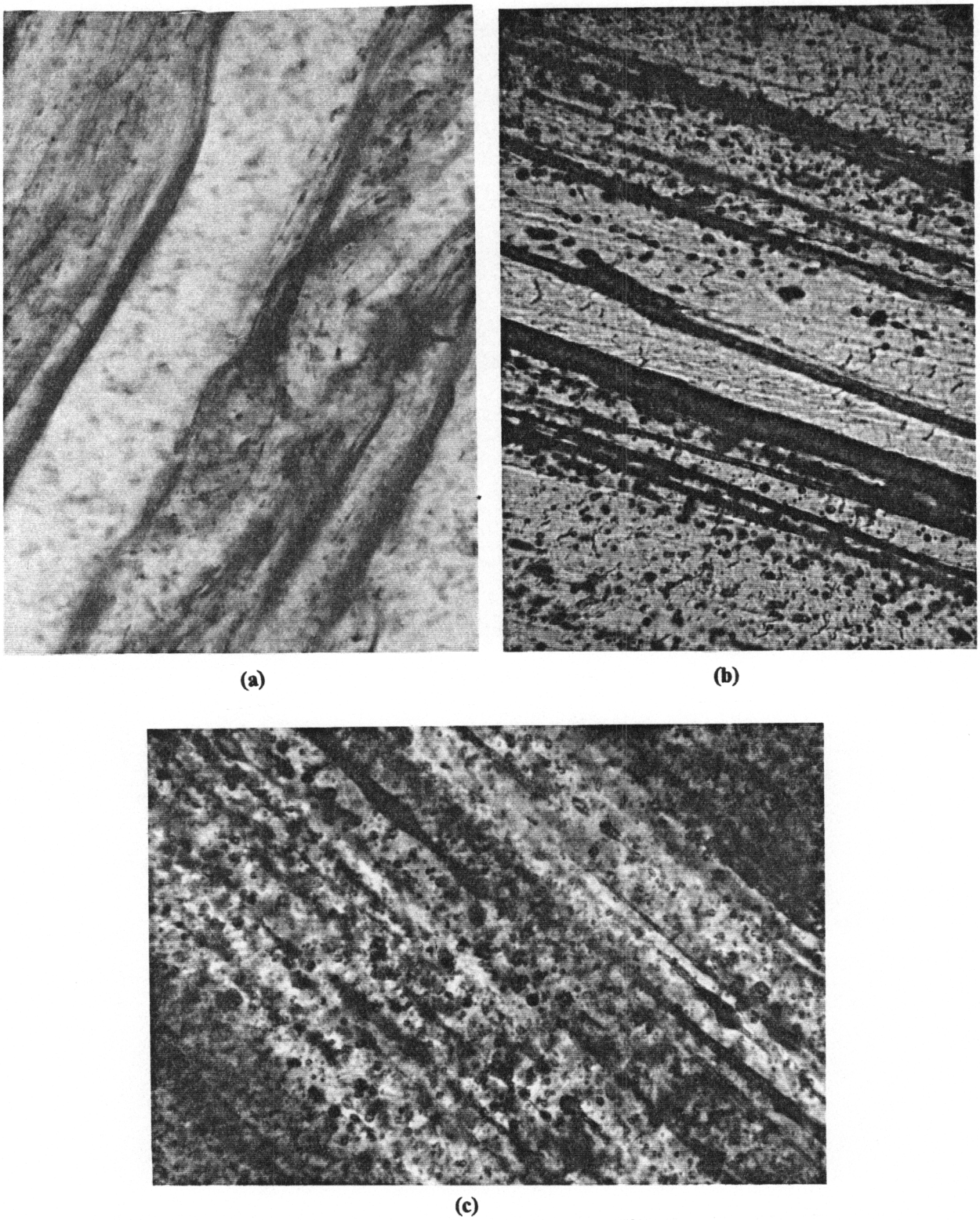

Figure 7: Optical micrographs taken parallel to the flow direction of 5.0 wt.% HX1000 rods produced using the DEP including (a) a total of 18 Kenics elements and (b) 4, and (c) 8 Koch mixing elements (—— 20 μm).

The development of the TLCP morphology in rods produced using single screw extrusion was also investigated for a concentration which inhibited coalescence. The goal of this work was to monitor the development of TLCP morphology in blends mixing in a single screw extruder prior to the formation of the strand. Specifically, rods (diameter ≅ 13 mm) of 5.0 wt.% HX1000 were prepared using single screw extrusion with and without additional mixing provided by 18 Kenics mixer elements. The static mixing elements were introduced to provide a direct comparison with materials produced using the DEP. Specifically, it is of interest to determine if the morphology seen in the rods produced using the DEP are the result of the static mixers solely or the result of the entire DEP.

The TLCP morphology seen in rods produced from blends mixed in a single extruder is not conducive to the formation of continuous reinforcing fibrils. The morphology as observed in Fig. 8, which shows photographs of extruded rods taken parallel to the flow direction, exhibits very few axially continuous TLCP fibrils. The TLCP phase is highly irregular and poorly dispersed and distributed both axially and radially within the rod. The visibly poor mixing could have been improved by a second extrusion step but this alternative would have exposed the blend to another processing step at temperatures above the thermally stable region of the PP.

Inspection of the cross sections of extruded rods produced using blending in a single screw extruder followed by 18 Kenics mixing elements showed a homogeneous morphology on the macroscopic scale. Rods did not exhibit the striations seen in the blends produced using the dual extrusion system with the same number of Kenics elements. Observation using optical microscopy revealed that the TLCP phase showed an irregular morphology consisting of predominantly dispersed droplets (Fig. 9).

The differences in the morphology of the rods produced using single versus dual extrusion blending could be attributed to differences in the mechanism of mixing. The morphology developed in the static mixers is the result of physically dividing and geometrically rearranging continuous fluid

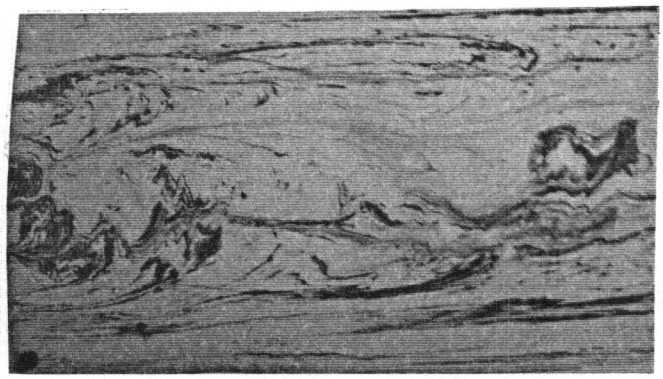

Figure 8: **Photographs taken parallel to the flow direction of 5.0 wt.% HX1000 rods produced from a blend mixed in a single screw extruder.**

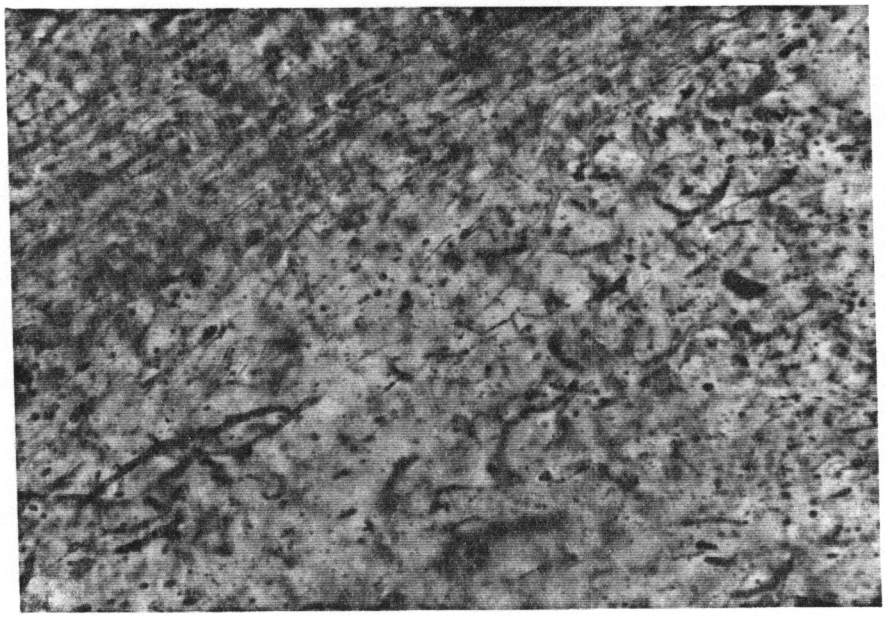

Figure 9: Optical micrographs taken parallel to the flow direction of 5.0 wt.% HX1000 rods produced from a blend mixed in a single screw extruder with 18 Kenics mixing elements (——50 μm).

streams at low shear rates. In particular the shear rate within the Kenics mixer was estimated as being of the order of 1 sec^{-1}. In contrast the single screw extruder relies on high strains and shear rates that initially elongate dispersed TLCP phases which subsequently breakup when an unstable state is reached [30]. The shear rate in this case was estimated as being over an order of magnitude larger than the shear rated estimated in the static mixing elements.

Another important factor governing the initial elongation process is the ratio of the viscosity of the dispersed phase, μ_d, to the viscosity of the matrix, μ_m, ($\lambda = \mu_d/\mu_m$). Specifically, it has been found that a viscosity ratio of between 0.1 and 1 will favor the elongational deformation of a dispersed droplet in simple shear flow [1,2]. In the initial stages of mixing in the DEP the viscosity ratios is of the order of 0.1 while the viscosity ratio during blending in the single screw extruder is of the order of 10 for the entire frequency range tested. Specifically, Fig 10 shows the complex viscosity of HX1000 as a function of frequency for samples which have first been preheated to 350°C then cooled to 310°C compared with a sample heated directly to 310°C from ambient conditions. This behavior has been observed in other TLCPs as well [34,35]. To determine if the reduction of viscosity could associated with thermal degradation, isothermal time sweeps were also conducted at 350°C. From the time sweeps it was found that the viscosity was stable and did not decrease for the period of time that the sample was in the rheometer (< 15 min.) From these observations it was concluded that the reduction of viscosity as a function of preheating was not caused by degradation of the TLCP. Hence, the DEP process offers a significant advantage over conventional blending processes in that there is some degree over the viscosity ratio of the blend components during mixing.

Comparing 5.0 wt.% HX1000 rods produced via dual and single extruder blending indicates that in some cases a similar TLCP structure is present. Specifically, rods produced from mixing in a single screw extruder in conjunction with 18 Kenics mixing elements or the DEP with 8 Koch mixing elements both produced a dispersed droplet morphology. However, the DEP with a total of 18 Kenics or 4 Koch mixing elements generated rods with a morphology consisting of predominately ribbons in

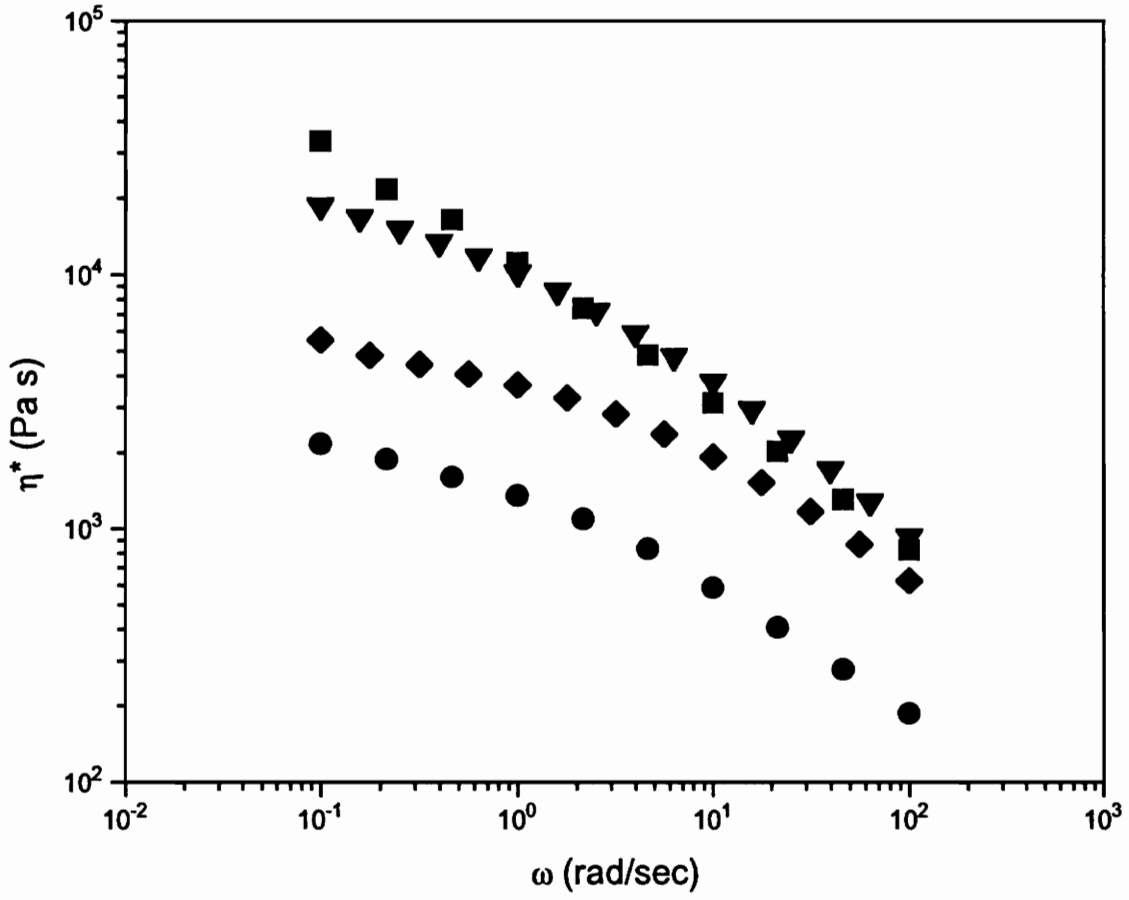

Figure 10: Complex viscosity versus frequency for HX1000 with the following temperature histories: (■) 310°C from 25°C, (●) 310°C from 350°C and PP at (▼) 260°C and (◆) 300°C.

addition to dispersed droplets. As is discussed in the following section, the morphology seen at the exit of the mixers was maintained when a capillary die was introduced and a strand was formed.

3.3.2 Morphology of Strands

In this section the morphology of 5.0 wt.% HX1000 strands formed from various mixer configurations is discussed. The objective was to investigate the correlation of the morphology seen in the strands to that developed prior to the die in the absence of significant coalescence. Specifically, strands were produced using the DEP consisting of a total of 18 Kenics mixing elements and both 4 and 8 Koch elements. Strands were also generated by mixing in a single screw extruder followed by 18 Kenics mixer elements placed between the extruder and the die. The strands produced from blends mixed in the single extruder with no static mixers exhibited visibly poor radial and axial mixing which caused the strand to be quite unstable and continuously break during the drawing process. Therefore, strands produced with this mixing history were not evaluated further.

Figures 11 and 12 show optical micrographs of drawn strands produced using the various mixer configurations described above. The morphology exhibited in the strands produced using both single extruder blending (with 18 Kenics elements) and DEP in conjunction with 8 Koch mixer elements was quite similar as was the extrudate taken prior to the die. The morphology of the strands consisted of elongated droplets aligned in the flow direction (Fig. 11a-b) with aspect ratios ranging from 1 to 20. In contrast, the morphology seen in the strands produced using the DEP with either a total of 18 Kenics mixer elements or 4 Koch mixer elements shows ribbons of infinitely high aspect ratio in addition to elongated droplets with aspect ratios of the order of 10 (see Fig. 12 a -b). Again there is a direct correspondence of the morphology of the strands to that seen in the extrudate taken prior to the die.

Scanning electron micrographs of cryogenically fractured strands reveal further similarities between the morphology seen at the exit of the static mixers and the drawn strands. Micrographs of

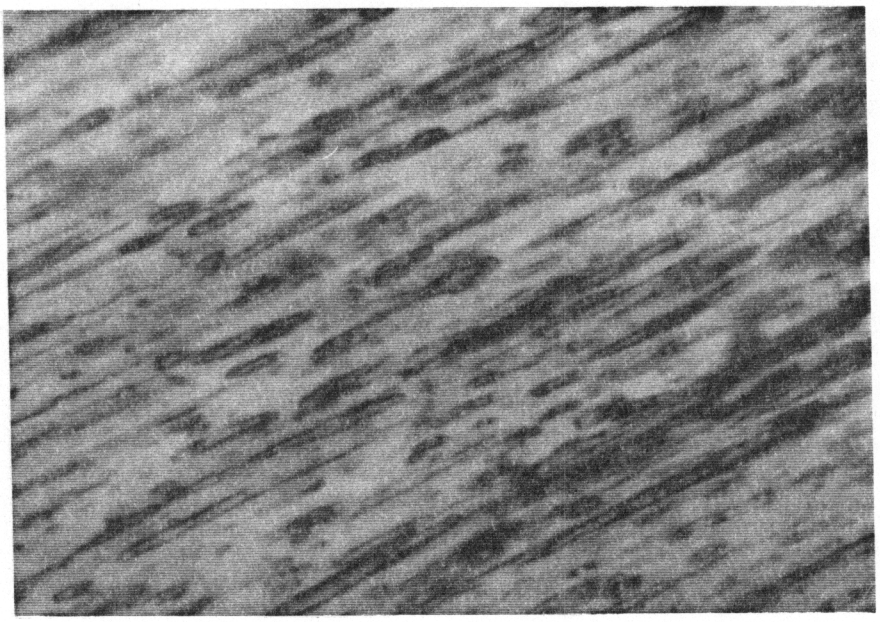

(a)

(b)

Figure 11: Optical micrographs of 5.0 wt.% HX1000 taken parallel to the axis of strands produced from blends mixed in a single extruder with 18 Kenics mixing elements attached and (b) the dual extrusion process with 8 Koch mixing elements (— 5 μm).

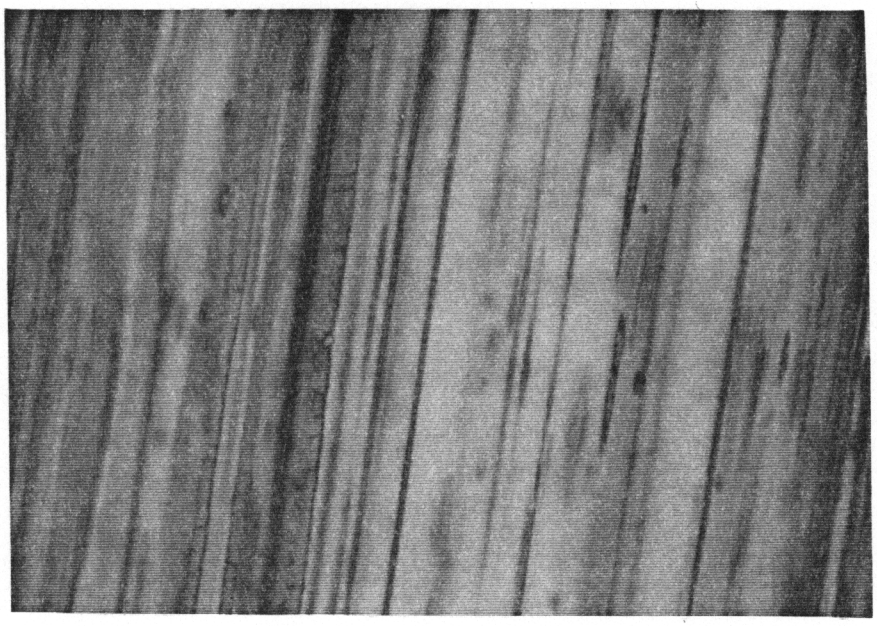

(a)

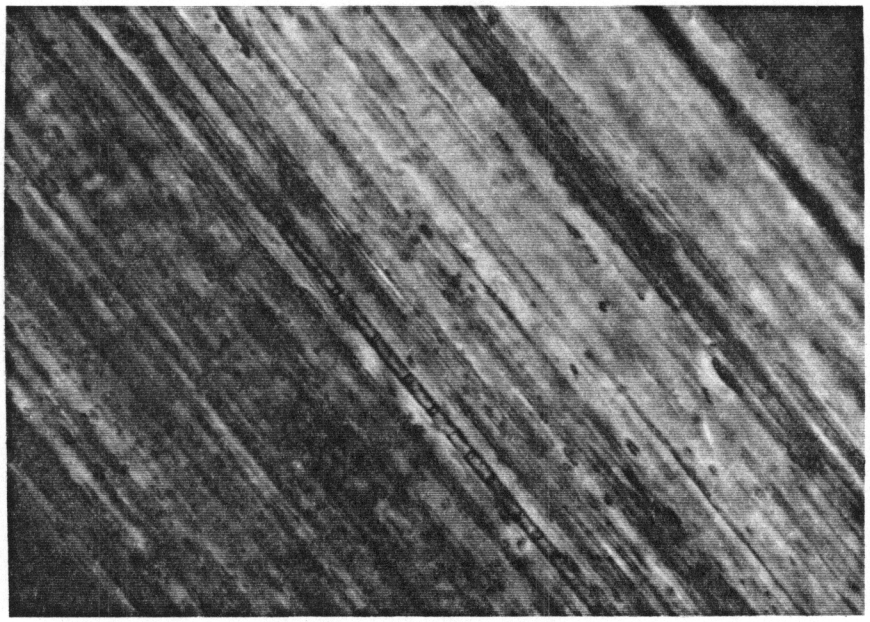

(b)

Figure 12: Optical micrographs of 5.0 wt.% HX1000 taken parallel to the axis of strands produced using the DEP (a) a total of 18 Kenics mixing elements and (b) 4 Koch mixing elements (— 5 μm).

the strands produced from blends mixed in a single screw extruder with 18 Kenics mixers and the DEP including 8 Koch mixer elements are shown in Fig. 13a and b, respectively. The morphology of the strands produced with both systems show an array of elongated TLCP droplets that are well distributed across the cross section of the strand. The elongated droplets in the strands produced using the DEP with 8 Koch mixing elements have an average diameter of approximately 1 μm while the average diameter of the dispersed phase in the strands produced by mixing both components in a single extruder is in the range of 2 to 3 μm. In contrast, the morphology of the strands produced using the DEP with a total of 18 Kenics mixing elements showed a morphology of ribbons which were aligned with the circumference of the strands with interspersed elongated droplets (Fig 14a). The morphology of the strands produced using 4 Koch mixer elements is quite similar in that ribbon structures and smaller scale TLCP fibrils can be seen (Fig. 14b). However, the ribbons are not aligned with the circumference of the strand as was seen in strands produced using Kenics mixers exclusively.

Similarities in the morphology of drawn strands produced by mixing in a single screw extruder with 18 Kenics mixing elements and the DEP with 8 Koch mixers indicates that the scale of mixing generated in both systems was similar. In particular blending in both the DEP with 8 Koch mixing element and a single screw extruder produced a TLCP morphology consisting of dispersed droplets. The absence of a significantly fibrillar TLCP morphology in the strands was attributed to the mixing histories which produced dispersed droplets which were too small to allow for deformation due to viscous forces [30]. Furthermore, the concentration of TLCP droplets was low which hindered substantial coalescence as the stream passed through the contraction into the capillary die. Thus, the two mechanisms generally attributed to the formation of the reinforcing fibrils in in situ composites produced by conventional methods were curtailed which lead to a poor morphology for self reinforcement.

The morphological observations of 5.0 wt.% HX1000 blends indicates that the morphology developed prior to the die is maintained in the resultant strand. This indicates that the mixing histories that generate fibrillar TLCP structure prior to the die can produce strands with more desirable

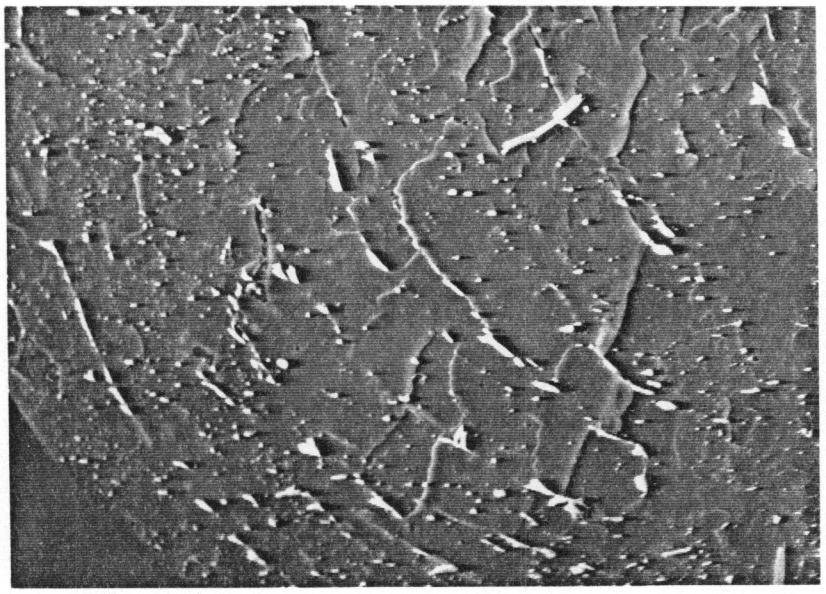

(a)

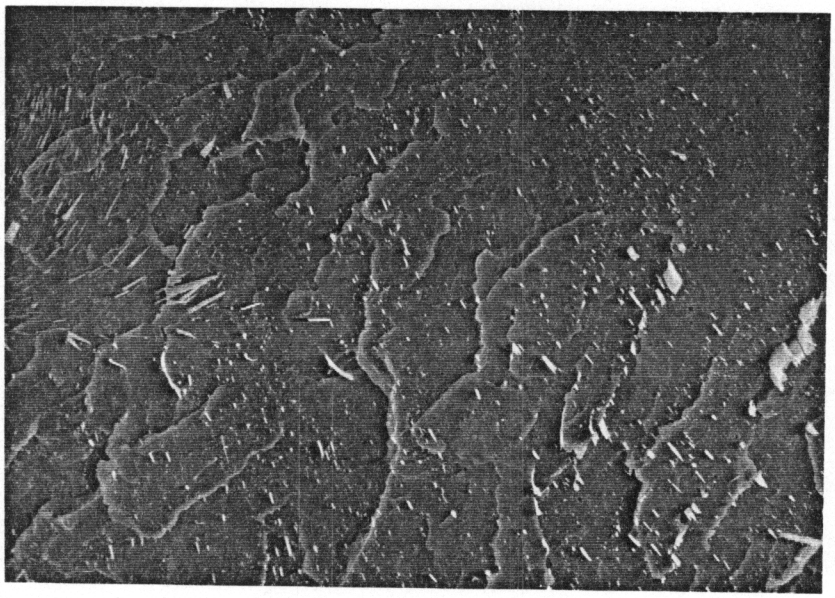

(b)

Figure 13: Scanning electron micrographs of 5.0 wt.% HX1000 drawn strands (draw ratio = 10) produced using (a) single extruder blending with 18 Kenics mixing elements and (b) the DEP with 8 Koch mixing elements (—— 30 μm).

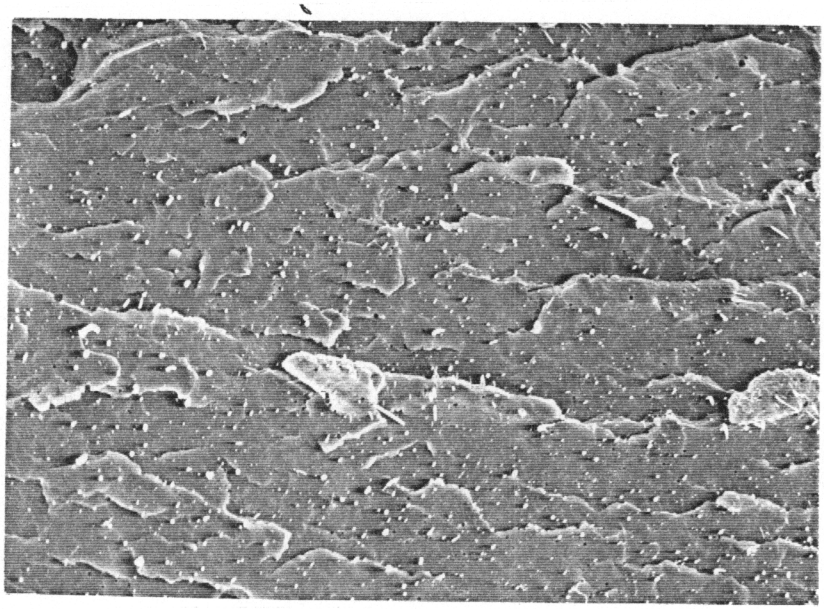

(a)

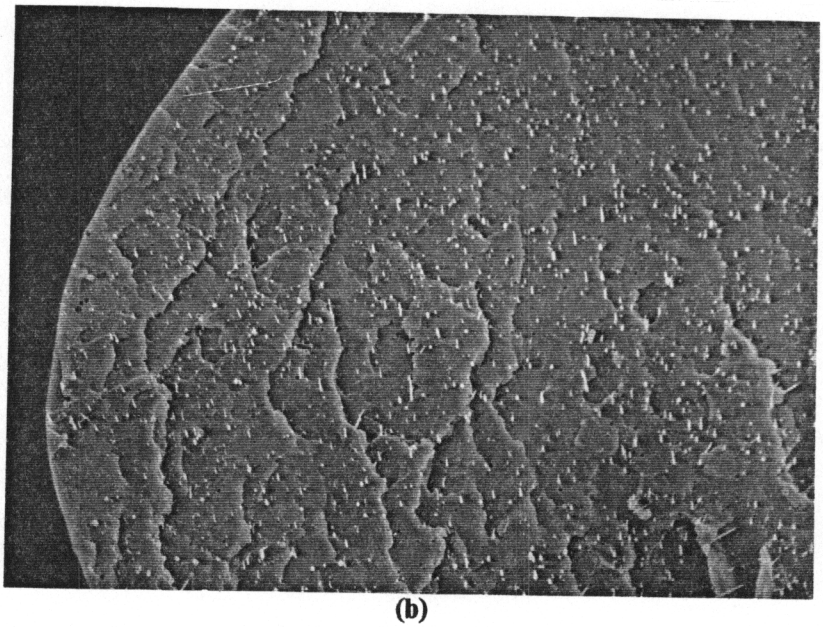

(b)

Figure 14: Scanning electron micrographs of 5.0 wt.% HX1000 drawn strands (draw ratio = 10) produced using the DEP with (a) a total of 18 Kenics mixing elements and (b) 4 Koch mixing elements (—— 30 μm).

morphologies for reinforcement. Specifically, the DEP (with appropriate mixing systems) can form axially continuous TLCP phases prior to the die which translate into a desirable morphology in the strands. In contrast, blending in a single extruder prior to strand formation forms dispersed droplets both prior to the die and in the resultant strand. The direct effect of the different morphologies on the tensile properties of the strands will be seen in the following section.

3.3.3 Tensile Properties of Drawn Strands

The tensile properties of 5.0 wt.% HX1000 strands produced using the various mixing configurations described above were measured as a function of the draw ratio of the strand and are discussed in this section. Measuring the tensile properties of the strands is important because the overriding objective of producing in situ composites is to generate morphologies which exhibit the highest possible mechanical properties.

Figure 15 shows the modulus as a function of strand draw ratio for neat PP and strands produced using single and dual extrusion processes with both employing a total of 18 Kenics mixing elements. Several important observations can be made from the data presented in Fig. 15. First, PP processed using the same conditions as the blend strands showed no improvement in modulus with increased draw ratio. This indicates that the property enhancement seen in the blends can be attributed to the TLCP phase which was shown to be highly affected by increased draw ratios [28]. The blend strands produced from both mixing systems increased with increased draw ratios but the average modulus of the strands produced using the DEP was 50% higher than the modulus exhibited by the strands produced from blends which were mixed in a single extruder. Specifically, it was found that the average modulus of the strands with draw ratios in excess of 3 produced from the single and dual extrusion blending processes were 1.58(0.45) and 2.37(0.31) GPa, respectively (standard deviations given in parentheses). This represents

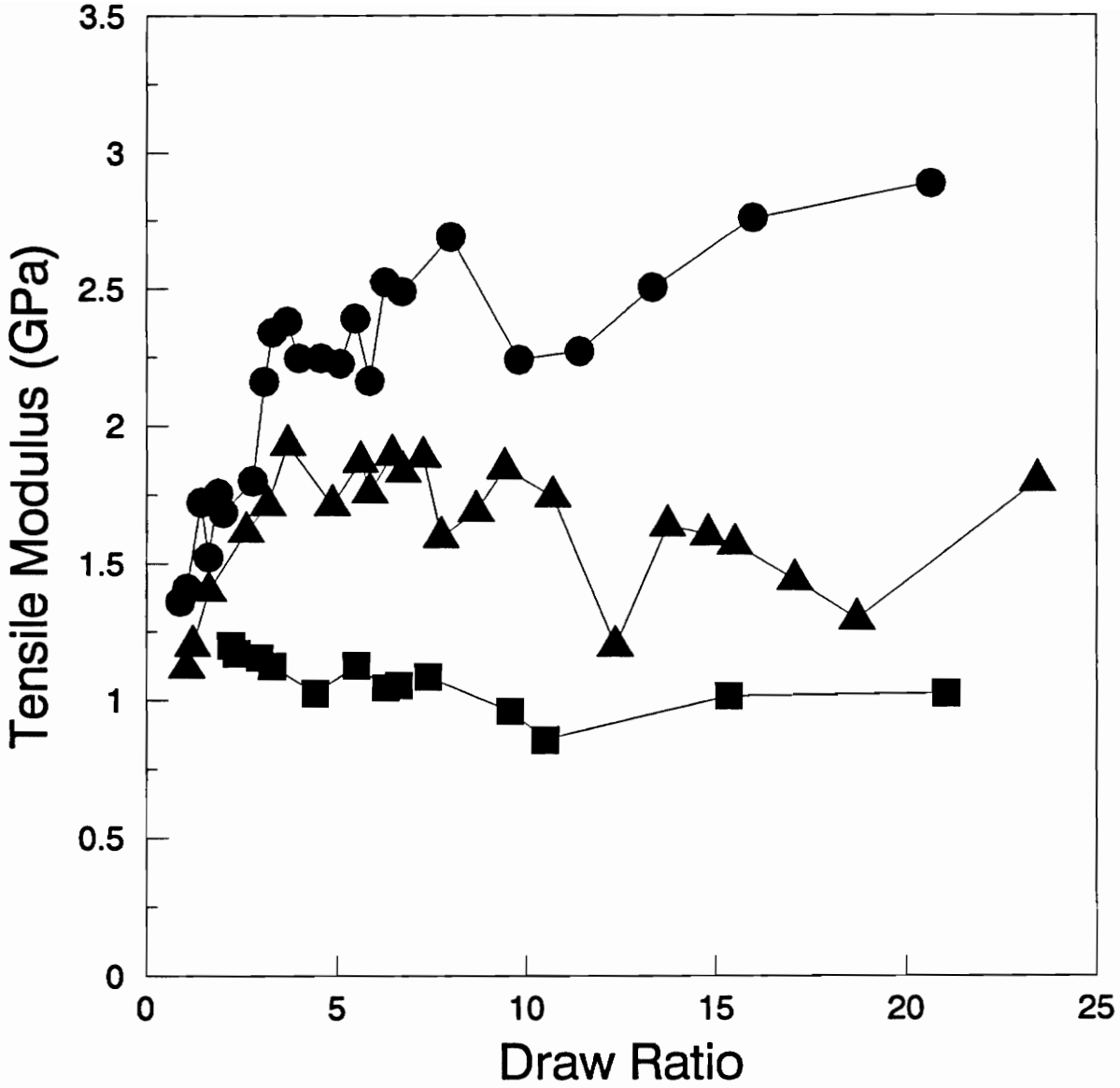

Figure 15: **Tensile modulus versus strands draw ratio for (■) neat PP and 5.0 wt.% HX1000 produced using a total of 18 Kenics mixing elements and (●) dual and (▲) single extruder blending.**

an average increase in modulus over 2.3 times the modulus of the neat PP.

The tensile strength of the strands as a function of increased draw ratio showed a similar behavior as was seen with modulus as shown in Fig. 16. The measured tensile strength of the neat PP was seen to slightly decrease as draw ratio was increased. In contrast, the strength of the strands produced using both blending methods was seen to initially increase with increased draw ratio. The strength of the strands produced using the DEP increased to an average tensile strength of 28.3(3.1) MPa while the average strength of the drawn strands produced from blending in a single extruder was 21.6(5.0) MPa (for draw ratios in excess of 3). The strength of the strands generated through single screw extrusion is actually less than the average strength of the neat PP which was measured as 23.2(3.9) MPa. The lack of property enhancement is a result of the morphology of the strands consisting of elongated droplets with very low aspect ratios.

The average tensile properties of strands with draw ratios in excess of 3 are summarized in Table 2 for all of the mixing histories examined. The properties indicate that the DEP with either a total of 18 Kenics mixing elements or 4 Koch mixer elements both show superior mechanical properties. Those produced using the DEP exhibit an improvement of over 2.3 times the modulus of neat PP. This comprises a significant improvement in modulus with only 3.6 vol.% HX1000 in the blends. Furthermore, the strands produced from both mixing histories approach 80 % of the optimal properties predicted by the rule of mixtures using the highest reported properties of HX1000 as the modulus of the reinforcing phase. The next highest strand properties are seen in the strands produced from the DEP with 8 Koch mixing elements and the lowest properties are seen in strands which were produced by mixing in a single extruder with 18 Kenics mixing elements. The poor property enhancement in these systems can be attributed to the TLCP morphology which consisted of elongated droplets with low aspect ratios.

The elongation at yield for the strands produced with the various mixing histories indicate further enhancement in properties in the strands produced using the DEP in conjunction with either a 18

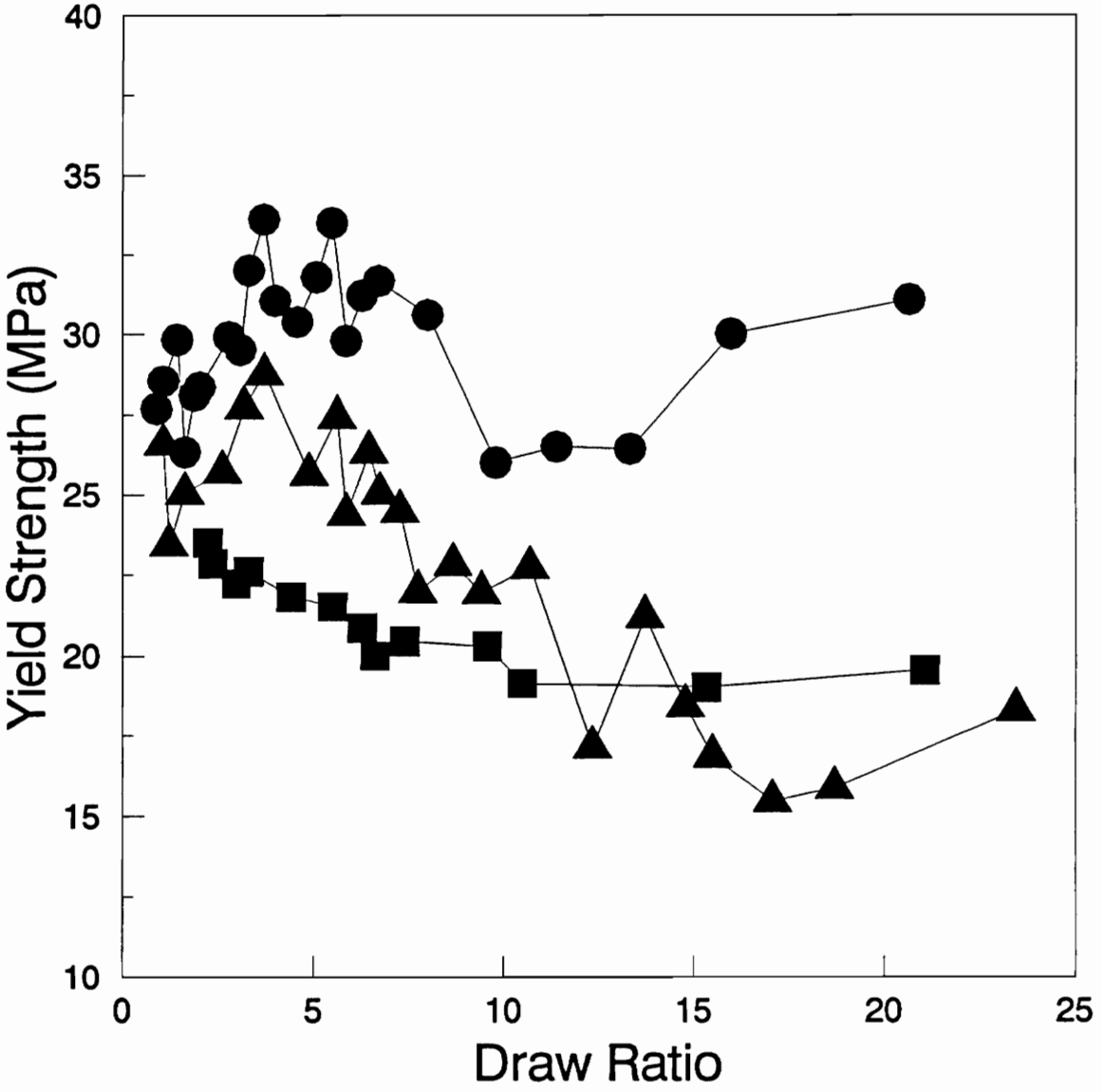

Figure 16: **Tensile strength versus strands draw ratio for (■) neat PP and 5.0 wt.% HX1000 produced using a total of 18 Kenics mixing elements and (●) dual and (▲) single extruder blending.**

Table 2: The effect of mixing history on the mechanical properties of drawn blend strands of 5.0 wt.% HX1000/PP (3.6 vol.%).

	Mixing System[a]	Tensile Modulus (GPa)	Yield Strength (MPa)	% Extension at Yield
Dual Extruder	(3 Kenics) 4 Koch	2.37 (0.31)	28.3 (3.1)	1.61 (0.24)
Dual Extruder	A total of 18 Kenics	2.34 (0.27)	29.4 (3.6)	1.64 (0.21)
Dual Extruder	(3 Kenics) 8 Koch	1.84 (0.23)	24.2 (2.7)	3.43 (0.50)
Single Extruder[b]	18 Kenics	1.58 (0.45)	21.6 (5.0)	2.40 (1.18)
Composite Theory[c]	-	2.9	-	-
neat PP	-	0.98 (0.18)	23.2 (3.9)	12.61 (3.16)
neat HX1000[d]	-	53.3 (4.1)	205 (53)	0.33 (0.10)

Notes: standard deviations given in parentheses, (a) the dual extrusion system included a multiple port injection nozzle, (b) drawn strands were not produced from blends mixed in a single extruder alone due to concentration variations along the strands, (c) assumes infinite aspect ratio of the TLCP reinforcing fibrils and (d) taken from reference 28.

total of Kenics or 4 Koch elements. Specifically, the elongation at yield of these strands was significantly lower than the those exhibited by the other blending processes. This might indicate that the TLCP is acting more effectively as a reinforcing phase in these in situ composite strands because the yielding point is closer to that of the neat HX1000. Furthermore, the standard deviation of the elongation at yield for strands produced through blending in a single extruder is virtually 50% of the average value. This was caused by the large axial concentration variations seen in the rods taken from the exit of the extruder. Specifically, the introduction of the static mixers acted to radially mix the material exiting the extruder but did not reduce axial concentration variation. In comparison, the standard deviation associated with the elongation at yield of the strands produced using the DEP are significantly lower than the those exhibited by strands produced through single extruder blending. This further supports the conclusion that the DEP (with appropriate mixer configurations) produces strands with a more uniform axial concentration in comparison with strands generated from one pass through a single screw extruder.

3.4 Conclusions

By monitoring the development of the morphology in the DEP from the point that the TLCP stream meets the matrix material to the final drawn strand, a clear mechanism for the development of the TLCP reinforcement has been presented. Specifically, it was found that under appropriate mixing configurations the fibrillar TLCP morphology seen in strands produced from this method originate at the onset of mixing in the phase distribution system and were subsequently refined as the melt passed though the static mixing elements. The axially continuous morphology seen at the entrance of the die was maintained and further developed as the blend passed through the die and was drawn. In contrast, strands produced using the single extruder blending or the dual extrusion method with excessive mixing produced a droplet morphology prior to the die. At a very low concentration of TLCP, the

droplets were too small and well dispersed to sufficiently coalesce and deform into fibrils in the elongational flow field of the die and drawing process. These phenomena resulted in an undesirable morphology for self reinforcement which was clearly seen in the measured mechanical properties of the strands.

3.5 Acknowledgments

The authors gratefully acknowledge the support of the Virginia Institute of Material Science and the Army Research Office (grant number DAAL 03-91-G-0166) for support of this work.

3.6 References

1 *La Mantia, F. P.:* Thermotropic Liquid Crystalline Polymer Blends. Technomic, Lancaster, PA., U.S.A. (1993).

2 *Weiss, R. A., Huh, W., Nicolais, L.:* Polym. Eng. and Sci. 27 p. 684 (1987).

3 *Kiss, G.:* Polym. Eng. Sci. 29 p. 410 (1987).

4 *Cogswell, F. N.,* in Recent Advances in Liquid Crystalline Polymers. *Chapoy, L. L.* (Ed.), Elsevier, London (1985).

5 *Cox, M. K.:* Mol. Cryst. Liq. Cryst. 153 p. 415 (1987).

6 *Baird, D. G., Sun, T.,* in: Liquid-Crystalline Polymers. *Weiss, R. A., Ober, C. K.* (Eds.), ACS Symposium Series, 1990.

7 *Ramanathan, R., Baird, D. G.,* in: Multiphase Macromolecular Systems. *Culbertson, B. M.* (Ed.), Plenum Press, New York 1989.

8 *Halpin, J. C., Kardos, J. L.:* Polym. Eng. and Sci. 16 p. 344 (1976).

9 *Coller, A. A., Clegg D. W.,* in: Mechanical Properties of Reinforced Thermoplastics. *Coller, A. A., Clegg D. W. (Eds.),* Elevier, London 1986.

10 *O'Donnell, H. J.:* Ph.D. Thesis Virginia Polytechnic Institute and State University, Blacksburg VA., U. S. A. 1994.

11 *de Souza, T.:* Ph.D. Thesis Virginia Polytechnic Institute and State University, Blacksburg VA., U. S. A. 1994.
12 *Seigman, A., Dagan, A., Kenig, S.:* Polymer 26, p. 1325 (1985).
13 *Isayev, A. I., Modic, M.:* Polym. Composites 8, p. 158 (1987).
14 *Sukhadia, A. M., Done, D., Baird, D. G.:* Polym. Eng. Sci. 30, p. 519 (1990).
15 *Kohli, A., Chung, N., Weiss, R. A.:* Polym. Eng. Sci. 29, p. 573 (1989).
16 *Beery, D., Kenig, S., Siegmann, A.:* Polym. Eng. Sci. 33, p. 1548 (1993).
17 *Bassett, B. R., Yee, A. F.:* Polym, Composites 11 p. 10 (1990).
18 *Tsebrenko, M. V.:* Intern. J. Polymeric Mater. 10 p. 83 (1983).
19 *O'Donnell, H. J., Baird, D. G.:* Presentation, at the SPE Antech Tech. Conference, March (1993).
20 *Bafna, S. S., Sun, T., De Souza, J. P., Baird, D. G.:* Polymer 34 p.708 (1993).
21 *Chung, T.:* Plast. Eng. Oct. p. 39 (1987).
22 *Blizard, K. G., Baird, D. G.:* Polym. Eng. Sci. 27, p. 654 (1987).
23 *Blizard, K. G., Federici, C., Federico, O., Chapoy, L. L.:* Polym. Eng. Sci. 30, p. 1442 (1990).
24 *Nobile, M. R., Awendola, E., Nicolais, L., Acierno, D., Carfagna, C.:* Polym. Eng. Sci. 29, p. 244 (1989).
25 U.S. Patent 5 225 488 (1993), *Baird, D. G., Sukhadia A. M.*
26 *Sukhadia, A. M., Datta, A., Baird, D. G.:* Intern. Polym. Process. 7 p. 218 (1992).
27 *Sukhadia, A. M.:* Ph.D. Thesis, Virginia Polytechnic Institute and State University, VA. U.S.A. 1991.
28 *Sabol, E. A.:* MS. Thesis, Virginia Polytechnic Institute and State University, VA, U.S.A. 1994.
29 *Taylor, G. I.:* Proc. Roy. Soc. A146 p. 501 (1934).
30 *Wu, S.: Polym.* Eng. Sci. 27 p. 335 (1987).
31 *Chen, S. J., MacDonald, A, R.:* Chem. Eng. March, p. 105 (1973).
32 *Mutsakis, M., Streiff, F. A., Schneider, G.:* Chem. Eng. Prog. July, p. 42 (1986).
33 *Wissburn, K. F.:* Brit. Polym. J. December p. 163 (1980).
34 *Lin, Y. G., Winter, H.H.:* Macromol. 21 p. 2439 (1988).

4.0 Composites Materials

Preface

The third objective of this work is the focus of this chapter. Specifically, the determination of the optimal properties attainable in a planar isotropic composite produced from blend strands is discussed. Furthermore the aspect of optimization of the properties of strands through melt drawing is also discussed (objective one). The chapter organized as a manuscript which will be submitted to *Polymer Composites* for subsequent publication.

Composites Based on Drawn Strands of Thermotropic Liquid Crystalline Polymer Reinforced Polypropylene

E. A. SABOL, A. A. HANDLOS *and* D. G. BAIRD

The Department of Chemical Engineering
Polymeric Materials and Interfaces Laboratory
Virginia Polytechnic Institute and State University
Blacksburg, VA 21041

(ABSTRACT)

This paper is concerned with the use of two thermotropic liquid crystalline polymers (TLCPs), HX1000 and Vectra B950, to reinforce a thermoplastic matrix of polypropylene (PP). The goal of this work was to pregenerate the optimal TLCP reinforcement in the PP then process the material at a lower temperature than the melting point of the TLCP to form a composite structure. Specifically, strands of the blend materials were produced using a dual extrusion process which resulted in the formation of axially continuous TLCP fibrils within the PP matrix. It was found that the mechanical properties of the strands were greatly improved by increased draw ratio and that optimal reinforcement, as predicted by the rule of mixtures, could be achieved. Initial studies indicated that injection molding and sheet extrusion of the pelletized strands caused the TLCP phase to agglomerate and deform which resulted in a reduction of the potential mechanical property enhancement. However, the TLCP fibrillar morphology of the pregenerated strands was maintained during compression molding which resulted in uniaxial composites with properties equal to or greater than the properties of the strands. In addition, composites were made using a compression molding process in which strands were randomly oriented prior to consolidation in order to show the limits of properties possible in composites produced from the pregenerated strands. It was found that this process could be used to produce composites in which the mechanical properties were isotropic in the plane of the sample and approached the property limits predicted by composite theory. Additionally, it was found that many of the mechanical properties of the VB/PP materials were greatly enhanced by the addition of a maleated PP throughout the composite forming process.

4.1 Introduction

The blending of polymers has been widely established as a cost effective method of producing materials with superior mechanical, thermal, and impact properties relative to those of the neat polymers (1). Recently, blends consisting of thermotropic liquid crystalline polymers (TLCP) and thermoplastics have been the focus of much academic and industrial interest (2-4). Much of this interest is due to the unique morphology that is formed in these blends during processing operations where extensional flow fields are developed. Specifically, the TLCP phase in these blends can form oriented fibrils that provide mechanical reinforcement to the matrix phase. These blends are called *in situ composites* because the fibril reinforcement is formed during processing.

The most important property of TLCPs for the reinforcement of thermoplastics is high strength and stiffness which is a result of their highly rigid molecular architecture, but the properties developed in a TLCP are dependent on the operation by which they are processed (2,5-7). For example, a thermotropic liquid crystalline polyesteramide consisting of 2-hydroxy 6-napthoic acid (HNA), terephthalic acid (TA), and 4'-hydroxy acetanalide, commercially known as Vectra B950 (VB), processed through fiber spinning develops a modulus of 75 GPa (9). However, the same material processed through injection molding has been reported to develop a machine direction modulus in the range of 16.5 to 29.2 GPa depending on the mold geometry and injection conditions (10). Hence, it is widely accepted that the highest properties possible for TLCPs are only achieved through processes like fiber spinning where uniaxial extensional flows are predominant and high molecular orientation of the TLCP can be achieved (2,11,12).

The properties of TLCPs also typically display a high degree of anisotropy due to their rodlike molecular structure which is easily aligned and oriented in the flow direction during processing (8). Directional dependence of properties is desirable in processes such as fiber spinning but proves to be a disadvantage in the production of materials such as films and injection molded parts where isotropic

properties are typically desired. For example, Jackson and Kuhfuss (8) investigated the properties of an injection molded TLCP based on poly(ethylene terephthalate) (PET) and HBA as a function of the mold thickness. They found that the TLCP exhibited a machine and transverse direction modulus of 17 and 1.4 GPa, respectively, when a mold thickness of 1.5 mm was used whereas machine and transverse direction properties of the samples produced with a mold with a thickness of 12 mm were the same but only equal to 2 GPa. Hence, the highest machine direction properties of TLCPs are associated with the highest degree of anisotropy.

Many of the same limitations seen in the pure TLCPs are also seen in their blends with thermoplastics. In particular in situ composites exhibit a high degree of anisotropy and process dependent properties. However, for in situ composites the properties are not only dependent on the molecular orientation of the TLCP phase but also the TLCP morphology. For example, injection molded in situ composites can exhibit both a high degree of anisotropy and a "skin core" type of morphology. Skin core morphology is characterized by the material close to the mold wall exhibiting highly oriented TLCP fibrils whereas the material closer to the center of the sample contains less oriented TLCP droplets (2). Because the morphology and molecular orientation of the TLCP phase are dependent on the strength and direction of the flow field, the properties of in situ composites are highly dependent on the processing operation.

It has been found that the highest properties in in situ composites, just as in neat TLCPs, are a product of processes that subject the material to a strong elongational flow field. Processes such as fiber spinning and strand and film drawing are all extensional in character. However, fiber spinning produces the strongest and most uniform extensional flow field and has been found to generate the highest properties of in situ composites (11-13). For example, in a study by Crevecouer (13) in situ composite sheets and fibers with 20 wt.% of a thermotropic liquid crystalline copolyester composed of HBA and 2-hydroxy 6-napthoic acid, commercially known as Vectra A (VA), in a miscible blend of polystyrene and poly(phenylene-ether) were produced. The machine direction modulus of the films was 4 GPa while

fibers of the same composition exhibited a modulus in excess of 10 GPa. Additionally, the sheets showed a large degree of anisotropy in physical properties as is seen in injection molding of in situ composites.

While fiber spinning has been shown to produce the highest properties in conventional in situ composites, the properties are still restricted by the necessity of overlapping processing temperatures of the blend constituents. Specifically, TLCPs of the highest strength and stiffness typically have processing temperatures in excess of the thermal processing range of many widely used and inexpensive thermoplastic polymers such as polypropylene and polyethylene. Thus, the range of possible combinations of TLCPs and matrix materials that can be used to produce in situ composites is limited.

To overcome the limitation of a required overlap of processing temperatures of the blend components and to exploit the benefits associated with drawing operations, a novel dual extrusion process (DEP) was developed. The DEP was initially developed and patented by Baird and Sukhadia (14-16) and subsequently improved by Sabol (17). This process (*Fig. 2-1*) utilizes two single screw extruders. One extruder plasticates the matrix material while the other plasticates the TLCP. The continuous polymer streams from each extruder are then joined in a phase distribution system which is followed by a series of static mixers that distribute the TLCP within the matrix phase. The blended material is then extruded through a die for final shaping of the in situ composite which is subsequently drawn to promote additional TLCP fiber formation and orientation. Several advantages of this system over typical methods of in situ composite formation include: (1) the TLCP and matrix materials can be processed when there is no overlap of the processing temperatures of the components with minimal degradation of the matrix; (2) the formation of the reinforcing fibrils relies on the splitting and geometric rearrangement of continuous TLCP phases as a result of the static mixers as opposed to the coalescence and elongation of dispersed droplets which is seen in traditional in situ composite processes; and (3) independent thermal histories can be imparted to the polymer streams prior to mixing.

The properties of drawn strands produced by means of the dual extrusion method have been shown to be higher than those of strands produced by blending in a single screw extruder. For example,

Sukhadia et al. (16) compared the properties of strands of 30 wt.% VA in a PET matrix produced using both single and dual extrusion techniques. Under the same drawing conditions (both draw ratios equal to 40), the strands produced from the dual extrusion process had a tensile modulus of 19 GPa while strands produced by blending in a single screw extruder had a modulus of 13 GPa. This 46% improvement in tensile modulus was attributed to the morphology of the strands produced using the dual extrusion process containing predominately axially continuous fibrils whereas the strands produced using the single screw extruder exhibited a skin-core morphology.

The purpose of this work is to use the dual extrusion process to produce strands in which the optimal reinforcing effect is provided by the TLCP phase and to then evaluate the properties of composite materials produced from the strands under processing conditions where the TLCP is not melted. In particular composites based on blends of TLCPs with PP in which the reinforcing fibrils were pregenerated under more optimal conditions than conventional in situ composites are produced and the effects of the pregenerated fibrils on the properties of the composites are investigated. Furthermore, the limit of possible properties of the blend strands and the composite materials based on the pregenerated strands is determined.

4.2 Experimental

4.2.1 Materials

Two TLCPs were used in this study. HX1000, supplied by DuPont, is an amorphous copolyester based on hydroquinone, terephthalic acid and other hydroquinone derivatives (2). It has a glass transition temperature of approximately 185°C (18) and a density of 1.25 g/cm^3. This material is typically processed in the range of 290 to 365°C. The second TLCP, Vectra B950 (VB), was purchased from the Hoechst Celanese Company. VB has a glass transition temperature of 110°C and a melting point of 280°C with a

density of 1.41 g/cm^3 (9,10). The rheology of HX1000 and VB, pertinent to processing via the dual extrusion method is discussed in references 17 and 15, respectively.

Polypropylene (PP) was used as the matrix in this study and was Profax-6823 purchased from the Himont Company. The PP has a melt flow index of 0.8 and the following characteristics: T_m =161°C, M_w ≅ 600,000, M_w/M_n = 5 and a density of 0.902 g/cm^3 (19). For the VB/PP blends the matrix PP was sometimes mixed with 10 wt.% maleic anhydride grafted polypropylene (MAP) supplied by Uniroyal. The MAP has a melt flow index of 50 and has been shown to contain 0.75 wt.% maleic anhydride (10). MAP was added to the blend by dry blending it with the PP prior to processing. Glass reinforced PP was also processed to provide a comparison of properties to composites based on pelletized drawn strands. The glass filled PP (PF072-2) was purchased from the Himont Company and contains 20 wt.% glass fibers.

4.2.2 Strand Processing

To determine the properties of the blend components as a function of draw ratio, strands of pure VB, HX1000 and PP were prepared using a single screw extruder with a capillary die with a diameter of 3.175 mm and L/D=1. The pure HX1000, VB and PP were extruded at melt temperatures of 310, 325 and 280°C, respectively, and drawn under ambient conditions.

Strands of HX1000/PP and VB/PP were generated using the dual extrusion process shown schematically in *Fig. 2-1*. The dual extrusion system consists of two single screw extruders (Killion model KL-100, diameter 24.5 mm with L/D=24) in which the matrix material and TLCP were plasticated separately. In some cases a Zenith 1.725 cc/rev gear pump was placed directly after the TLCP extruder to accurately meter the melt flow rate. The melt streams were then joined in a phase distribution system which introduced the TLCP phase through twelve injection ports. The injection ports were symmetrically

aligned before the first element in a series of 18 Kenics mixing elements (12.7 mm diameter) which blended the materials. The blend was extruded through a 3.176 mm capillary die with L/D=1 to form a strand that was subsequently drawn in a vertical drawing chimney (12 m long and 90 mm in diameter). The drawing chimney was introduced to increase the temperature during drawing as well as to insulate the strand from air currents inherently present in the processing environment which caused strand instabilities at high take-up velocities. After drawing, the material was quenched in a water bath to solidify the molten blend strand and freeze the resultant morphology and orientation.

The composition of the blend was determined using several methods. For the experiments in which the gear pump was used, the gear pump RPM versus flow rate was initially determined at the final processing temperature and pump inlet pressure (2700-3500 psig). The resulting linear calibrations were used to set a fixed TLCP flow rate into the blending system. The rotational speed of the screw in the matrix extruder was then adjusted to maintain a constant total blend flow rate of 40 g/min. Prior to the installation of the gear pump, the compositions of the blends were determined by timing the disappearance of a known weight of polymer in the TLCP extruder while monitoring the total blend flow rate. The output of each extruder was then adjusted to the final blend composition and total flow rate. The composition in both cases was measured by removing the PP after the blend was prepared by heating a known weight of the blend in an oven at 290°C for at least two hours. This caused the PP to be completely oxidized leaving only the TLCP. The composition was determined by the residual weight of TLCP compared to the original blend weight. The compositions determined by this test correlated well with the compositions determined by the gear pump method described above.

4.2.3 Secondary Processing of Strands

Once strands were produced using the dual extrusion system, they were further processed through various methods to form composite materials. Composite materials were formed from pelletized strands through sheet extrusion, injection molding and compression molding of both uniaxially and randomly aligned strands.

Injection molding of pelletized strands was carried out by using an Arburg Allrounder injection molder (model 221-55-250). Strands were first pelletized with an average length of approximately 6 mm then used as the feed for the molding process. Plaques were made in an end-gate mold (T-distribution manifold) with dimensions of 75 x 80 mm with mold thickness of 1.5 mm. Neat PP was also injection molded to determine the properties of the matrix processed under the same conditions as the composite materials.

Undrawn films were produced from pelletized in situ composite strands by using a 101.6 mm wide sheet die (coat hanger distribution manifold) with a gap thickness equal to 1.5 mm attached to a single screw extruder. The melt temperature was maintained at approximately 205°C. Neat and glass filled PP were also processed under the same processing conditions to serve as a comparison with the sheets produced from blend strands. Due to the irregular surface appearance of composites sheets, it was necessary to compression mold the samples prior to mechanical property testing. This was done by using a water cooled Carver laboratory press (Model 2696) and a 76 x 76 mm picture frame mold. The samples were initially heated to 180°C then pressed under an initial pressure of 300 psig which subsequently declined during sample solidification.

Composite samples in the form of plaques were produced by compression molding drawn blend strands. To determine if the properties of the blend strands produced as a function of draw ratio were maintained through the compression molding process, uniaxially compression molded plaques were produced. Samples were produced from approximately 11.5 g of strands cut to a length of 70 mm. The

strands were placed in a 76 x 76 mm picture frame mold and aligned. The mold was then heated to a temperature of 190°C and subsequently pressed in the water cooled laboratory press to a final thickness of 1.5 mm under an initial pressure of 300 psig.

A second compression molding process (*Fig. 2-5*) was used to produce composite samples with more planar isotropic mechanical properties. The process is composed of multiple compression molding steps of randomly arranged strands. Initially, 4 g of strands were cut and arranged in a 152 x 152 mm picture frame mold. The material was then heated to 220°C and pressed at an initial pressure of 700 psig. Three 152 x 152 mm samples were made in this fashion. These laminates were then cut into four 76 x 76 mm laminates. The twelve total laminates were then placed in a 76 x 76 mm picture frame mold, heated to 205°C and pressed to a final thickness of 1.5 mm under an initial pressure of 875 psig to form the final plaque.

4.2.4 Mechanical Testing

The tensile modulus and strength of individual strands were measured using an Instron mechanical tester (model-4204). An initial gap length of 148 mm was used with a crosshead speed of 0.5 mm/min. The cross sections of the strands were typically elliptical. Therefore, the cross sectional area of the strands and subsequently the draw ratios (the ratio of the cross sectional area of the die to that of the strand) were determined using the major diameter, D_1, and minor diameter, D_2, of the strand and the equation for the area of an ellipse ($A = \pi/4 D_1 D_2$). The tensile properties of the strands are the average of properties at specific take-up velocities with an average error of 4 and 5 % for tensile modulus and strength, respectively. Tensile strength values are not reported for neat TLCPs due the samples breaking in the grips which lead to high errors and tensile strengths that were unrealistically low.

The tensile and flexural properties of composite samples (injection molded, compression molded strands and extruded sheets) were also measured. The samples were cut into 9 mm wide rectangular bars and sanded to minimize cutting marks. The tensile properties of the bars were evaluated using the Instron testing machine and an extensiometer (Instron model 2630-25). The crosshead speed was maintained at 1.27 mm/min for all tensile tests. Samples were also tested for flexural properties by using a three-point bending test and the Instron testing machine. The crosshead speed during flexural property testing was determined with respect to sample thickness according to ASTM standards (ASTM D 790M-86).

4.2.5 Morphology

The morphology of strands and plaques was observed by using optical and scanning electron microscopy. Optical microscopy was performed using a Zeiss Polarizing light microscope. Scanning electron microscopy was done using a Stereoscan-S200 with an accelerating voltage of 15kV. Samples were prepared by means of cryogenic fracture after immersion in liquid nitrogen for at least 5 minutes. The fractured samples were fixed to aluminum stubs and coated with a layer of gold using a SPI Sputter Coater to enhance conductivity.

4.3 Results and Discussion

The results of this work are organized as follows. The effects of drawing on the properties of the neat materials are presented in an effort to facilitate the comparison of properties with the composite materials. Second, the properties developed in the composite strands produced using the dual extrusion process are discussed The properties of secondary composite formation through injection molding and

sheet extrusion are then discussed. Finally, compression molding of both uniaxially and randomly arranged strands is discussed. Furthermore, the effect of the presence of 10 wt.% MAP on the properties of VB/PP composites is presented.

4.3.1 Neat Polymer Properties

The neat PP and both TLCPs were extruded as strands and drawn in order to ascertain the properties of the blend components prior to composite formation. Specifically, the objective was to determine the effects that draw ratio has on the properties of the pure materials and to determine the ultimate properties possible in these materials attained using a similar processing method as the blend strands. The role played by the processing conditions described in this section will facilitate a clearer understanding of the properties developed in the composite materials.

The moduli of both HX1000 and VB strands were dramatically improved as the draw ratio was increased (*Fig. 3*). In particular the modulus of HX1000 increased monotonically from less than 35 GPa in the undrawn state to a plateau modulus of 53.3(4.1) GPa for draw ratios in excess of 50 (standard deviations given in parentheses). The measured modulus of VB was found to be similar to HX1000 in the undrawn state but continued to increase for draw ratios of up to 100. This behavior is similar to that reported by the manufacturer (9), but their data indicates that the ultimate properties are achieved at a draw ratio of approximately 30. This difference might be attributed to differences in processing conditions which were not reported in the product literature. Nevertheless, the ultimate measured modulus of 70.4(5.2) GPa for VB corresponds well with the as-spun fiber modulus of 75 GPa reported by the manufacturer (9).

Polypropylene was also extruded and drawn to determine the effect that the draw ratio had on the properties of the matrix material. The tensile modulus and strength of the PP remained unaffected by the

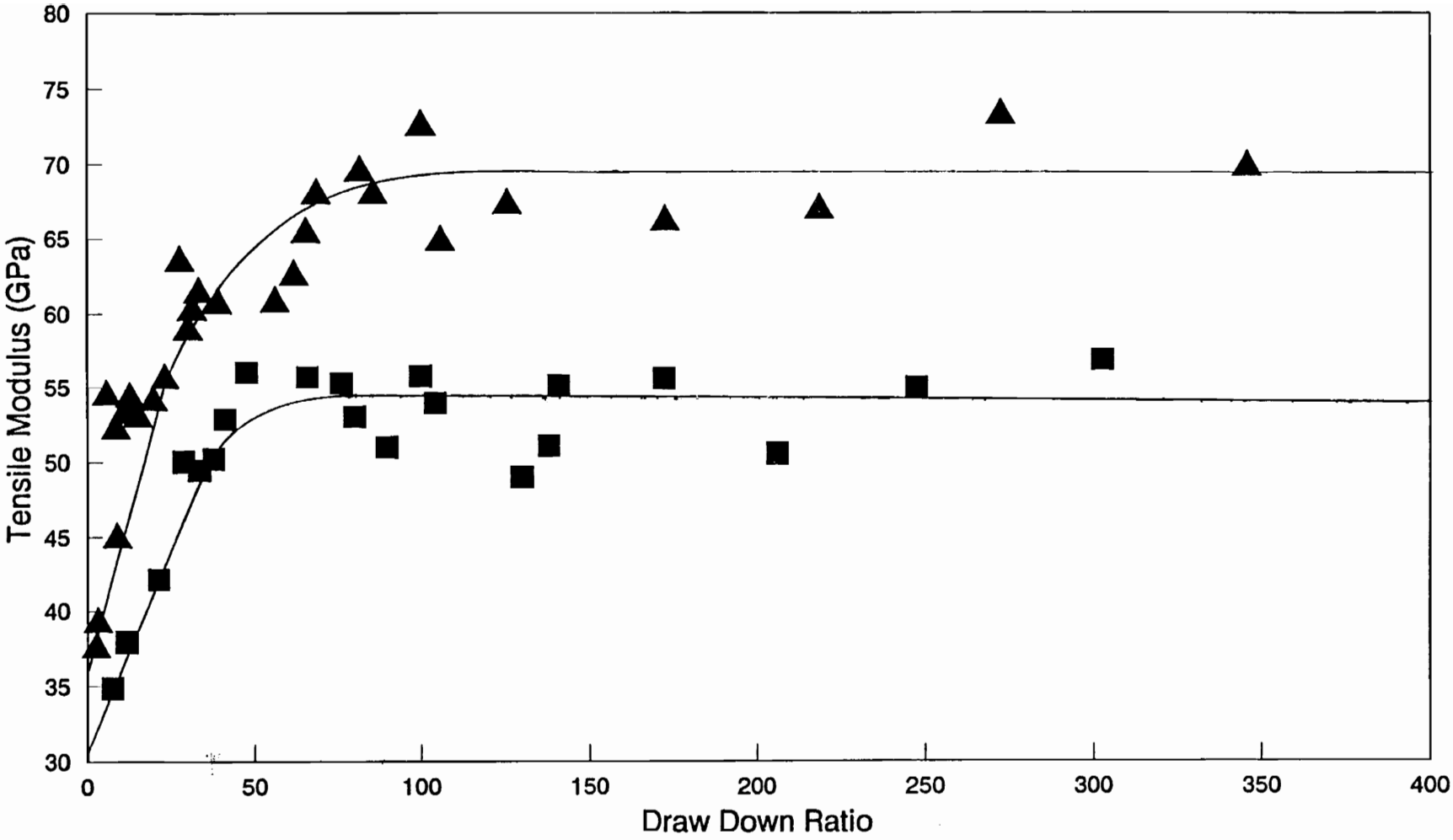

Figure 3: Tensile modulus versus draw ratio for TLCP strands (▲) Vectra B950 and (■) HX1000.

draw ratio over the range of draw ratios examined. The modulus was found to be 0.98(0.18) GPa while the strength was 23.2(3.9) MPa for the entire range of draw ratios tested. The lack of property enhancement in neat PP with increased draw ratio was attributed to the time scale of drawing being greater than the relaxation time of the PP. Therefore, there was insufficient transfer of stress between the PP molecules to induce orientation and subsequent property enhancement. In comparison with flexible chain polymers, TLCPs have very long relaxation times which allow them to orient at much lower extension rates and maintain orientation for longer periods of time once stresses are removed (2). From these experiments it can be concluded that trends seen in the properties of the blend strands with draw ratio can be attributed to changes in the orientation of the TLCP and not the PP matrix.

4.3.2 Drawing of Blend Strands

As was seen in the neat TLCP strands, as the draw ratio of composite strands was increased the modulus also increased. As illustrated in *Fig. 4,* the tensile modulus of the 18 wt.% HX1000 strands increased from 5 GPa to 8 GPa as the draw ratio was increased from 5 to 25, respectively, while the tensile modulus of the 27 wt.% composition increased from 5 to over 12 GPa as the draw ratio was increased from 5 to 20, respectively. Both blends show a monotonic increase in modulus with increasing draw ratio with no plateau region at high draw ratios (as was seen with the neat TLCP). The lack of a plateau region in the blend strands was attributed to the limited amount of data obtained at draw ratios higher than those reported. The production of higher draw ratios was hindered by the blend strand slipping in the nip rollers at high take-up velocities and tensions when the strand was correspondingly quite small. Nevertheless, the highest measured modulus values of the blend strands compare quite favorably with the values predicted by the rule of mixtures using the ultimate fiber modulus of HX1000 as the modulus of the reinforcing phase. In this case, the predicted moduli of the 18 and 27 wt.% blends are

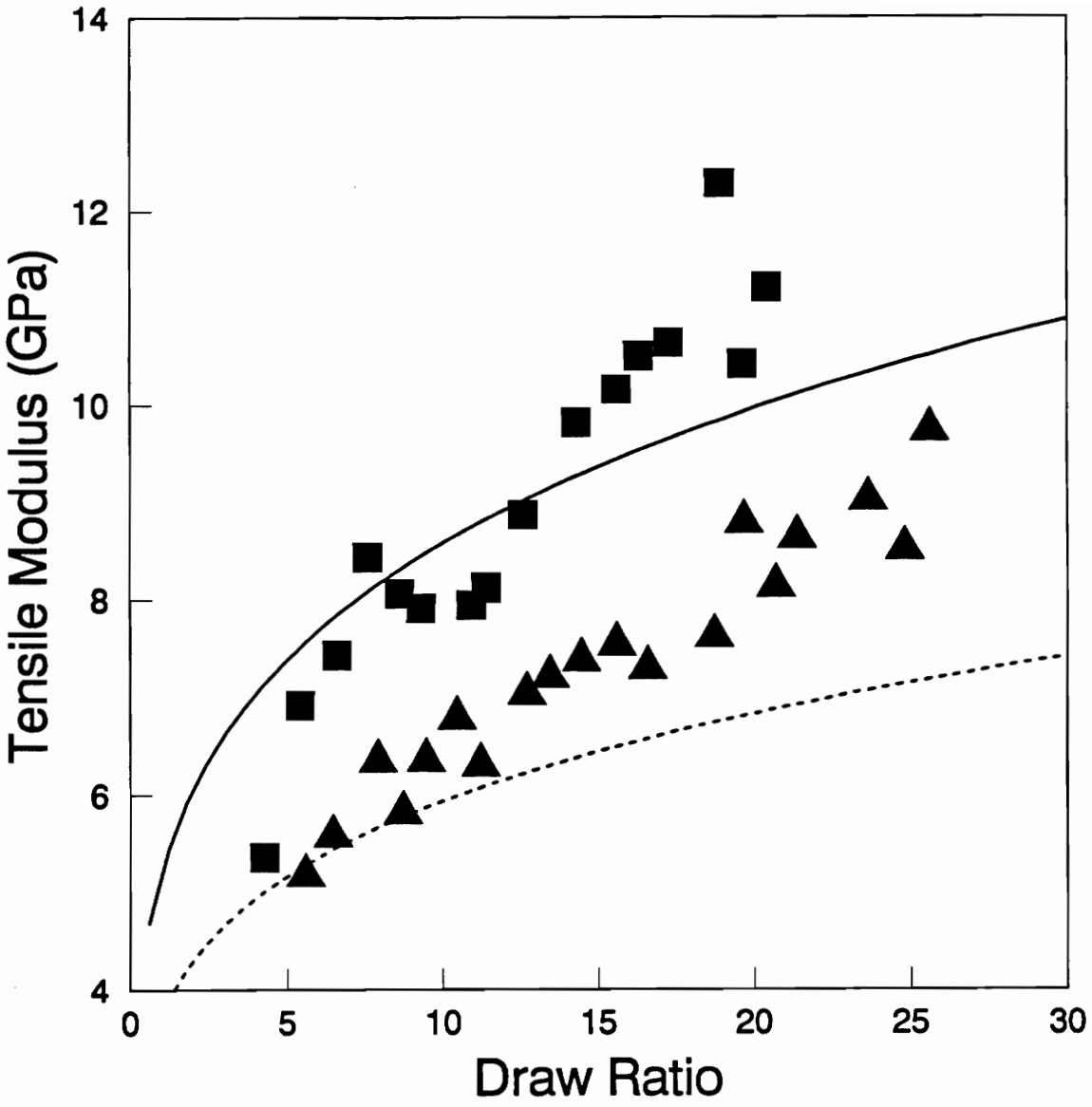

Figure 4: Tensile modulus versus draw ratio for HX1000/PP strands: (▲) and (■) are experimental experimental data and (·····) and (——) are the rule of mixtures predictions based on using the modulus of VB as a function of draw ratio for a 18 and 27 wt.% HX1000 compositions, respectively.

8.2 and 12.0 GPa, respectively. However, if the modulus of the blend strands is calculated by means of the rule of mixtures and the modulus values of HX1000 measured at each draw ratio, the prediction does not correspond well with the experimental data. In particular the experimentally determined moduli of the blend strands increased at a much higher rate with draw ratio than was predicted by the rule of mixtures. This might indicate that the TLCP fibrils within the blend strands are orienting more readily at the higher draw ratios tested in comparison with the neat materials.

The HX1000/PP blends showed an increase in tensile strength with increased draw ratio (*Fig. 5*). However, the data exhibits a clear difference between the strength of the 18 and 27 wt.% compositions only at the highest draw ratios tested. This is probably the result of the tensile strength data being more inaccurate due to irregularities in the strand cross sections which caused the strands to break prematurely. Nevertheless, the measured tensile strength for the 18 wt.% HX1000 strands increased from 52 to 68 MPa as draw ratio increased from 5 to 25 while the strength of the 27 wt.% HX1000 strands increased from 52 to 72 MPa as the draw ratio was increased from 5 to 20.

The morphology of the 18 wt.% HX1000/PP strands consisted of axially continuous fibrils and ribbons that decreased in cross sectional area with increased draw ratio. The TLCP morphology can be observed in the scanning electron micrographs of cryogenically fractured strands presented in *Fig. 6.* The strand with lower draw ratio (*Fig. 6a*) exhibits TLCP fibrils and ribbons in the range of 1 to 10 μm in diameter and width, respectively. In the more highly drawn strand (*Fig. 6b*) the TLCP phases are no larger than 5 μm in width and the majority of fibrils are under 1 μm in diameter. The TLCP phase size reduction combined with the increasing physical properties as a function of increasing draw ratio both indicate that the TLCP remained molten throughout the drawing process. This is significant because premature freezing of the TLCP phase has limited the achievable draw ratios of other in situ composites processed as fibers (13, 21,22).

While properties measured in the strands produced using the HX1000/PP achieved the limits predicted by the rule of mixtures, the blend of VB/PP required the use of maleic anhydride grafted

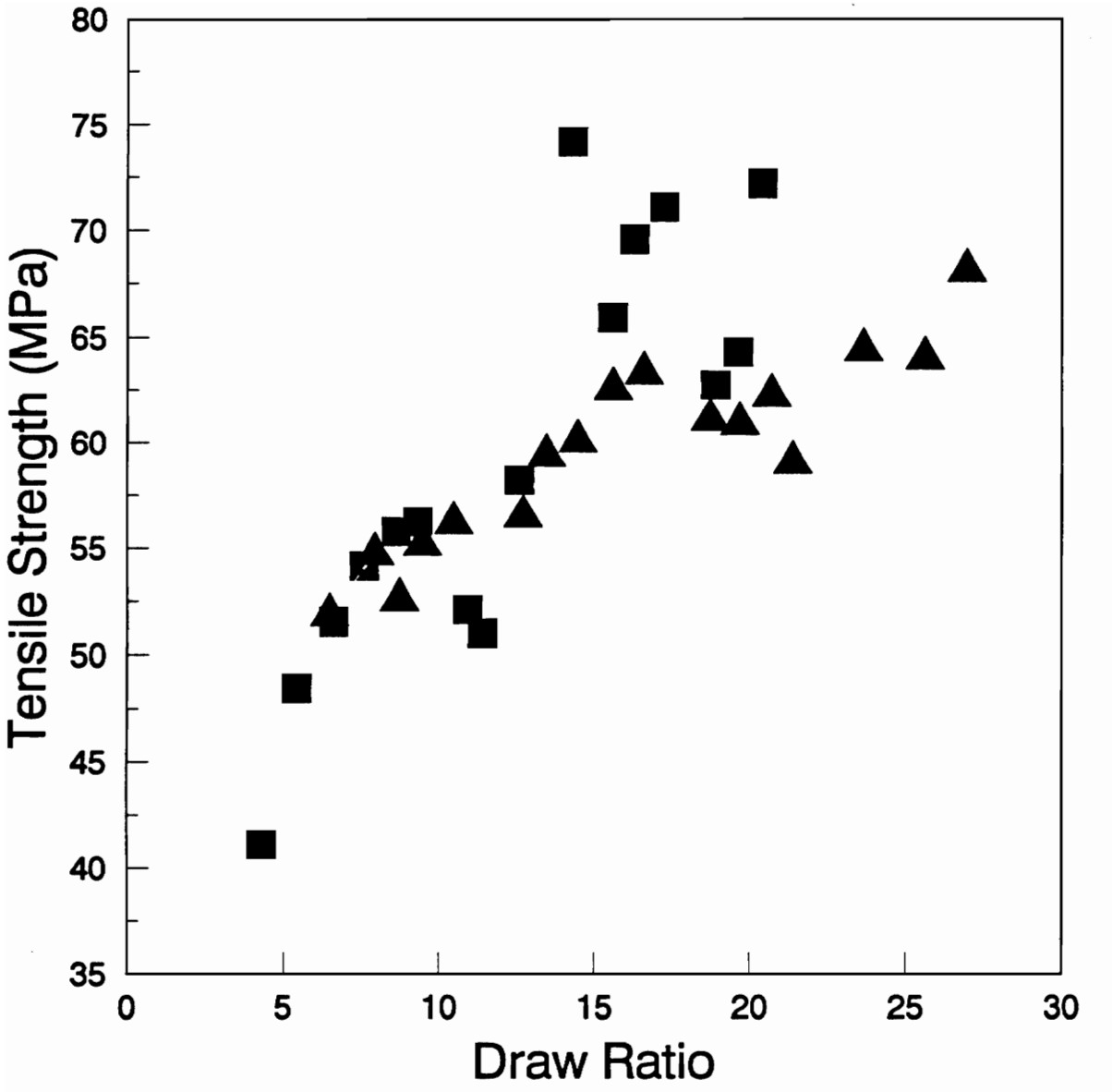

Figure 5: Tensile strength versus draw ratio for HX1000/PP blends produced using the dual extrusion process with (▲) 18 and (■) 27 wt.% HX1000.

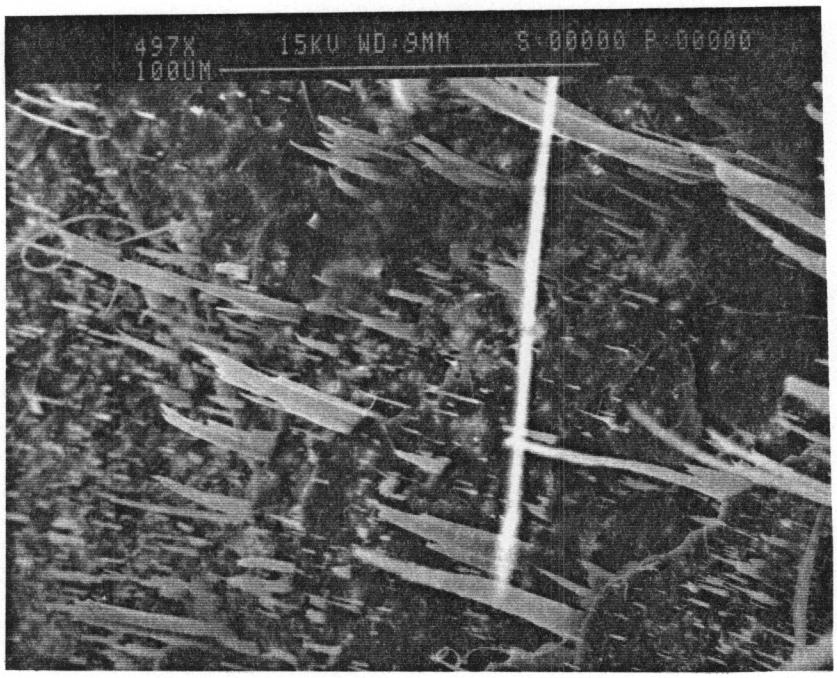

(a)

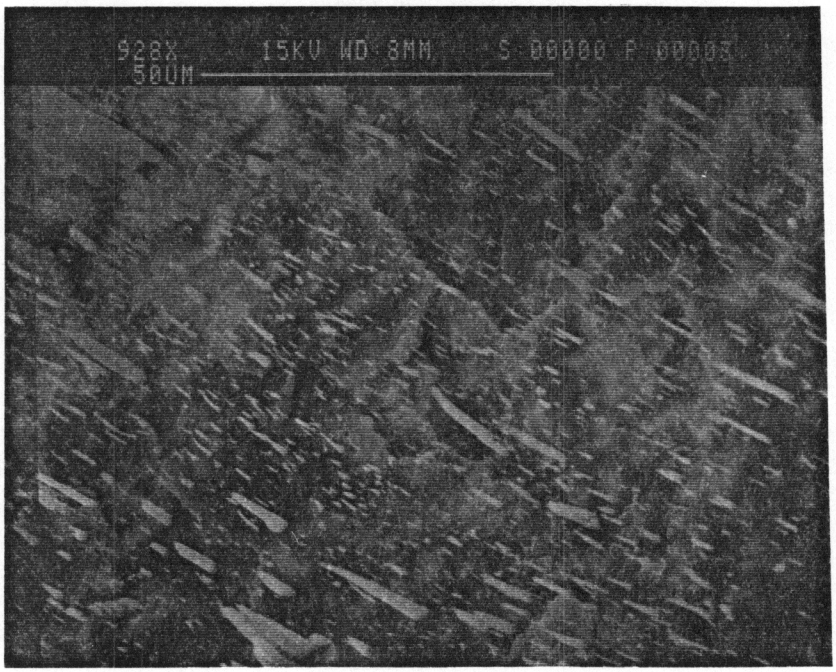

(b)

Figure 6: Scanning electron micrograph of 18 wt.% HX1000/PP strands with the following draw ratios of (a) 6.3 and (b) 13.0.

polypropylene (MAP) to reach optimal properties. The presence of MAP lead to higher draw ratios in this blend because to acted it stabilize the drawing process. Furthermore, the modulus of the strands which contained MAP showed an improvement in modulus at a given draw ratio as compared to blends where MAP was not used. For example, the presence of 10 wt.% MAP increased the tensile modulus of 25 wt.% VB strands by at least 15% for each of the draw ratios tested as seen in *Table 1*. However, the tensile strength did not show consistent improvement with the addition of 10 wt.% MAP. Scanning electron microscopy revealed no perceivable difference in the morphology of the strands with the addition of the MAP. Thus, the presence of the MAP is likely to have improved the properties by affecting the adhesion of the TLCP and PP in contrast to causing a change in morphology which is indicative of a change in compatibility of the materials (23). However, the role of MAP in the enhancement of the properties of the drawn strands is not exhaustive as only one level of MAP was used.

The full range of tensile properties as a function of the draw ratio is illustrated for a 30 wt.% VB/PP(10 wt.% MAP) blend in *Figs. 7 and 8*. Qualitatively, the effect of draw ratio on the properties of the blend strands is very similar to the blend of HX1000 and PP. In particular, the tensile modulus of the VB/PP strands increased from approximately 9 GPa for the undrawn sample to over 16 GPa for draw ratios in excess of 60 (*Figs. 7*). The tensile strength of the strands also increased over the range of draw ratios from less than 90 MPa to 160 MPa (*Fig. 8*).

The highest measured tensile properties for the VB/PP blend compared quite favorably with the predicted properties using the rule of mixtures. Similar to HX1000 the measured moduli of the blend strands were in excess of the modulus predicted by using the rule of mixtures and the modulus of VB at each draw ratio but a significant deviation is seen only at the highest draw ratios tested (*Fig. 7*). Nevertheless, the properties of the strands produced at the highest draw ratios corresponded well with the properties predicted using the rule of mixtures and the manufacturer reported properties for VB which are 75 GPa and 650 MPa for modulus and strength, respectively. In particular the predicted modulus of the 30 wt.% VB blend is 17 GPa and the predicted strength is 160 MPa. Thus, it appears that the use of a

Table 1: The effects of 10 wt.% MAP and draw ratio on the mechanical properties of 25 wt.% VB/PP drawn strands.

	0 % MAP		10 wt.% MAP	
Draw Ratio (V_f/V_o)	Strength (MPa)	Modulus (GPa)	Strength (MPa)	Modulus (GPa)
1.8	76.3 (7.5)	6.8 (0.7)	79.1(9.1)	8.3 (1.0)
8.2	99.0 (9.9)	9.8 (1.0)	91.1 (7.6)	11.26 (0.4)
20.6	110.4 (16.3)	11.4 (1.3)	114.0 (10.0)	13.41 (1.4)

Note: Standard deviations give in parentheses

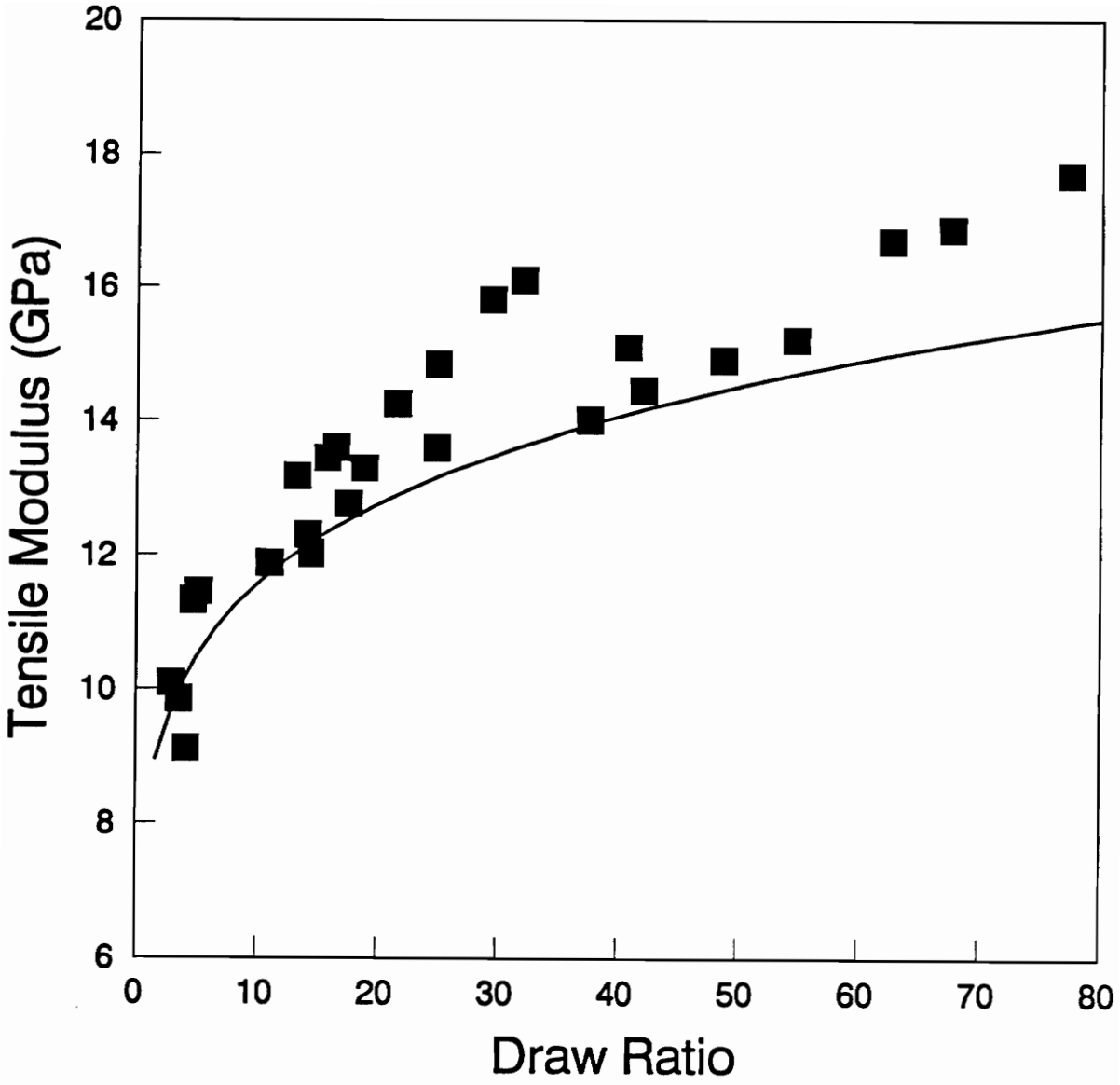

Figure 7: Tensile modulus versus draw ratio for 30 wt.% VB/PP(10 wt.% MAP) strands produced using the dual extrusion process: (■) experimental data and (——) the rule of mixtures based on using the modulus of VB as a function of the draw ratio.

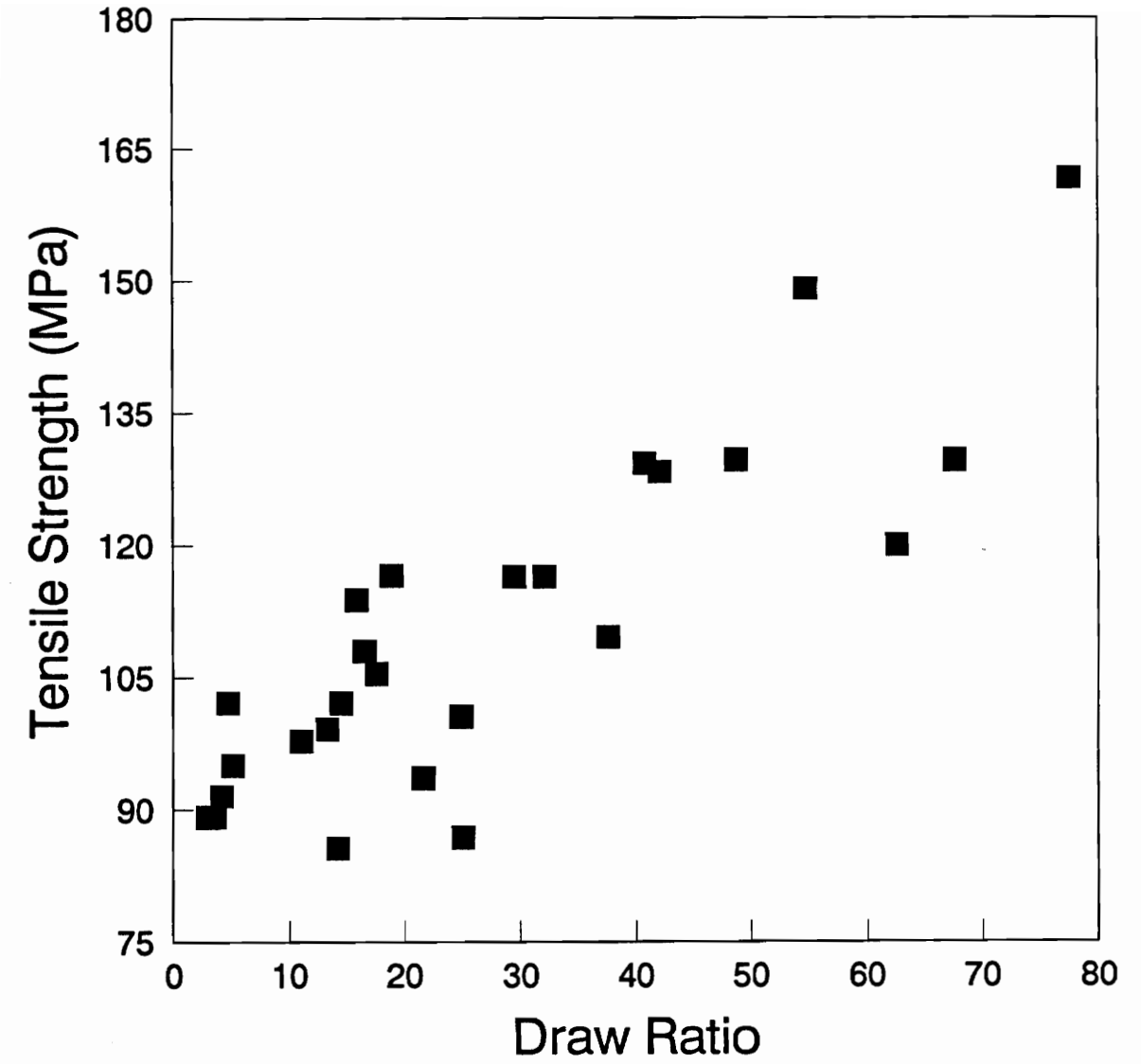

Figure 8: Tensile strength versus draw ratio for 30 wt.% VB/PP(10 wt.% MAP) strands produced using the dual extrusion process.

simple rule of mixtures, in combination with the as-spun fiber properties of the TLCP, predicts the ultimate properties of blend strands produced using the dual extrusion process quite well.

4.3.3 Injection Molding

To test the concept of using the drawn strands as a short fiber composite material, drawn strands of 24 wt.% VB/PP (10 wt.% MAP) were used as the feed for the production of injection molded samples. The goal of this work was to determine if injection molding of pelletized strands below the melting point of the TLCP could generate plaques with improved mechanical properties and reduced anisotropy over those produced above the melting point of the TLCP. In particular, strands were initially drawn to a draw ratio of 28 and had a modulus and strength of 10.4(1.6) GPa and 80.5(12.5) MPa, respectively. The strands were then pelletized and processed. The temperature of the last heating zone and nozzle of the injection molder was varied from 250 to 300°C in steps of 10°C which encompassed a range of processing temperatures from above to below the melting point of VB which is 280°C.

The tensile moduli of the injection molded plaques determined in both the machine and transverse direction are presented in *Fig. 9* as a function of the temperature in the last heating zone of the injection molder. The machine direction modulus for processing temperatures below 270°C was approximately 2.3 GPa. As the processing temperature was increased through the melting point of the TLCP the modulus increased to a value in excess of 3.7 GPa. The modulus transverse to the machine direction was not significantly affected by the processing temperature and remained below 1.8 GPa. The tensile modulus of the blend materials did improve over the properties of the neat PP which exhibited a machine and transverse modulus of 1.12(0.04) and 1.00(0.81) GPa, respectively.

A very similar trend was seen in the behavior of the tensile strength as a function of the processing temperature (*Fig. 10*) for injection molded VB/PP strands. The transverse direction strength

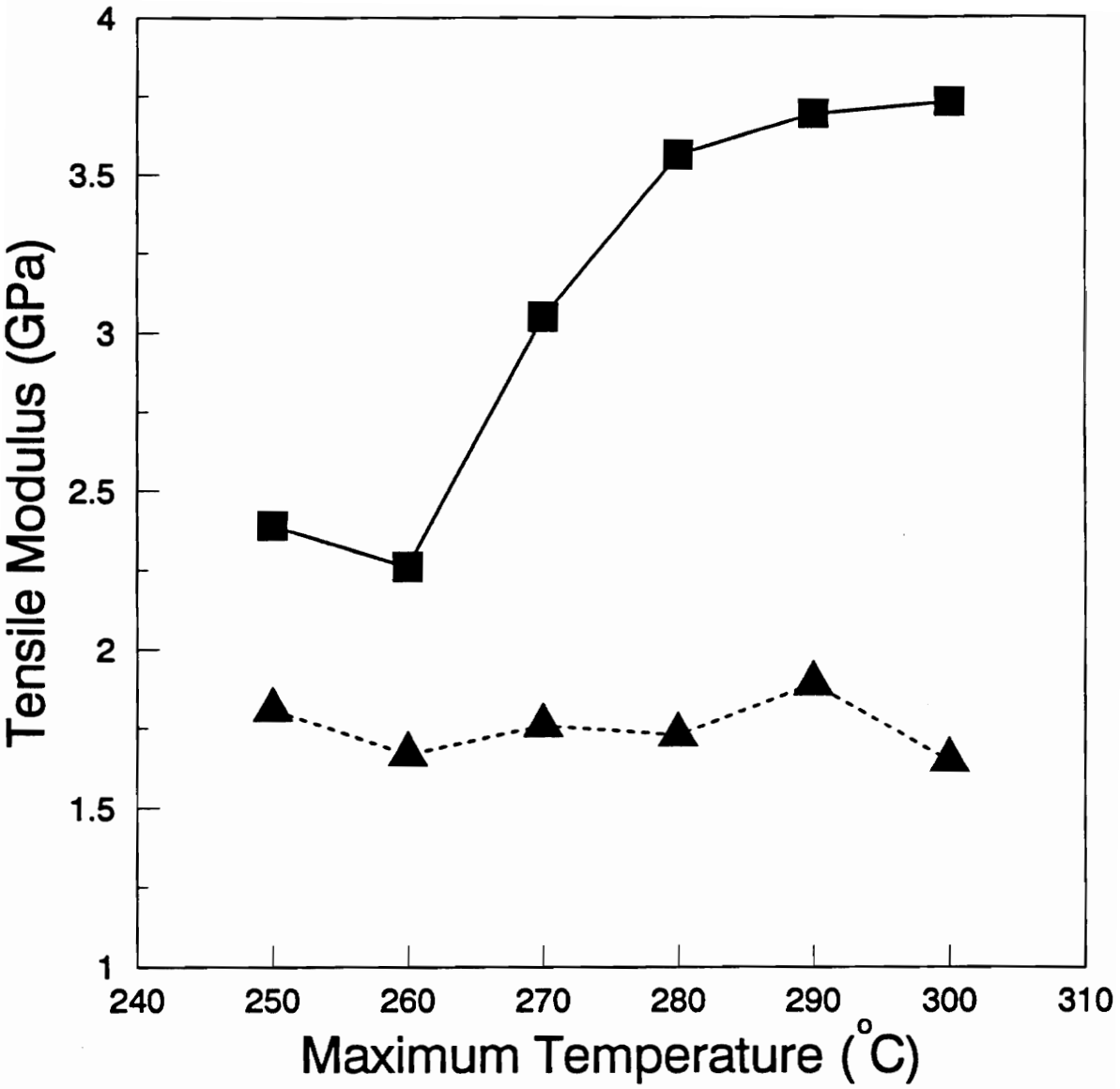

Figure 9: Tensile modulus versus third zone temperature for injection molded samples produced from pelletized strands of 24 wt.% VB/PP(10 wt.% MAP), (■) machine and (▲) transverse direction properties.

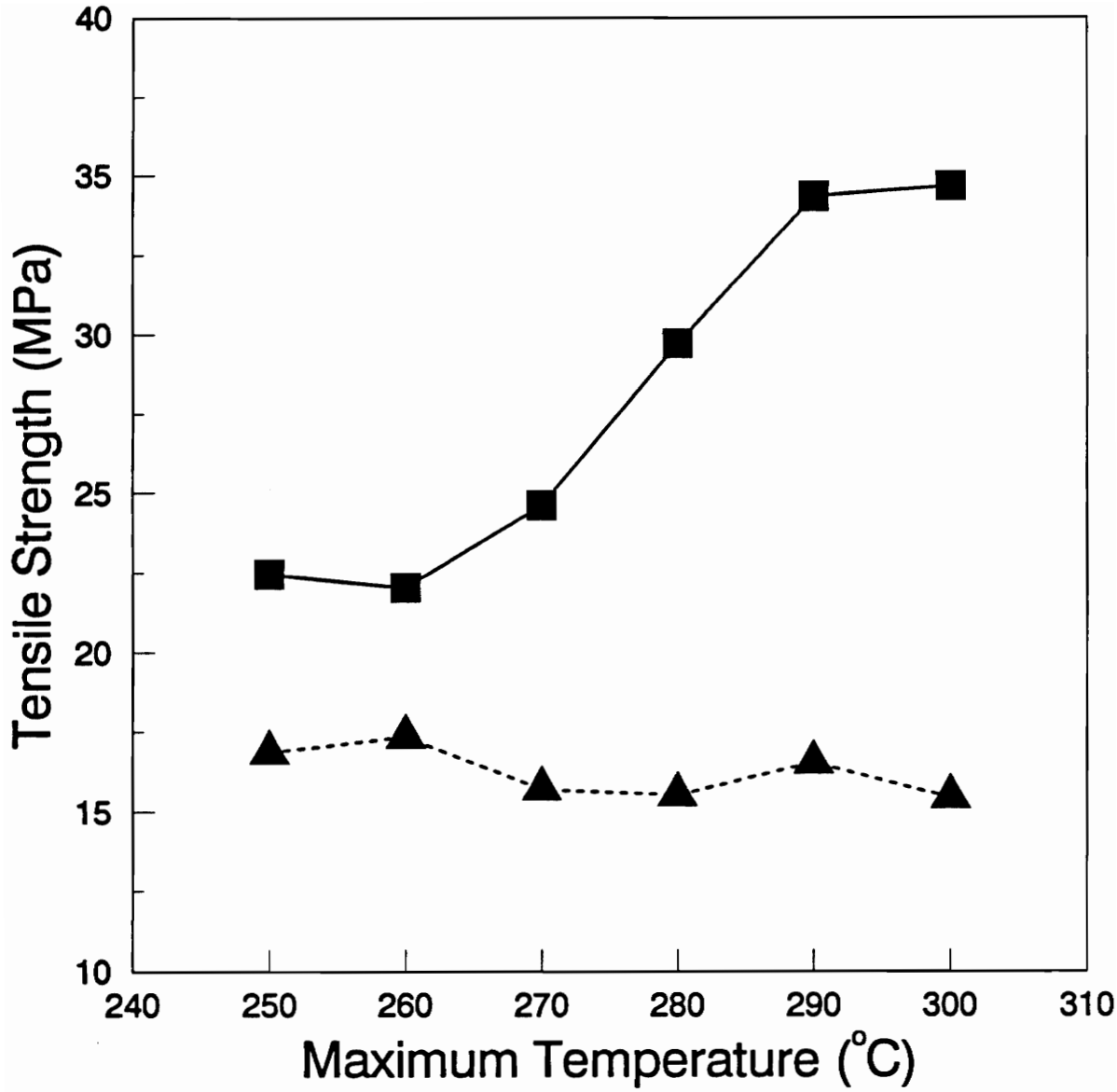

Figure 10: Tensile strength versus third zone temperature of injection molded samples produced from pelletized strands of 24 wt.% VB/PP(10 wt.% MAP), (■) machine and (▲) transverse direction properties.

was on the average 17 MPa and not measurably affected by the transition from a solid to molten TLCP phase. In addition the transverse tensile strength was less than that of pure PP, which was found to be 25.6(0.61) MPa. The strength of the composite in the machine direction was 22 GPa for processing temperatures below 270°C and reached a value of 34 GPa at the highest processing temperatures. This represents poor reinforcement except at high processing temperatures when compared with the machine direction strength of pure PP, which is 28.1(0.81) MPa.

The significant effect of processing temperature on the directional dependence of properties is related to the transition from a molten to a solid TLCP phase. The properties generated in the material processed at temperatures below 270°C are close to being isotropic, but this is due to the machine direction properties being quite low. The plaques produced above the melting point of the TLCP are essentially conventional in situ composites because all of the original morphology and orientation imparted during the strand formation process has been lost due to the TLCP melting prior to the mold filling step. Hence, they show a high degree of directional dependence in properties as is characteristic of injection molded in situ composites.

The poor property enhancement seen in the plaques produced at the lower temperatures is attributed to the TLCP fibrils present in the precursory strands deforming and breaking up as a result of the injection molding process. The morphology of the plaques processed at a temperature of 250°C can be seen in the optical micrograph shown in *Fig. 11.* As can be observed in the micrograph, the TLCP fibrils are clearly not being maintained as rigid reinforcing fibrils.

The morphology seen in the composites might be attributed to processing significantly above the Tg of the TLCP in the severe environment of the injection molding process. Specifically, the screw in the injection molder rotated at 200 rev/min. Furthermore, the apparent shear rate, γ_a, in the injection nozzle, given by $\gamma_a = 4\langle V_z \rangle / R$, where $\langle V_z \rangle$ is the average velocity and R is the radius of the capillary, was estimated as being on the order of 10,000 sec^{-1} (24). These harsh processing conditions contributed to the destruction of the TLCP fibrillar morphology during processing and the lack of property enhancement in

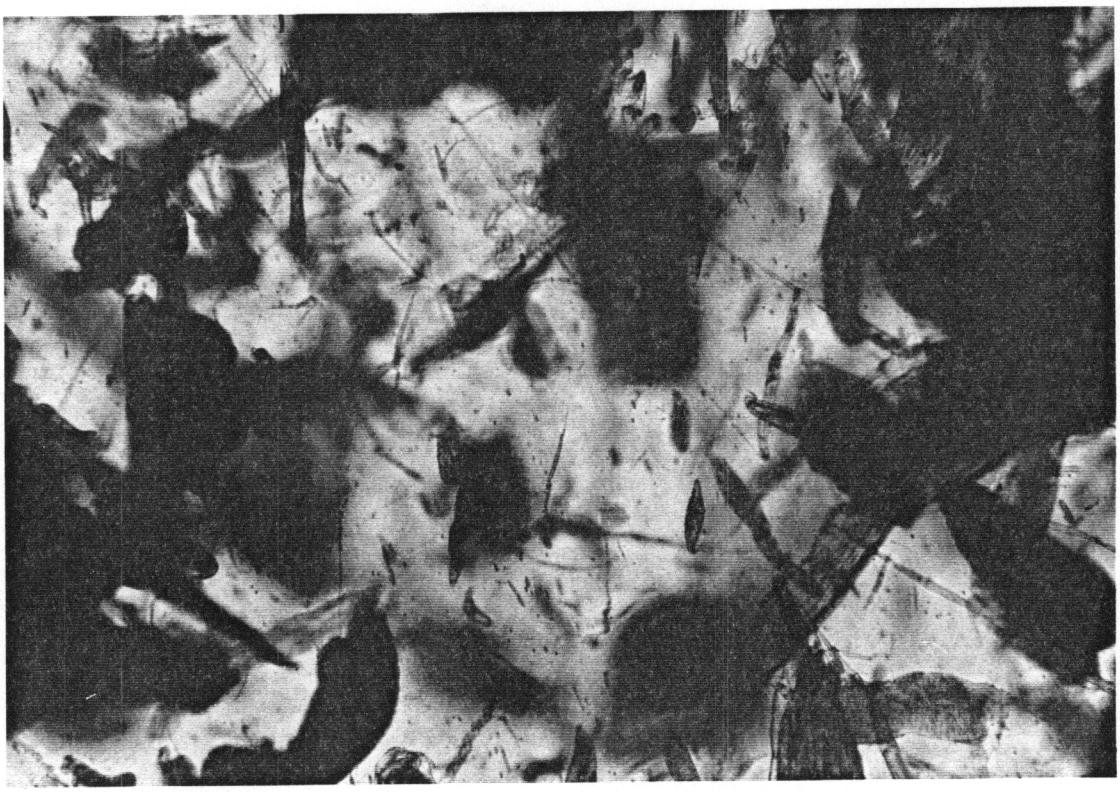

Figure 11: Optical micrograph of an injection molded samples produced from pelletized drawn blend strands and processes at a maximum temperature of 250°C (—— 60 μm).

the resulting composites. The processing temperatures were below the melting point of the TLCP but they were still significantly above the Tg of VB, which is 110°C. Hence, the use of TLCPs with higher glass transition or melting temperatures or processing at greatly reduced temperatures might lead to a better morphology and transfer of properties from the drawn strands to those of the injection molded samples.

4.3.4 Extrusion of Sheets

Pelletized strands were processed through sheet extrusion which is a continuous process which can produce materials with planar isotropic properties but is a much less harsh processing environment as compared with injection molding. Specifically, pelletized drawn strands of 29 wt.% HX1000 were processed by means of sheet extrusion to determine if the properties generated in the strands as a result of increased draw ratio could be transferred to the properties of the sheets. The process was operated at 205°C and the speed of the extruder screw was maintained at only 7 rev/min to minimize stress on the TLCP fibrils. Thus, the sheet extrusion process was much less rigorous than the injection molding process discussed in the previous section. Additionally, the HX1000 has a higher processing temperature than VB indicating that it may retain its properties through the sheet extrusion process. Sheets of 20 wt.% glass filled PP were also processed into extruded sheets to provide a comparison with a more conventional short fiber composite material.

The machine direction tensile properties of 29 wt.% HX1000 sheets are reported in *Table 2.* The tensile strength and modulus of the sheets do not show significant reinforcement due to the presence of the TLCP phase nor are there any clear trends in the properties with increased draw ratio of the precursor strands. The tensile strength of the composite sheets was lower than that of the matrix material while the modulus showed an average improvement of only 55% over the modulus of the neat

Table 2 : Mechanical properties of extruded sheets produced from pelletized strands of 29 wt.% HX1000/PP.

Precursor Strand Draw Ratio	Strength (MPa)	Modulus (GPa)
2.27 (0.20)	18.6 (1.5)	1.58 (0.36)
6.67 (1.35)	20.0 (1.1)	1.68 (0.44)
15.39 (4.18)	21.6 (0.6)	1.35 (0.19)
26.83 (3.29)	17.3 (0.6)	1.60 (0.12)
PP Machine Direction	25.6 (0.15)	1.01 (0.07)
PP Transverse Direction	26.3 (0.55)	0.99 (0.04)
20 wt. % Glass/PP Machine Direction	41.8 (1.9)	2.10 (0.12)
20 wt. % Glass/PP Transverse Direction	42.1 (0.8)	2.18 (0.10)

Note: Standard deviations given in parentheses

PP. The properties of the 20 wt.% glass reinforced PP, while higher than the HX1000/PP sheets, also showed only a slight improvement in modulus relative to the neat PP. This is only a qualitative statement because the matrix material and fiber loading were different. However, the glass filled system did show significant enhancement of the tensile strength not seen in the sheets generated from the pelletized drawn strands. In addition, the properties of extruded sheets showed no machine or transverse direction dependence.

The poor tensile strength measured in the extruded sheet obtained from pelletized strands was caused by the TLCP fibrils deforming and agglomerating during processing. An optical micrograph of glass filled PP is presented in *Fig. 12a* and shows glass fibers of approximately 10 microns in diameter with measured aspect ratios from 2 to over 100 which were oriented randomly on a global scale. This fibrillar arrangement is in contrast to the arrangement seen in *Fig. 12b* obtained from the film based on HX1000/PP strands (26.8 draw ratio). In this sample, the TLCP phase is in the form of bundles of fibers in excess of 10 μm in diameter. This indicates that the bundles of TLCP fibrils (each having a diameter on the order of one micron) formed in the drawn strands are remaining partially intact through the extrusion process. This morphology is believed to be due to the TLCP being flexible and having a very high aspect ratio which allows them to entangle during processing. In contrast, the rigid glass fibers either break in the stress fields generated in the extruder and die or remain intact. However, it may be possible to reduce agglomeration in blend systems by using TLCPs with higher melting points and larger scale processing equipment.

In an attempt to reduce the degree of agglomeration of the TLCP fibrils, HX1000/PP sheets were also made from pellets with much lower aspect ratios. Specifically, pregenerated strands (draw ratio of 28.3) were cut into pellets of less than 2 mm in length. This effectively reduced the reinforcing fiber aspect ratio by a factor of five compared with the strands used to produce the films discussed above. Still, the actual TLCP fibrils in these strands had aspect ratios on the order of 1000

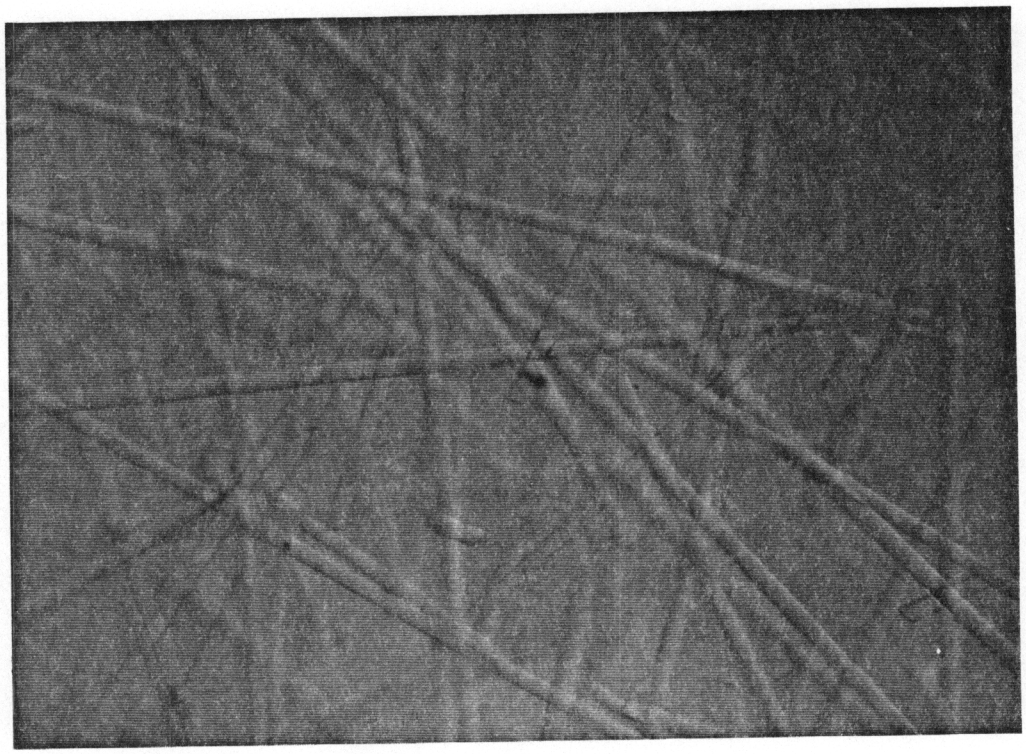

A

B

Figure 12: Optical micrographs of extruded sheets (a) 20 wt.% glass reinforced PP and (b) sheet produced from pelletized HX1000/PP strands (— 10 μm).

which should have been adequate to provide significant property enhancement to the composite sheets. However, the TLCP phase in these sheets also showed a high degree of agglomeration leading to mechanical properties even lower than the sheets produced from the longer pellets. In particular the tensile modulus and strength of the sheets produced from the shorter pellets were 0.79(0.06) GPa and 17.1(0.7) MPa, respectively.

From this section, it was found that the properties of the composite sheets based on pelletized strands were balanced in the machine and transverse direction but not as high as would be expected if the TLCP fibrils were to have remained rigid and randomly oriented on a global scale. Additionally, it was found that the properties of the sheets were reduced as the length of the strand precursor was reduced. This indicated that to achieve the highest properties in a planar isotropic composite based on drawn strands the length of the precursor material must be high and must be maintained through the processing operation. These findings prompted the use of compression molding as a method of processing pregenerated strands because both the length and morphology of the strands can be controlled through processing.

4.3.5 Compression Molding of Uniaxially Aligned Strands

In situ composite strands produced using the dual extrusion method were further processed through compression molding. The goal of this work was to determine if the properties measured in the strands could be maintained through the compression molding process. Specifically, strands of both HX1000/PP and VB/PP were processed at a temperature of only 190°C to minimize loss of orientation and

mechanical properties of the TLCP phase during processing. Furthermore, the blend of VB/PP was processed with and without 10 wt.% MAP to determine if the property enhancement seen in the strands was maintained in the compression molded materials. Many of the properties of the VB/PP uniaxial composites increased with the presence of 10 wt.% MAP, but it should be noted that the full effect of MAP on the physical properties of the uniaxially aligned compression molded materials is not yet completely understood because only one level of MAP was used.

The results of compression molding of drawn strands of 29 wt.% HX1000/PP are presented in *Table 3*. The data indicates that the uniaxial composite strength and modulus (measured in the strand direction) are similar or higher than the properties measured by the single strand method. For example, the tensile modulus of the most highly drawn strands and uniaxial composites based on those strands are 12.55 and 13.55 GPa, respectively, which compare well with the modulus of 12.9 GPa predicted by the rule of mixtures using 53.3 GPa as the modulus of the HX1000 fibrils. Similarly, the tensile strength of the strands of the highest draw ratio was 62.2 MPa while the uniaxial composite strength was measured as 67.0 MPa. Again indicating that the properties of the strands are directly transferred to uniaxially aligned composites.

The flexural strength and modulus of the HX1000/PP uniaxial samples also increased with increased draw ratio of the pregenerated strands (*Table 3*). In particular the flexural strength and modulus of the composite samples increased by 46 and 76 %, respectively, as the draw ratio of the precursor strands increased from 2.27 to 26.83. The flexural properties in the fiber direction of the uniaxial composites also showed a significant improvement over the neat matrix material. The highest flexural strength and modulus measured in the composites were 96.7 MPa and 11.45 GPa, respectively. This represents an improvement of the flexural strength of PP by a factor 2.3 while the flexural modulus improved by a factor of 10 over that of PP.

The tensile strength of the uniaxially aligned plaques produced from VB/PP strands showed slight improvement with increased draw ratio but no measured effect with addition of the 10 wt.% MAP

Table 3: Mechanical properties of 29 wt.% HX1000/PP compression molded samples produced from drawn blend strands.

Draw Ratio ⇩		Tensile Strength (MPa)	Tensile Modulus (GPa)	Flexural Strength (MPa)	Flexural Modulus (GPa)
2.27 (0.20)	Strand	37.7 (5.5)	4.42 (0.68)	-	-
	Uniaxial	60.5 (2.1)	8.06 (0.63)	66.2 (1.5)	6.49 (0.25)
	Random [2 mm]	9.6 (0.9)	1.73 (0.18)	29.3 (4.3)	2.01 (0.18)
	Random [10 mm]	13.6 (2.8)	1.87 (0.37)	37.7 (7.7)	2.24 (0.24)
	Random [20 mm]	20.2 (4.7)	2.81 (0.68)	39.0 (3.5)	2.60 (0.18)
	Random [30 mm]	24.5 (2.4)	2.84 (0.62)	47.5 (7.9)	2.67 (0.70)
6.7 (1.4)	Strand	42.0 (6.7)	7.66 (1.24)	-	-
	Uniaxial	66.9 (5.4)	12.15 (1.03)	83.0 (4.4)	9.42 (0.06)
	Random [2 mm]	13.1 (1.6)	1.99 (0.22)	28.1 (0.8)	1.94 (0.14)
	Random [10 mm]	17.6 (2.7)	2.98 (0.25)	46.8 (5.8)	3.11 (0.31)
	Random [20 mm]	21.3 (3.4)	3.40 (0.73)	44.6 (3.1)	3.13 (0.12)
	Random [30 mm]	30.1 (4.3)	4.29 (0.47)	50.3 (6.9)	3.07 (0.13)
15.4 (4.2)	Strand	68.6 (9.2)	12.36 (2.09)	-	-
	Uniaxial	73.2 (5.4)	12.19 (0.65)	95.2 (3.6)	10.37 (0.60)
	Random [2 mm]	15.3 (0.5)	2.57 (0.22)	38.7 (1.4)	2.67 (0.08)
	Random [10 mm]	24.1 (2.3)	3.15 (0.45)	46.8 (9.2)	3.04 (0.22)
	Random [20 mm]	28.2 (0.4)	4.77 (0.92)	54.0 (4.9)	3.52 (0.37)
	Random [30 mm]	29.0 (3.0)	4.73 (0.76)	55.2 (6.1)	3.32 (0.21)
26.8 (3.3)	Strand	62.2 (8.8)	12.55 (1.60)	-	-
	Uniaxial	67.0 (4.2)	13.55 (2.75)	96.7 (1.8)	11.45 (0.21)
	Random [2 mm]	15.2 (1.1)	2.54 (0.09)	40.3 (2.9)	2.67 (0.16)
	Random [10 mm]	25.6 (2.7)	2.95 (0.53)	59.2 (1.8)	3.69 (0.13)
	Random [20 mm]	32.3 (1.3)	4.55 (0.45)	56.3 (2.1)	3.53 (0.29)
	Random [30 mm]	34.9 (3.5)	4.42 (0.34)	61.9 (2.5)	3.88 (0.23)
Composite[a]	Uniaxial	-	12.9	-	-
Theory	Random	-	5.6	-	-
	PP	25.9 (0.4)	1.00 (0.06)	41.0 (1.8)	1.13 (0.07)

Notes: Strand length in the compression molding process given in brackets and standard deviations given in parentheses and (a) composite theory using measured fiber modulus of 53.3 GPa.

(*Table 4*). The tensile strength of the uniaxially aligned plaques with 0 and 10 wt.% MAP increased from 92.7 and 89.9 GPa to 101.0 and 100.0 GPa, respectively, when draw ratio was increased from 1.8 to 20.6. The measured tensile strength of the uniaxial plaques is higher for the low draw ratio strands as compared with the properties measured in the strands (*Table 1*). For example, the lowest draw ratio strands with 0 % MAP shows a strength of 79.0 MPa while the composite plaque had a measured strength of 92.7 GPa. This dissimilarity may be due to differences in the testing methods of the strands compared with the plaques. Specifically, the composite materials were tested with an extensiometer while the strain in the strand samples was calculated by displacement of the grips which held the strand.

The tensile modulus of the uniaxially aligned VB/PP plaques increased with increased draw ratio and presence of 10 wt.% MAP as was seen in the properties of the strands. The tensile modulus increased for each draw ratio by approximately 1 GPa with the addition of the 10 wt.% MAP. The tensile modulus of the plaques also increased with increased draw ratio. For example, the plaques produced with 10 wt.% MAP increased from 11.4 to 12.7 GPa as draw ratio of the precursor strands was increased from 1.8 to 20.6, respectively. Again the properties of the compression molded plaques were higher than the strands at the lower draw ratios but became similar at higher draw ratios (*Table 1*). In addition, the highest tensile modulus of 12.7 GPa is only 10 % lower than the modulus of 14 GPa predicted by the rule of mixtures (calculated using the 75 GPa as the modulus of VB).

The flexural properties of the uniaxially oriented compression molded VB/PP plaques also increased as a result of increased draw ratio but only strength was measurably increased by the presence of MAP. The flexural strength of the 0 and 10 wt.% MAP uniaxial composites increased from 91.7 and 103.5 MPa to 113.8 and 116.0 MPa, respectively, as the draw ratio of the precursor strand increased from 1.8 to 20.6. The flexural modulus increased an average of 10% over the same range of draw ratio but the highest modulus of 11.9 GPa was measured in the material with no MAP. Many of the properties of the VB/PP uniaxial composites increased with the presence of 10 wt.% MAP but its' full effect on the physical

Table 4: The effect of 10 wt.% maleated PP on the mechanical properties of 25 wt.% VB/PP compression molded samples produced from drawn blend strands.

Draw Ratio ⇨ (V_f/V_0)		1.8		8.2		20.6		Composite Theory[a]
Sample		Tensile Properties						
	Maleated PP	Strength (MPa)	Modulus (GPa)	Strength (MPa)	Modulus (GPa)	Strength (MPa)	Modulus (GPa)	Modulus (GPa)
Uniaxial	0 %	92.7 (8.3)	10.7 (1.0)	95.4 (9.9)	10.6 (0.6)	101.0 (6.9)	11.8 (0.6)	14
	10 wt.%	89.9 (4.7)	11.4 (1.0)	95.6 (7.5)	11.7 (1.1)	100.0 (3.8)	12.7 (1.0)	14
Random	0 %	29.0 (3.4)	3.6 (0.3)	29.4 (2.8)	2.8 (0.4)	40.8 (0.8)	3.9 (0.2)	5.9
	10 wt.%	33.8 (4.5)	3.4 (0.8)	39.9 (1.6)	4.4 (0.4)	46.2 (1.0)	5.0 (0.5)	5.9

Sample		Flexural Properties						
	Maleated PP	Strength (MPa)	Modulus (GPa)	Strength (MPa)	Modulus (GPa)	Strength (MPa)	Modulus (GPa)	Modulus (GPa)
Uniaxial	0 %	91.7 (2.7)	9.1 (0.5)	106.5 (5.9)	9.4 (0.5)	113.8 (3.9)	11.9 (0.5)	-
	10 wt.%	103.5 (3.5)	10.5 (0.3)	112.2 (2.1)	11.5 (0.5)	116.0 (4.0)	11.6 (0.3)	-
Random	0 wt.%	51.4 (4.2)	2.7 (0.5)	59.0 (5.2)	2.5 (0.1)	63.1 (3.1)	3.5 (0.3)	-
	10 wt.%	50.6 (8.6)	2.6 (0.4)	65.2 (7.3)	3.5 (0.6)	67.2 (2.5)	3.5 (0.1)	-

Note: Standard deviations given in parentheses and a) composite theory using the the as spun fiber modulus of VB, which is 75 GPa, as the modulus of the reinforcing phase.

properties of the uniaxially aligned compression molded materials is not yet completely understood because only one level of MAP was used.

The results of the compression molding of the drawn blend strands below the melting point of the TLCP indicate that the tensile properties of the in situ composite strands produced using the dual extrusion system are being maintained through the compression molding process. This is qualitatively in agreement with a study by Bassett and Yee (24) in which uniaxially aligned compression molded composites of 40 wt.% VB in a polystyrene matrix were generated from fibers produced through conventional in situ composite processing (i.e., blending in the same extruder). They found that the moldings exhibited properties that approached the properties of the original in situ composite strands. In another study, Handlos and Baird (25) found that blend strands of VA/PP produced via the dual extrusion system could be compression molded below the melting point of the TLCP to form uniaxially aligned plaques with properties similar to the strands.

Thus, it was found that the conditions of the compression molding process are such that the reinforcing fibrils within the blend strands are being maintained. However, the properties of the uniaxially aligned compression molded plaques were highly anisotropic, and therefore this process can produce enhanced properties only in the strand direction. This motivated the development of a process that utilizes compression molding to maintain the high properties of the TLCP phase but produces materials with isotropic properties in the plane of the plaque.

4.3.6 Compression Molding of Randomly Oriented Strands

To utilize the advantages of compression molding and to generate samples with planar isotropic properties, the process illustrated in *Fig. 2* was developed. The process consists of multiple compression molding steps of randomly oriented strands to generate a composite with isotropic properties in the plane

of the plaque. The purpose of this approach was to evaluate the upper limit of the properties of composite materials produced from pregenerated strands. In particular, the process allows strict control of the morphology of the composite with limited loss of molecular orientation of the reinforcing TLCP fibrils.

To determine the effectiveness of the process to generate the highest possible properties in composite material, the properties of the samples were compared to those predicted using composite theory (26). Specifically, the materials were modeled as conventional random fiber composites whose tensile modulus can be predicted by,

$$E_R = \frac{3}{8} E_P + \frac{5}{8} E_T \qquad (1)$$

where E_R is the modulus of the random composite and E_P and E_T are the modulus parallel and transverse to the fiber in a uniaxially aligned composite of the same material, respectively. For composites with reinforcing fiber aspect ratios approaching infinity, the Halpin-Tsai equation indicates that E_P is given by a simple rule of mixtures (27) while E_T is predicted by an inverse rule of mixtures (28).

Compression molded plaques containing fibers of 29 wt.% HX1000 with random orientation increased in tensile strength with both increased draw ratio and initial length of the pregenerated strands as is seen in *Table 3*. In particular the tensile strength of the plaques increased by an average of 2.3 times as the initial length of the strands was increased from 2 mm to 30 mm for all draw ratios tested. Additionally, the strength of the plaques produced with the longest strands increased from 24.5 to 34.9 MPa as the draw ratio increased from 2.27 to 26.83, respectively. The highest strength indicates an improvement of 74% over the properties of the pure PP which is a significant improvement compared to the properties generated through sheet extrusion discussed previously.

The effects of strand length and draw ratio on the tensile modulus of the HX1000/PP plaques is similar to the tensile strength behavior although the properties appear to level off at high draw ratios and strand lengths. Specifically, the tensile modulus of the plaques increased by an average of 85% as the initial length of the strands increased from 2 to 30 mm for all draw ratios. The tensile modulus of the plaques produced with the longest precursor strands increased from 2.84 GPa to in excess of 4.4 GPa over

the range of draw ratios tested. The tensile modulus of the plaques produced with the higher draw ratio strands does not increase for strands in excess of 20 mm in length. Specifically, the highest tensile modulus of 4.77 GPa was observed in the plaque produced using 20 mm long strands with a draw ratio of 15.4. This represents an improvement of 4.7 times the modulus of the neat PP and approaches the modulus predicted by composite theory (*Eqn. 1*) of 5.6 GP (using 53.3 GPa as the modulus of the reinforcing fiber).

The flexural modulus and strength of the HX1000/PP composite plaques with randomly oriented fibers also show a distinct increase with increased draw ratio and length of precursor strands. From *Table 3* it is observed that the flexural strength and modulus increase by an average of 59 and 35%, respectively, for an increase in precursor strand length of 2 to 30 mm. The flexural strength and modulus of composites based on the longest initial strand lengths increased from 47.5 to 61.9 MPa, and 2.67 to 3.88 GPa, respectively, as the draw ratio of the initial strands was increased from 2.3 to 26.8. The highest flexural modulus of the plaques produced from randomly arranged fibers is more than 3.8 times the flexural modulus exhibited by neat PP. The corresponding flexural strength increased 20% over the strength of neat PP. Furthermore, comparing the properties of the random lay up samples to the properties of the uniaxially compression molded material shows an extremely favorable transfer of flexural properties from the strands to the composites. In particular, the flexural modulus and strength of the random lay up are 40 and 70%, respectively, of the properties measured in the uniaxial configurations.

The planar isotropic enhancement of properties in the compression molded composites is attributed to the laminar random arrangement of the strands. The morphology of the compression molded samples consisted of domains of TLCP fibrils that are randomly oriented on a global scale (*Fig. 13*). The domains originated from the strand precursor material and subsequently flatten as a result of compression molding. Thus, the high strength TLCP fibrils, produced in the drawing process, are being arranged

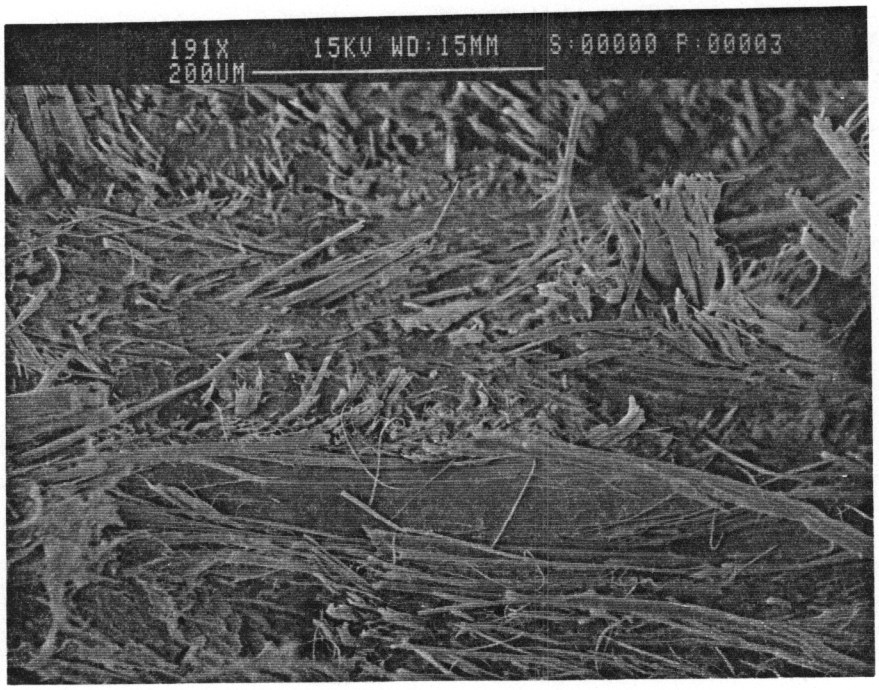

Figure 13: Scanning electron micrograph of a 29 wt.% HX1000/PP compression molded sample produced from a random configuration of draw strands.

randomly in a highly planar manner and result in the high isotropic mechanical properties in the plane of the composite sample.

Many of the same effects of draw ratio seen in the random lay up of HX1000/PP strands are also reflected in the VB/PP composites. In this case, the initial strand length was maintained at 50 mm to minimize effects due to strand length. In addition, the effect of MAP on the resultant mechanical properties was also investigated. Specifically, 25 wt.% VB/PP strands with and without 10 wt.% MAP were produced using the dual extrusion system and were compression molded in a random configuration.

The tensile strength of the samples produced from a random lay up of VB/PP strands was seen to increase with both increased draw ratio and with the presence of MAP (*Table 4*). In particular the tensile strength samples produced with 0 and 10 wt.% MAP increased from 29.0 and 33.8 MPa to 40.8 and 46.2 MPa, respectively, as the draw ratio of the precursor strands increased from 1.8 to 20.6. These findings are significant because the strength in both the strands and compression molded plaques with uniaxially oriented fibers was not seen to improve with the presence of MAP. This might suggest that the MAP is acting to increase the adhesion between the VB and PP because these effects would not be as readily seen in the properties of either the strands or the uniaxially aligned plaques where the reinforcing phase is aligned in the testing direction.

The tensile modulus of compression molded plaques produced from a random lay up of drawn strands of VB/PP increased with draw ratio but the addition of 10 wt.% MAP only affected the properties seen in the samples produced from the most highly drawn strands. Specifically, the tensile modulus of the plaques increased for the 0 and 10 wt.% MAP from 3.6 and 3.5 MPa to 3.9 and 5.0 MPa, respectively, as the draw ratio of the strands was increased from 1.8 to 20.6. Hence, the MAP lead to an increase of the modulus by almost 30% for samples produced with the highest draw ratio strands, but there was no improvement seen for strands produced with the lowest draw ratio. This might be attributed to the MAP acting to improve adhesion between the phases. The effect of adhesion (i.e., presence of MAP) would be much more evident in the material produced from higher draw ratio strands simply because the interfacial

area would be greatly increased. The effect of the MAP on the properties of the compression molded samples is not completely clear because the properties of the original strands were also seen to increase due to the presence of MAP. Hence, the improvement in the composite properties could also be attributed to the original strands having an increased modulus.

The flexural properties of the VB/PP plaques produced from a random arrangement of drawn strands improved with increased draw ratio while the presence of MAP did not show a consistent effect. The flexural modulus was seen to be unaffected by the presence of 10 wt.% MAP and increased from about 2.6 to 3.5 GPa as the draw ratio of the precursor strands was increased from 1.8 to 20.6. The flexural strength of the random composite produced with 0 and 10 wt.% MAP increased from 51.4 and 50.6 MPa to 63.1 and 67.2 MPa, respectively, as the draw ratio of the initial strands was over the same range. Thus, the MAP seemed only to measurably improve the flexural strength for the materials produced from the most highly drawn strands. However, higher levels of MAP might show a more significant effect.

The improvement in properties of VB/PP blends containing MAP are in qualitative agreement with the results of O'Donnell (10) for injection molded in situ composites. His results showed that the addition of 10 wt.% MAP to a 30 wt.% blend of VB in PP processed through injection molding resulted in an increase of the machine direction strength from 23.1 to 28.3 MPa and the machine direction modulus from 3.7 to 4.2 GPa. The tensile strength transverse to the machine direction was also improved from 11.8 to 14.6 MPa and the transverse direction modulus increased marginally from 1.5 to 1.6 GPa with the same concentration of MAP. The improvement in properties was attributed to the presence of MAP enhancing the hydrogen bonding between the TLCP and the matrix. Furthermore, his work showed that the properties continued to increase for concentrations of MAP up to 50 wt.% indicating that the properties of the materials produced from pregenerated strands might also increase with higher MAP concentration.

The properties generated in the samples produced from the random lay up of pregenerated strands were higher than the properties seen in the injection molded in situ composites of O'Donnell (10). For example, the tensile strength of the compression molded samples of 25 wt.% VB/PP (10 wt.% MAP) was 60% higher than the machine direction strength and over 3 times the transverse direction strength of the injection molded in situ composites. Furthermore, the compression molded materials were produced with 20% less VB than the injection molded in situ composites. This indicates that the compression molding of pregenerated strands produces mechanical properties in composite samples that are both higher than those obtained by means of injection molding as well as being isotropic in the plane of the sample.

In both HX1000/PP and VB/PP blends it was found that higher properties in the pregenerated strands, as a result of higher draw ratio, were are also reflected in the properties of compression molded samples containing fibers in a random orientation. This result is a direct consequence of the preservation of properties of the strands through the compression molding process as was seen in the uniaxially aligned compression molded samples discussed in the previous section. Furthermore, the compression molding process produced a TLCP morphology which is random in the plane of the sample. This is the ideal morphology that was desired in the composites processed through injection molding and sheet extrusion. Therefore, the compression molding process is believed to produce the upper limit of properties attainable in a planar isotropic composite produced from pregenerated strands.

The compression molded samples produced using randomly arranged pregenerated strands show a significant utilization of the mechanical properties of the reinforcing phase. For example, the highest tensile strength and modulus of the 25 wt.% VB/PP composite was 46.2 MPa and 5.0 GPa, respectively while the strength and modulus of the extruded sheets produced from 20 wt.% glass filled PP were approximately 42 MPa and 2.15 GPa, respectively. This is significant when one compares the tensile strength of VB to that of glass fibers. In particular the tensile modulus of VB and glass are essentially the same and equal to 75 GPa (28). Furthermore, the tensile strength of glass is in the range of 2000 to 3500

MPa (28,29) while the tensile strength of VB is only 650 MPa. Hence, the reinforcement produced in the composites based on TLCPs seems to better utilize the properties of the reinforcing material as compared to that offered by glass filled system.

4.4 Conclusions

In this study a dual extrusion process was used to pregenerate strands of VB/PP and HX1000/PP from which composite materials were produced by processing the strands at temperatures below the melting point of the TLCP. It was found that the mechanical properties of the neat TLCPs and their blends with PP, produced using a dual extrusion process, were much improved as a result of melt drawing. It was also found that the properties of the strands at the highest draw ratios corresponded quite well with the properties predicted by the rule of mixtures based on the use of the as-spun fiber moduli of the TLCPs.

The limit of properties in composite materials produced from pregenerated strands was provided by compression molding of the strands. Compression molding of uniaxially aligned pregenerated strands resulted in composite materials whose mechanical properties were the same or higher than the properties measured in the strands from which they were derived. Similar property enhancement was seen in compression molded materials produced from a random arrangement of pregenerated strands. The properties of the samples produced improved with increased draw ratio and length of the precursor strands with the highest measured properties approaching the theoretical limit predicted by using composite theory. The property enhancement seen in the compression molded materials resulted from achieving the optimal properties of the reinforcing phase in the drawing process and then maintaining the aspect ratio of the TLCP fibrils during composite formation. Thus, the compression molding of randomly oriented strands can serve as a tool to predict the limits of properties possible in composites produced from pregenerated strands. These results indicate that processes which use the high mechanical properties of

the pregenerated strands to form composite materials could be used to generate composite materials with properties which are not only higher but also more isotropic that those observed for in situ composites.

The initial studies of the use of pelletized pregenerated strands to form composites through injection molding and sheet extrusion lead to a less than ideal morphology for mechanical property enhancement. These processes caused the TLCP fibrils, formed in the strand process, to agglomerate and deform leading to poor mechanical reinforcement of the matrix. However, the properties of the composites produced in this manner might be improved by using higher melting TLCPs and processing at lower temperatures.

To achieve the highest properties in both the strands and the composites produced through compression molding in the VB/PP blends, the use of 10 wt.% maleic anhydride grafted polypropylene was required. However, a complete understanding of the effect of MAP on the properties is unclear at this point because only one level of MAP was used. Further studies are being conducted to completely evaluate the importance of the using MAP to improve the properties of the blend materials. It should be noted, however, that the presence of the MAP served to stabilize the strand during the drawing operation allowing higher draw ratios to be achieved than was possible without MAP.

4.5 Acknowledgments

The authors gratefully acknowledge the support of the Virginia Institute of Material Systems and the Army Research Office (Grant No. DAAL 03-91-G-0166) for support of this work.

4.6 References

1 D. R. Paul and S. Newman, *Polymer Blends, Vol. 1.* Academic Press, New York (1978).

2 F. P. La Mantia , *Thermotropic Liquid Crystalline Polymer Blends.* Technomic, Lancaster, PA (1993).

3 R. A. Weiss, W. Huh and L. Nicolais, *Polym. Eng. and Sci.,* **27**, 684 (1987).

4 A. Kohli, N. Chung and R. A. Weiss, *Polym. Eng. and Sci.,* **29**, 573 (1989).

5 A. J. East, L. F. Charbonneau and G. W. Calundann, *Mol. Cryst. Liq. Cryst.,* **157**, 615 (1988).

6 F. N. Cogswell in *Recent Advances in Liquid Crystalline Polymers.* ed. L. L. Chapoy, Elsevier, London (1985).

7 M. K. Cox, *Mol. Cryst. Liq. Cryst.,* **153**, 415 (1987).

8 W. J. Jackson and H. F. Kuhfuss, *J. Polym. Sci., Polym. Chem. Ed.,* **14** 2043 (1976).

9 Product literature from Hoechst Celanese

10 H. J. O'Donnell, Ph. D. Thesis, Virginia Polytechnic Institute and State University (1994).

11 W. C. Lee, A. T. Dibenedetto, J. M. Gromek, M. R. Nobile, and D. Acierno, *Polym. Eng. and Sci.,* **33**, 156 (1993).

12 Q. Lin, J. Jho and A. F. Yee, *Polym. Eng. and Sci.,* **33**, 789 (1993).

13 G. Crevecoeour, Ph.D. Thesis. Katholiede Universiteit Leuven, 1991.

14 D. G. Baird and A. M. Sukhadia, U. S. Patent No. 5,225,488 (1993).

15 A. M. Sukhadia, Ph. D. Thesis, Virginia Polytechnic Insitute and State University (1991).

16 A. M. Sukhadia, A. Datta and D. G. Baird, *Intern. Polym. Process.* 7 218 (1992).

17 E. A. Sabol, M.S. Thesis, Virginia Polytechnic Institute and State University (1994).

18 S. S. Bafna, T. Sun, J. P. de Souza and D. G. Baird, *Polymr,* **34** 708 (1993).

19 Supplier Data sheet Himont Co.

20 C. Carfagna, E. Amendola, L. Nicolais, D. Acierno, O. Francescangeli, B. Yang and R. Rustichelli, *J.Appl. Polym. Sci.,* **43** 839 (1991).

21 K. G. Blizard, C. Federici, O. Federico and L. L. Chapoy, *Polym. Eng. and Sci.,* **30** 1442 (1990).

22 R. L. Markham, *Adv. in Polym. Tech.,* **10** 231 (1990).

23 R. B. Bird, R. C. Armstrong, and O, Hassager, *Dynamics of Polymeric Liquids, Vol. 1, Fluid Mechanics,* John Wiley & Sons, Inc., New York (1987).

24 B. R. Bassett and A. F. Yee, *Polym, Composites,* **11** 10 (1990).

25 A. A. Handlos and D. G. Baird, SPE Antec '93 Prep., 1170 (1993).

26 P. K Mallick, *Fiber Reinforced Composites.* Marcel Dekker, New York (1988).

27 J. C. Halpin and J. L . Kardos, *Polym. Eng. and Sci.,* **16** 344 (1976).

28 A. A. Coller and D. W. Clegg eds., *Mechanical Properties of Reinforced Thermoplastics.* Elevier, London (1986).

29 C. E. Knox in *Handbook of Composites.* ed. G. Lubin, Van Nostrand Reinhold Co., New York (1982).

5.0 Recommendations

- The morphology developed in the dual extrusion system when Kenics mixing elements were used consisted of axially continuous TLCP ribbons. Preliminary investigations have suggested that the ribbon like structure can be maintained in sheets formed when the strand die of the dual extrusion process is replaced with a film die. This structure may be useful in producing materials with enhanced barrier properties as the barrier properties of TLCPs are typically much better than those of thermoplastics.

- The compression molding of randomly oriented strands indicated that properties generated in composite materials could reach the theoretically determined limits. One processing operation that could similarly produced composite materials with exceptional properties is the formation of weaves of pregenerated strands which could be subsequently consolidated through compression molding or thermoforming at a temperature below the melting point of the TLCP. This process would allow for clear control over the anisotropy of the composite material while utilizing the highest possible properties in the blend fibers. The production of fabrics from pregenerated strands would require that the dual extrusion process be further developed so that strands of a much smaller diameter could be produced. Dmaller diameters are required to produce a material which is flexible enough to be maintained through the weaving process.

- The multiple phase distribution system was shown to improve the degree of mixing and the axial continuity of the TLCP phase prior to the blend material entering the static mixing elements. However, the improvement could be greatly enhanced through an improved phase distribution system design.

Specifically, an initial improvement could be to decrease the diameter of the inlet ports in order to inject the secondary phase at an accelerated velocity. This could lead to the formation of individual streams if TLCP entering the matrix material further enhancing the degree of mixing prior to the blend entering the static mixers. Other improvement could include multiple injection stems or individual injection through a radial array of static mixing elements within the an advanced phase distribution system. Furthermore, the development of improved injection technology would be greatly complimented by a flow visualization study of the entry behavior of a secondary polymer stream entrring a matrix polymer stream (as in the phase distribution system).

- The dual extrusion system shows much utility in the blending of TLCPs and thermoplastics when there was limited overlap of the processing temperatures of the blend constituents. It could be worhwil would be of great utility to extend the process to other blending applications where similar limitations exist. For example, the injection of low melting temperature impact modifiers or plastisizing agents to higher melting thermoplastics could utilize the benefits of the dual extrusion technology for unique applications. Furthermore, the dual extrusion system has been shown to produced blends of low dispersed phase concentrations with improved axial concentration uniformity as compared to blending in a single screw extruder. Thus, a low concentration modifiers could be introduced with a uniform concentration as well. These factors could lead to the utilization of a process similar to the dual extrusion system for a wide variety of applications.

Appendix A : General Operating Procedure for the Dual Extrusion Process

A detailed operating procedure for the dual extrusion apparatus described in Chapter 2.0 is given in this appendix. A preexisting knowledge of the methods used in simple extrusion and the melt behavior of the matrix and dispersed phase material (i.e., appropriate process temperature settings) is assumed in this procedure. A detailed procedure for the assembly of the gear pump, piping, and mixing system is not discussed. This procedure is focused mainly on the unique aspects of the dual extrusion system operation. Safety precautions, calibration steps, and practices intended to maintain the system in good working order are also included.

A.1 System Set-up

The dual extrusion system is schematically depicted in figure 2-1 with a secondary schematic of the heater control zones presented in Figure 1-1 The system can be set up for one or two floor operation. In the case of two floor operation, the extruders and gear pump are placed on the second floor and the blend strand is extruded though grating or a hole of the floor and subsequently quenched and taken up on the first floor. The extruders should be placed such that the extrudate free falls though the center of the

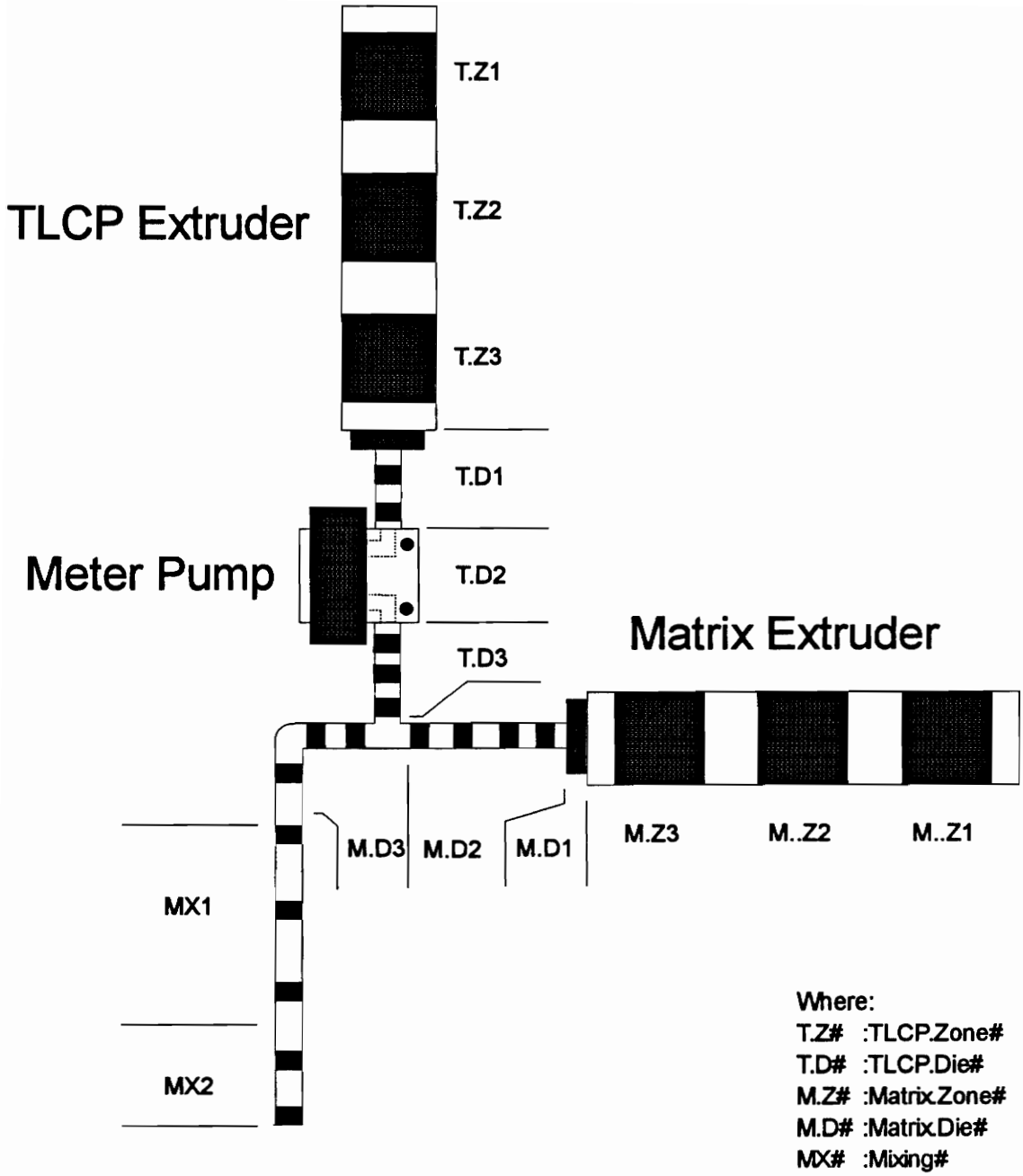

Figure A-1: **A schematic of the heating zones of the dual extrusion system.**

opening in the floor. The drawing chimney consists of two sections of schedule 40 PVC pipe. A free standing section of 2 1/2" pipe is placed between the die and the second floor grating. A secondary perforated 4" pipe is fixed to the underside of the second floor centered on the opening and hangs vertically between the second floor grating and the water bath on the first floor. Two floor operation requires two water baths to adequately cool the strand. Both water baths are placed on a table on the first floor. The first water bath (8" × 8" × 4') should be placed such that the extruded strand falls between the stationary 4" roller and the front end of the first water bath. There are two secondary freely rotating 1 1/2" rollers at the back of the water bath which are placed so that the strand is guided smoothly out of the water bath. The second water bath (12" × 4" × 3') is placed directly behind the first. The strand is guided through this water bath by weights, and finally out through the air jet that removes excess water on the strand. The rollers are placed on a table of equal height to the water baths directly behind the second water bath. Two floor operation results in the highest possible draw down ratios.

In the case of single floor processing, the systems set up and operation is much simpler. One (8" × 8" × 4') water bath placed directly under the die is typically adequate to quench the strand. Although the system can be operated with no drawing chimney, a free standing 2 1/2" PVC pipe can be placed between the die and the water bath to act as a drawing chimney. While this set-up is adequate for many applications, draw ratios as high as those possible in the two floor system are not possible.

A.2 System Start-up

A.2.1 Fill the water bath(s) with cold tap water.

A.2.2 Connect the power supply to the nip rollers

A.2.3 Connect and turn on the air supply for the air jet if used. A low flow rate of air (the amount necessary to just disturb the surface of the water is a good guideline) should be maintained throughout

system operation.

A.2.4 Initially, place a suitable collection container under the die to collect the extrudate prior to the system reaching operating conditions

A.2.5 Turn ON the cooling water to each extruder and maintain the cooling water flow throughout system operation.

A.2.6 With all individual heater controllers turned OFF, turn ON the main power supply to each extruder.

A.2.7 Set all heating zone temperatures to the desired set points utilizing the following guidelines. The controllers designations are presented in Table A-1 as well as the heater specifications.

- Set the controller temperature of T.Z1 and M.Z1 at 20 to 40°C below the melting points of the polymers in each respective extruder.
- Set the controller temperature of T.Z2 and M.Z2 at 5 to 10°C above the melting point of the polymers in each respective extruder.
- Set the controller temperatures of T.Z3 and M.Z3 to the desired temperatures and adjust as necessary during operation.
- Upon initial start-up, set the temperatures of T.D1, T.D2 (gear pump) and T.D3 to at least 100°C below the melting point of the TLCP.
- Set the controller temperatures of M.D1 and M.D2 to the desired melt temperature of the matrix material.
- Set all controller temperatures of M.D3, MX1 and MX2 to matrix materialsmeltingtemperature plus 30°C. Adjust these temperatures only after flow is maintained in the system

A.2.8 Turn ON the power supply to the temperature control zones T.Z3, T.D1, T.D2 and T.D3 and wait for the temperature to reach the set points. Once the set points are achieved, raise the

Table A-1: Heater specifications and controller designations for the dual extrusion process.

	Controller Designation Procedure[a]	Controller Designation on System[b]	Heaters
TLCP Extruder	T.Z1	Zone 1	Internal
	T.Z2	Zone 2	Internal
	T.Z3	Zone 3	Internal
	T.D1	Clamp Ring	1- 500W clamp ring heater 2- 1" x 1" 125W Band Heater
	T.D2	Adaptor	1- 800W pump heater 4- 50W 0.25"dia. x 1.5" Cartage heater
	T.D3	Die	3- 1" x 1" 125W band heater
Matrix Extruder	M.Z1	Zone 1	Internal
	M.Z2	Zone 2	Internal
	M.Z3	Zone 3	Internal
	M.D1	Die	1- 500W clamp ring heater
	M.D2	Die 1	4- 1" x 1" band heater
	M.D3	Die 2	3- 1" x 1" band heater
Auxiliary Controller[c]	MX1	C 1	4- 1" x 1" band heater
	MX2	C 2	2- 1" x 1" band heater

Notes: (a) These controller designations were used in the operting procedure, (b) these controller designations were the ones labelled on the actual system during opertion and correspond to the following extruder identification numbers: matrix extruder No. 8743.F and TLCP extruder No. 10657 and (c) auxiliary controller was 110V all other controllers were 220V

temperature setting in increments of 50°C. Wait for the temperature to reach the set points proir to increasing the setpoint. Finally, set these temperatures to the desired injection temperatures. The gear pump and injection piping might take as long as 45 minutes to reach the final deasired temperature depending on the final temperature.

A.2.9 Turn ON all heaters except zones T.Z1 , T.Z2, M.Z1, and M.Z2 and allow time for the system to heat to the set point temperatures. The set point temperatures are typically reached in less than 15 minutes but may take longer for higher set points.

Safety Note: Initial heating is the most dangerous period during operation. Under no circumstance should ones face or hands be under or near the die during this time. Build up of gases due to the decomposition of polymer in the system will periodically cause molten polymer and superheated gases to be violently expelled from the die causing the potential for serious personal injury.

A.2.10 Turn heating Zones 1, 2 and 3 controllers in each extruder to the AUTO position. Temperatures should reach the set point values in 10 to 15 minutes.

A.2.11 After the temperatures in both extruders, gear pump, piping and mixing section have reached the final set points, start the screw motor in the matrix extruder at a low speed (~10 RPMs) and wait for the pressure to rise and level off in this extruder. If the pressures should rise at a drastic rate or rise above 3500 psi, slow the screw speed. If the pressure continues to rise, turn OFF the matrix extruder and allow the system to heat for a longer period of time. Once flow has been maintained and the pressure is stable, increase the speed of the matrix extruder screw to ~ 20 RPMs to begin to purge the system.

A.2.12 Start the gear pump at a speed setting of approximately 5 RPMs.

Note: Starting the metering pump at a temperature below the melting point of the TLCP could cause catastrophic failure of the coupling between the driving shaft and the gears within the pump. This

condition will require extensive maintenance and should be avoided.

A.2.13 Start the screw in the TLCP extruder at a setting of approximately 3 RPMs. Slowly increase the RPMs to a final setting such that the pressure in the extruder is maintained in the range of 2500 to 3500 psig. This range of "stuffing" pressures (TLCP extruder pressure) is required for accurate metering of the flow rate by the gear pump. The final RPMs of the TLCP extruder should be roughly equal to or slightly less than the RPMs of the gear pump, but exact RPM settings are material dependent and could deviate from this rule of thumb. The screw RPMs will require slight adjustment during operation to maintain an appropriate stuffing pressure, and therefore must be monitored throughout operation.

A.2.14 Pump both materials through the system until the extrudate is uniform in appearance. While the system is purging, make final adjustments to system operating temperatures and matrix RPMs as necessary to achieve final desired settings since they will change due to viscous heating.

A.2.15 Adjust the flow rate of the TLCP. This must be done in a specific order. If the flow rate of TLCP is to be increased, first increase the RPMs of the meter pump, then adjust the RPMs of the TLCP extruder to maintain an appropriate stuffing pressure. If the flow rate of TLCP is to be reduced, first reduce the TLCP extruder RPMs to a value substantially below the expected final set point, then reduce the RPM set point of the gear pump to the final set point. Adjust the RPMs of the TLCP extruder to maintain an appropriate stuffing pressure to the meter pump. The specific set point of the gear pump is determined from a material specific calibration as is described in section A.4.

A.3 Process Operation

A.3.1 After the system has reached the desired operating conditions, remove the collection container and allow the extrudate strand to fall directly onto the stationary roller.

A.3.2 Start the nip rollers at a speed considerably below the desired set point (refer to Figure A.3 for speed calibration). An initial motor setting of 4 is appropriate for most processes.

A.3.3 Using a pair of scissors, quickly scrape the die face effectively cutting the strand, and remove the excess extrudate that has collected in the water bath.

A.3.4 Using the scissors as tongs hold the extrudate strand and quickly string under the stationary roller, then under the first freely rotating roller and above the last rotating roller.

A.3.5 Continually pull the extrudate though the rollers. At this point the strand can be handled with your bare hands.

A.3.6 If the system is being operated on a single floor, the strand is ready to be taken up by the nip rollers. For two floor operation the strand must now be placed in the second water bath and weighted so that the strand remains submerged in the cooling water. The strand is then fed through the air jet of the second water bath.

A.3.7 As you pull the extrudate, increase the speed of the strand until the process operates smoothly. At this point cut the strand close to the air jet and quickly feed it into the nip rollers.

A.3.8 Slowly increase the speed of the nip rollers until the desired set point is reached.

A.3.9 The system is now fully operating and strands can be collected

A.4. System Purging and Shut Down

A.4.1 After sufficient strand material has been collected place an appropriate container under the die to collect excess extrudate during purging and shut down

A.4.2 Remove all feed from the TLCP extruder using a vacuum cleaner. Allow the TLCP extruder to pump material until the extruder pressure is less than 500 psig. This indicates that the extruder screw is empty.

A.4.3 Lower the temperature setting of T.Z1 to 125°C, and allow this zone to cool for approximately 10 minutes. The extruder screw should still be rotating during this period.

A.4.4 Flush the TLCP extruder and gear pump with Dynapurge. Use several different screw speeds and gear pump settings to facilitate cleaning of the system.

Note: Failure to allow the feed zone of the TLCP extruder to properly cool (to ~125°C) prior to the addition of the purge material might cause the Dynapurge to block the feed section of the extruder. This condition will require that the screw be removed from the extruder and manually cleaned

A.4.5 The matrix extruder should be purged with Profax-6823 polypropylene. This may require the temperatures in this extruder to be adjusted depending on the matrix material that has been extruded. Again use various screw speed settings while purging.

A.4.6 Purge the system until all traces of TLCP have been removed in the extrudate.

A.4.7 Remove the excess Dynapurge feed from the TLCP extruder and allow the system to operate until the pressure in the TLCP extruder decreases to a pressure less than 500 psi.

A.4.8 Turn the RPMs of the screw in the TLCP extruder to zero. Turn off the power supply to the motor of the TLCP extruder.

A.4.9 Reduce the RPMs of the gear pump to zero. Turn off the main power supply to the gear pump.

A.4.10 Turn heating zones T.Z2, T.Z2, and T.Z3 to the ON position (this will start the cooling fans of these zones). Turn OFF heating zones T.D1, T.D2 and T.D3 of the TLCP extruder.

A.4.11 Turn off the main power supply to the TLCP extruder.

A.4.12 Continue pumping Profax-6823 through the system until all traces of the Dynapurge have been removed from the extrudate.

A.4.13 Set the RPMs of the screw in the matrix extruder to zero and turn OFF the power supply to the motor. Turn the heater controllers of M.Z1, M.Z2 and M.Z3 to the ON position. Turn OFF all remaining temperature controllers. Finally, turn OFF the main power spply to the matrix extruder.

A.4.14 After the system has cooled down for 15 minutes, turn OFF the cooling water and the main power supply for both extruders.

A.5 Calibrating the Gear Pump

The gear pump, which meters the flow of TLCP into the injection nozzle, is highly accurate but must first be calibrated. They procedure for the calibration of the meter pump is described below.

A.5.1 The TLCP piping should be disconnected from the exit of the gear pump assembly, and a short 1/4" nipple should be fitted into the gear pump discharge.

A.5.2 The gear pump and TLCP extruder should be heated up as described in Section A.3.0. Temperatures should be set to the same conditions that are to be used when the blend is produced.

A.5.3 The flow of TLCP should be started and maintained as discussed in Section A.3.0.

A.5.4 After the system has been adequately purged with the TLCP and no traces of Dynapurge are in the extrudate, calibration of the gear pump can begin. Calibration is accomplished by collecting and weighing the extrudate for a fixed period of time and gear pump RPM. The flow rate is then calculated and correlated to the gear pump set point. The gear pump should be calibrated in the RPM range of 1 to

10. At least 5 samples should be taken at each gear pump set point. The sample time for RPM setting of less than 3 RPMs should be at least one minute while higher gear pump setting can be calibrated with only a half minute sample times. Representative calibration curves are presented in Figure A.3.

Appendix B : Miscellaneous Figures

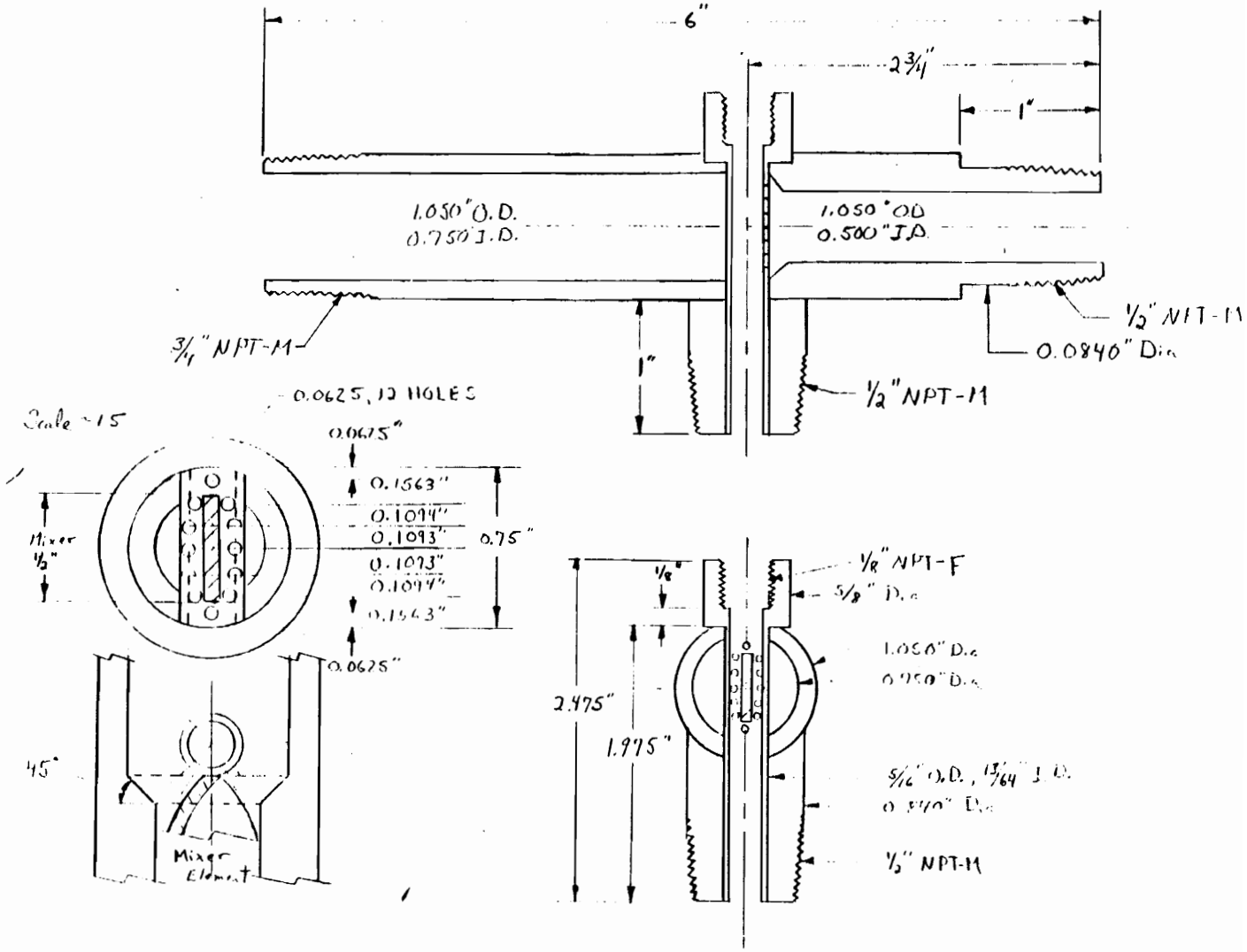

Figure B-1: Mechanical drawing of the multiple port phase distribution system

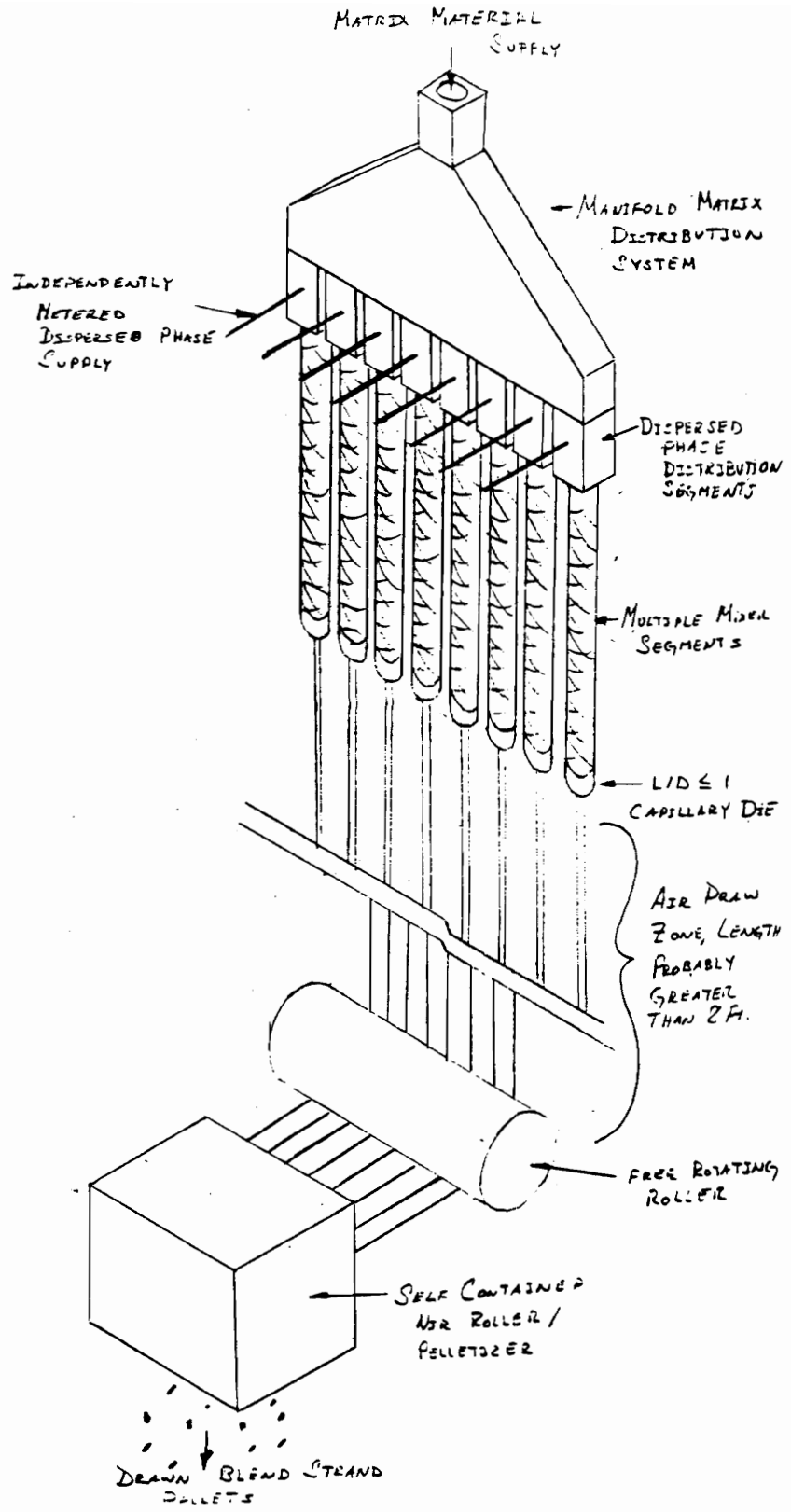

Figure B-2: Sketch of a possible scale-up option for the dual extrusion process.

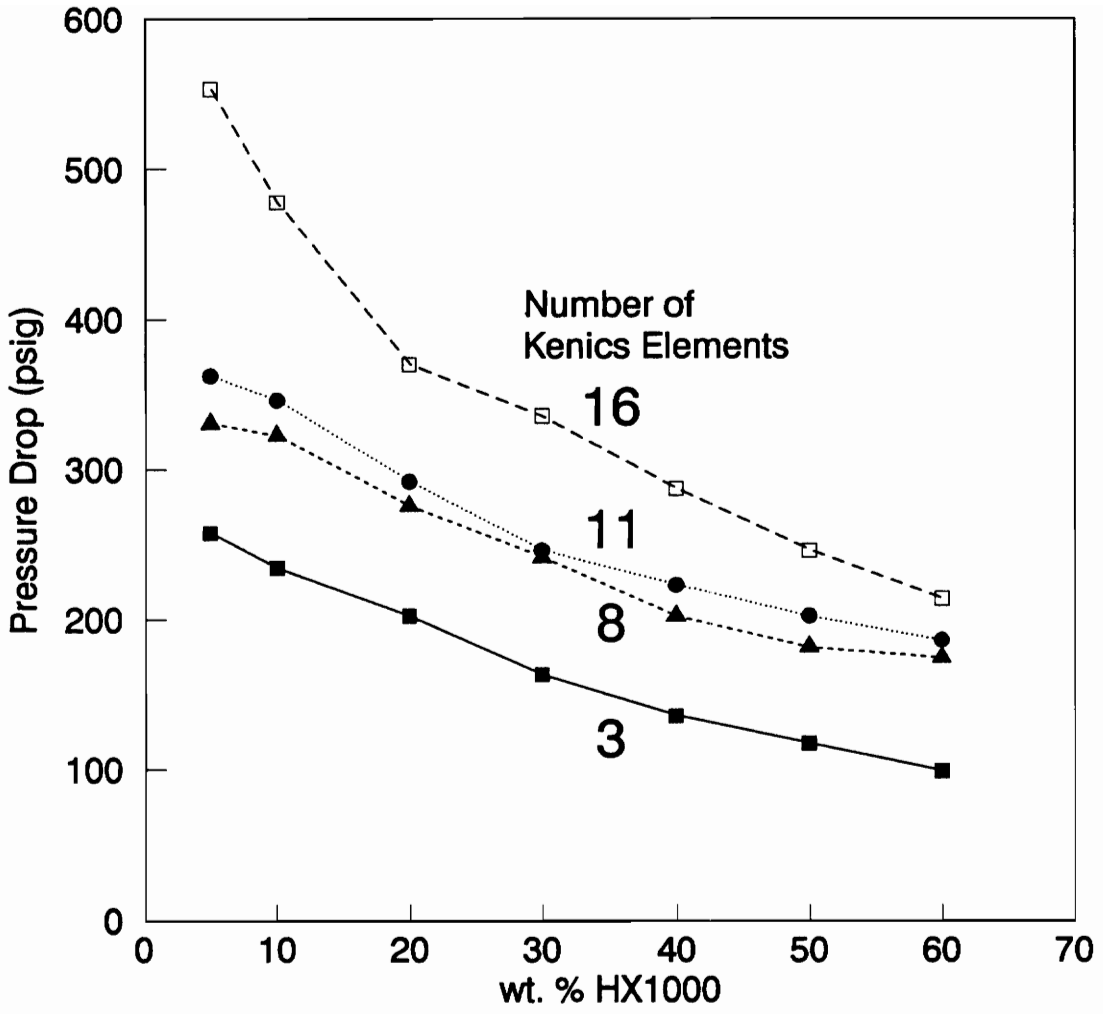

Figure B-3: Pressure drop through Kenics mixing elements as a function of HX1000 concentration and number of elements.

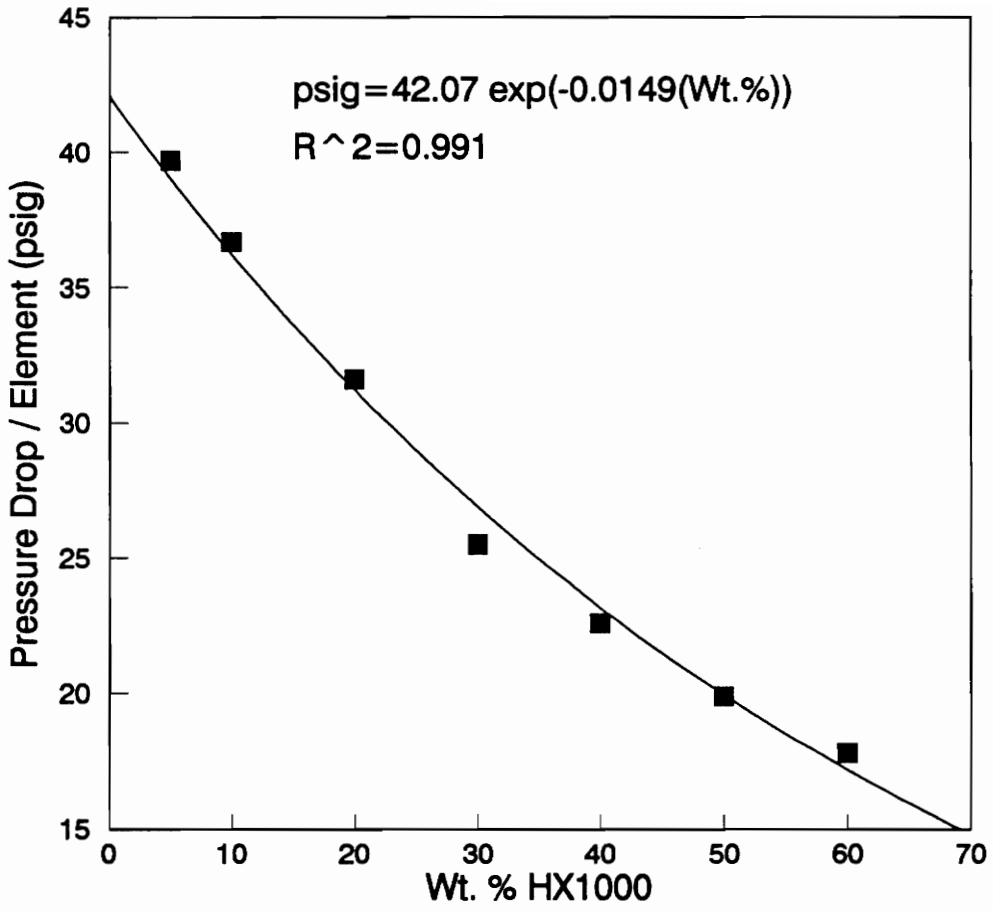

Figure B-4: Pressure drop per Kenics mixing element versus HX1000 concentration.

Vita

The author was born in Philipburg Pennsylvania on January 15, 1970. His academic career began in May of 1987 at the Pennsylvania State University in the Department of Chemical Engineering. His undergraduate work was supplemented by three semesters of cooperative education with the E.I. DuPont Company at a nylon fibers facility in Seaford Delaware. After received a B.S. degree in May of 1992, he came to the Chemical Engineering Department of the Virginia Polytechnic Institute and State University where he was granted a M.S. degree in May of 1994. In February of 1994, he was offered and accepted a position in process development engineering at W. L. Gore & Associates Inc. in Elkton Maryland.